# ABSTRACT

MCMECHEN, MICHAEL ALAN. Structural Impact of Aza-amino Acid Substitution in β-hairpin Model Systems. (Under the direction of Dr. Caroline Proulx).

Aza-amino acids are peptide mimics where the carbon has been substituted to a nitrogen atom in the α-position of one or more amino acids. The single atom substitution causes an increase in stability and a loss of a defined chiral center, while also inducing local conformational constraints and changing the hydrogen bonding properties (semicarbazide *vs* amide). Previously, the introduction of aza-amino acids has been found to stabilize β-turn secondary structures with the aza-amino acid in the $i + 1$ or $i + 2$ position, as well as to induce hyperstability in collagen peptide mimics.

In this thesis, the potential of using the unique hydrogen bonding properties of aza-amino acids (semicarbazides) to stabilize extended conformations in β-sheet peptidomimetics was explored. β-hairpins serve as a minimalistic β-sheet systems composed of two β-strands aligned in an antiparallel fashion and are used as model systems to understand the non-covalent associations that promote β-sheet formation and protein aggregation. Here, we have integrated aza-amino acids into three different 12mer β-hairpin model systems of varying stability to probe the impact of aza-amino acid substitution on conformation and stability. Specifically, singular aza-amino acids were incorporated in the center of the upper β-strand ($azaVal^3$ or $azaGly^3$) and compared with D-$val^3$ and $Gly^3$ substitutions, as well as the parent model peptide ($Val^3$). The effect of aza-amino acid substitution in β-hairpin analogs were assessed using NMR and circular dichroism spectroscopy. All azapeptides derivatives were found to severely weaken the β-hairpins model peptides, with the $Val^3$ to $azaVal^3$ substitution leading to a complete loss of β-hairpin formation.

Structural Impact of Aza-amino Acid Substitution in β-hairpin Model Systems.

by
Michael Alan McMechen

A thesis submitted to the Graduate Faculty of
North Carolina State University
in partial fulfillment of the
requirements for the degree of
Master of Science

Chemistry

Raleigh, North Carolina
2018

APPROVED BY:

Caroline Proulx
Chair of Advisory Committee

Gavin Williams

Wei-Chen Chang

## DEDICATION

I dedicate this work to my family and my love.  Your support and guidance made me who I am today.

## BIOGRAPHY

Michael McMechen was born on September 9$^{th}$, 1992 in Jacksonville, Florida. He lived in Cooper City, Florida until the age of 14, then moved to Black Mountain, North Carolina where completed middle and high school. He attended the University of North Carolina at Asheville to attain a BS in Chemistry in 2016. He promptly came to North Carolina State University to continue his academic career under the guidance of Caroline Proulx.

# ACKNOWLEDGEMENTS

I would like to thank Dr. Caroline Proulx for the direction and mentorship she has provided me during my time at NC State, and my group mates for their support and good humor keeping the laboratory cheerful.  I would also like to thank Dr. Melander, Dr. Chang, and Dr. Williams, as well as their group members for all of their assistance.  Lastly, I would like to thank Dr. Peter Thompson, who facilitated the NMR work in this research.

**TABLE OF CONTENTS**

## LIST OF TABLES

## LIST OF FIGURES

## LIST OF SCHEMES

# CHAPTER 1

# Introduction

## 1.1 Peptides as Therapeutic Agents

Peptides are comprised of sequences of 2 to 50 amino acids, which are considered one of the basic building blocks of the human body. They are ubiquitous and play critical roles as neurotransmitters[1] (*e.g.* enkephalin, substance P) and hormones in receptor-mediated signal transduction[2] (*e.g.* insulin, oxytocin, vasopressin). Synthetic peptides derived from protein segments can also serve as important modulators of protein-protein interactions (PPIs). In 2016, > 50 noninsulin peptide-based drugs were on the market, with many therapeutic peptides deriving their activity from modulating PPIs or binding to cellular membrane receptors.[3] Peptide based therapeutics have proven to be advantageous through their high binding efficacy, cheap production costs, biological safety, and vast structural and chemical versatility.[4] However, peptides suffer from several critical disadvantages. First, they are highly susceptible to degradation from the body's enzymes, which lead to a shortened duration of action. Second, peptides may suffer from low bioavailability. Finally, acyclic peptides can be highly flexible, which can lead to non-specific binding events and lower binding affinities.[5,6]

In order to maximize binding interactions with their target, peptides must adopt a stable secondary structure, such as an α-helix or β-sheet.[7] These secondary structures are promoted by a network of hydrogen bonds, electrostatic interactions, and hydrophobic interactions within the peptide.[8,9] Figure 1 shows representations of two prominent secondary structures found in nature, α-helices and β-sheets, which differ primarily in their hydrogen bonding patterns (shown in green) and backbone dihedral angles.[10] β-sheets are composed of two or more β-strands, which can align either in a parallel (Figure 1b) or anti-parallel (Figure 1c) fashion. Two β-strands, connected by a short (2-3 amino acids) turn sequence known as a β-turn, form a β-hairpin (Figure 1c and d).[11]

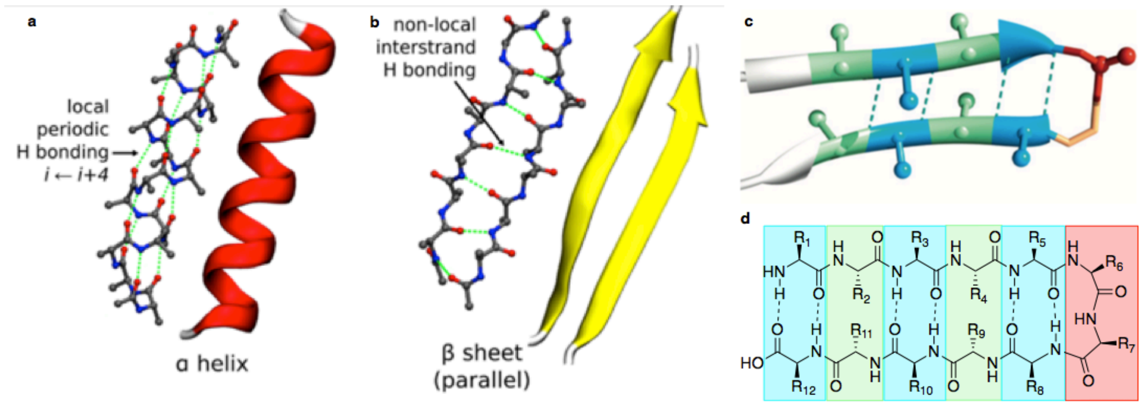


**Figure 1.1.** Depiction of peptide secondary structures. a) α-Helix[10]. b) Parallel β-sheet[11] c) Schematic representation of a β-hairpin with the hydrogen bonding (HB) regions in blue, non-hydrogen bonding (NHB) regions in green, and the turn sequence shown in red/orange.[11] d) Chemical structure of the β-hairpin.

β-strands and further β-sheets can be found throughout protein tertiary structures and are often implicated in protein dimerization, protein-protein interactions, oligomerization, and aggregation. [12] β-sheet interactions go beyond normal regulation of biological processes, and have been implicated in diseases such as Alzheimers, Parkinsons, type II diabetes, and prion diseases.[13,14,15] Such diseases result from the misfolding of native peptides and the uncontrolled formation of β-sheet-rich insoluble aggregates called amyloids, which can form toxic fibrils.[16] In order to improve our mechanistic understanding of amyloid formation, deepen our knowledge of factors that stabilize and destabilize β-sheets, and better guide the design of β-hairpin-folded peptide therapeutics, model systems had to first be made.

## 1.2 β-hairpin model systems

Compared with α-helices, the discovery of adequate β-hairpin model systems was long complicated by their tendency to self-associate in aqueous solution and form insoluble aggregates.[17] In essence, the design of good model hairpin systems required three features: 1) β-strand segments with good "β–sheet propensity" and favorable cross-strand interactions,[18] 2) a tight and stable two- or three-residue β-turn region that promotes nucleation of β-hairpins,[19] and 3) reduced propensity for aggregation.[20] The first isolated β-hairpin was characterized by NMR in 1993 as an isolated peptide sequence from tendamistat.[21] The initial peptide folded weakly and the need for a more effective model was apparent. Gellman *et al.* later proposed two model acyclic β-hairpin systems, RYVEV**X̲**GOKILQ-$NH_2$ (where X = L-Asn or D-Pro),[22] which have since been used by various other groups in independent studies to quantify the (de)stabilizing effects of cross-strand interactions and/or backbone modifications (*vide infra*).[23] The peptide is designed to maintain a charged state of +3 to avoid self-association through unfavorable electrostatic interactions, includes favorable cross-strand side-chain associations, and contains one of two turn sequences with D-Pro or Asn at the *i* + 1 and Gly at the *i* + 2 position. Having a D-proline residue at the *i* + 1 position was previously shown to favor the formation of type II' β–turn, while L-Asn-Gly dipeptides induce type I' β–turns.[24] Gellman *et al.* systematically demonstrated through a combination of CD spectroscopy and NMR analyses that the D-Pro-Gly turn sequence is superior to Asn-Gly for β-hairpin induction.[22] Specifically, long-range NOE interactions and the downfield shifting of α-protons relative to random coils were used to assess β-hairpin formation (Figure 1.2), with larger downfield chemical shifts being attributed to a greater population of β-hairpin-folded peptides.[17] The L enantiomer of proline, which forms a type II “mirror image” β-turn when incorporated at the $i + 1$ position, disrupts β-hairpin formation and can serve as a negative control.

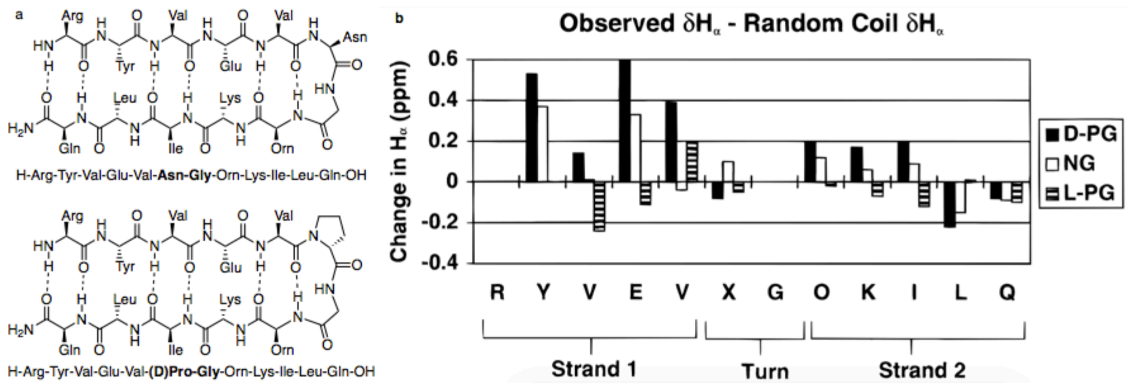


**Figure 1.2.** a) Chemical structures of the two 12-residue model β-hairpin peptides. b) observed $\delta H_\alpha$- random coil $\delta H_\alpha$ for 3.5 mM D-Pro-Gly peptide (solid bars), 4.6 mM Asn-Gly peptide (open bars) and 3.1 mM L-Pro-Gly peptide (striped bars) in aqueous (9:1 $H_2O$: $D_2O$) sodium deuterioacetate buffer, pH 3.8 (uncorrected), 4 °C. Figure reproduced from reference 22.

The following equation (eq. 1) was subsequently introduced to quantify the stability of the β-hairpins in model peptides, where $\delta_0$ and $\delta_{100}$ correspond to the chemical shifts of protons on the amino acid α-carbons (αCH) in either random coil peptides (negative control), or a cyclic fully folded peptide (positive control), respectively.[25]

$$\text{Fraction folded} = (\delta_{\text{observed}} - \delta_0)/(\delta_{100} - \delta_0) \quad \text{eq. 1}$$

The % population of the β-hairpin folded state in linear peptides is now commonly calculated with this equation, often reporting the αCH chemical shift variations for amino acids at specific, hydrogen-bonded positions away from the *N*-terminus and the D-proline residue (*i.e.* $Val^3$, $Orn^8$, and $Ile^{10}$ residues in the model peptides seen in Figure 1.2). In addition to this, the chemical shift difference (Δδ) between the two diastereotopic glycine protons (Hα and Hα’) in the turn region has also been used as a simplified method to quantify peptide folding (eq. 2).[26]

$$\text{Fraction Folded} = \Delta\delta_{\text{Gly Obs}} / \Delta\delta_{\text{Gly 100}} \quad \text{eq. 2}$$

Since the signals for Gly Hα/Hα' are usually found in a distinct region of the NMR spectrum, away from the αCH signals of all other amino acids, this is a relatively quick and easy method to determine β-hairpin stability. However, in sequences that employ D-Pro-Gly as a turn inducer, calculations of hairpin stability using glycine splitting (eq. 2) has been found to be less reliable and to overestimate the percentage of folded peptide.[23a] As such, β-hairpin population in these sequences should be primarily based off of the downfield shifting of the αCH (eq. 1), albeit glycine splitting is often still used to afford a quick, qualitative assessment of β-hairpin stability in these systems.[23d] In sum, while D-Pro-Gly is a stronger β-hairpin promoter, there are still advantages to using an Asn instead of D-Pro residue at the *i* + 1 position of the β-turn in model β-hairpin peptides.

## 1.3 β-sheet peptidomimetics

Peptidomimetics are compounds that are designed to closely mimic the structure, conformation, or bioactivity of peptides while increasing overall stability.[27] Such modifications can range anywhere from fully synthetic molecules, to predominantly natural peptides with minor chemical modifications. Figure 1.3 shows some examples of the various modifications made on peptides and have all been used with varying success to mimic peptide secondary structures and bioactivity.

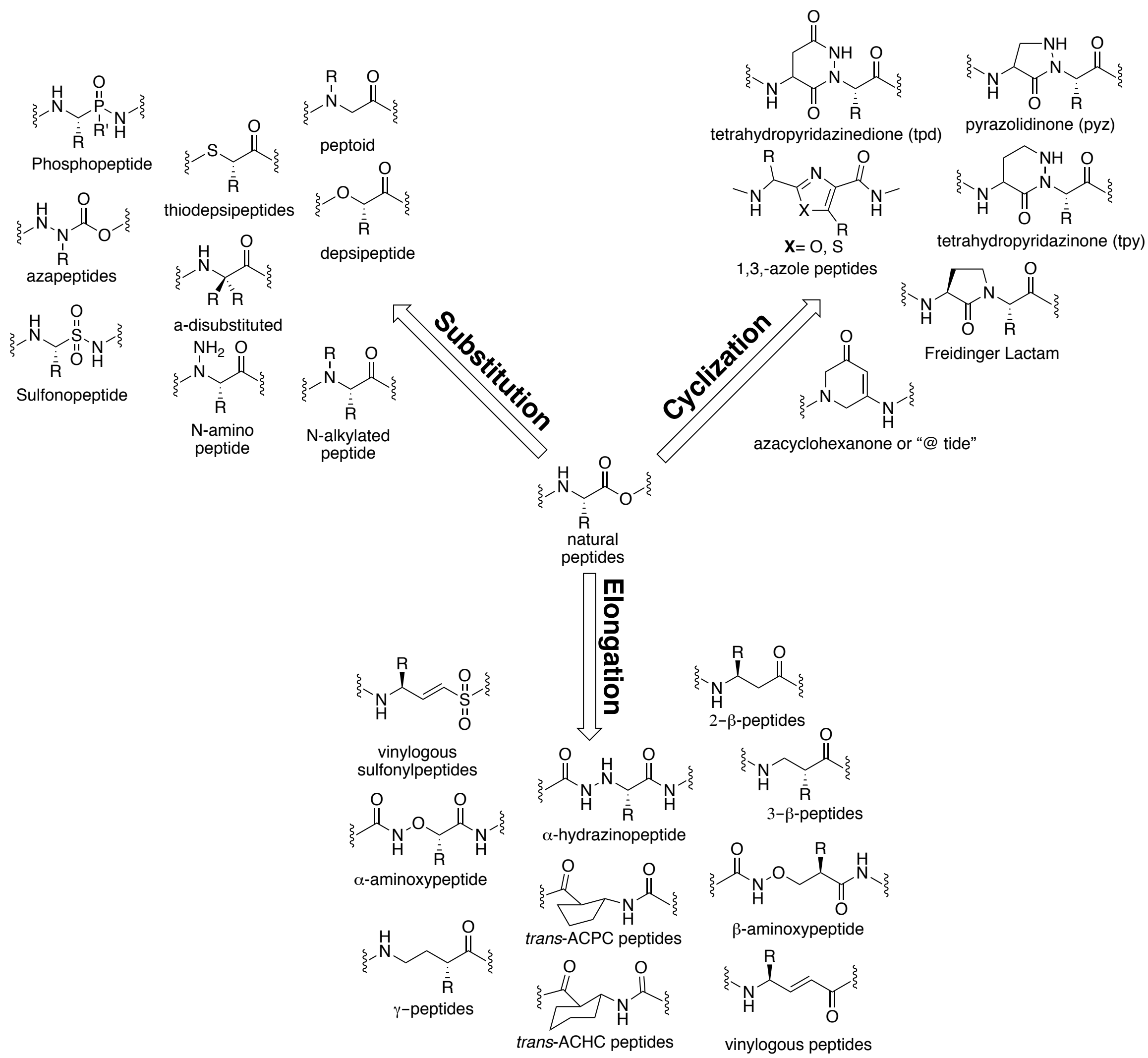


**Figure 1.3.** Examples of peptidomimetics, including cyclic constraints, backbone elongations, and various other substitutions.

### 1.3.1 Hao mimetics

In particular, β-hairpins have been mimicked by rigidifying either the turn region, or by using molecular scaffolds that serve to template the β-strand regions. For example, Nowick *et al.* were able to stabilize β-hairpin motifs by constructing a heterocyclic template composed of three sequential moieties: a **h**ydrazine, a 5-**a**mino-2-methoxybenzoic acid, and an **o**xalic acid residue, named "Hao" for short (Figure 1.4).[28] The Hao mimetic was designed to mimic the hydrogen-bonding network of a natural tripeptide on one face, while “blocking” – or minimizing hydrogen bond donors and acceptors – on the other (solvent exposed) face.

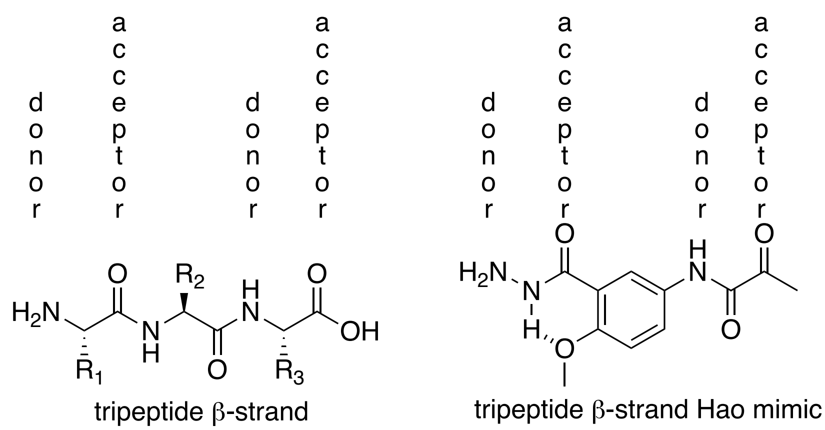


**Figure 1.4.** The hydrogen bonding network of a natural peptide sequence (left) and Hao peptidomimetic (right).[30]

Strategic incorporation of this unnatural Hao tripeptide mimic in peptide sequences, coupled with macrocyclization, has afforded many interesting β-sheet peptidomimetics.[29] Even in high concentrations, as the peptidomimetic forms dimers and higher orders of association, the inert external surface of the Hao prevents uncontrolled aggregation.[30] This controlled association was proven through NMR analyses, as well as X-ray crystallography. Figure 1.5 shows a representative example of a macrocyclic β-sheet mimic that was designed to inhibit amyloid fibril formation in Alzheimer’s desease, containing a peptide fragment from amyloid β peptide (Aβ) in the upper strand as a recognition element, and a Hao residue in the lower strand to prevent aggregation.[31] The obtained X-ray crystal structure revealed the formation of dimers adopting both antiparallel (Figure 1.5 c) and parallel (Figure 1.5 d) orientations in the solid state.[31]

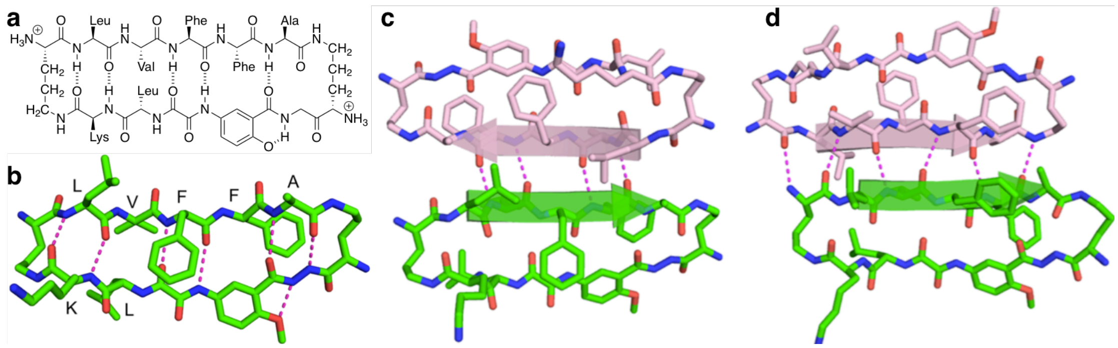


**Figure 1.5.** Example of a macrocyclic β-sheet possessing a Hao unit in the bottom strand, and residues 17-21 of Aβ peptide in the upper strand. a) Chemical structure of the mimetic. b) Crystal structure showing intramolecular hydrogen bonds with dashed lines. c) Crystal structure of a dimer in an *antiparallel* orientation showing intermolecular hydrogen bonds with dashed lines. d) Crystal structure of a dimer in a *parallel* orientation showing intermolecular hydrogen bonds.[31]

Many other macrocyclic β-sheet mimics have been created by varying the peptide sequence and length of the recognition (upper) strand while maintaining one or more Hao residues in the templating (bottom) strand. Using peptide sequences designed to bind to known fibril-forming peptides from protein misfolding diseases, taylor made macrocycles were created to selectively associate with the peptide strands and prevent aggregation. Specifically, peptide fragmentsfrom $A\beta_{40}$, $A\beta_{42}$, $h\beta_2M$, and $h\alpha Syn_{1\text{-}100}$ believed to be implicated in Alzheimer's, human $\beta_2$-Microglobulin amyloidolysis, and Parkinsons disease respectively were used to study the inhibition of amyloid aggregation.[32] Using transmission electron microscopy (TEM) and thioflavin T (ThT) fluorescence assays, Nowick *et al.* demonstrated that certain Hao-containing sequence-specific macrocycles were able to significantly stunt the growth of Aβ aggregates.[32]

### 1.3.2 Peptide *N*-amination

Other methods of improving β-hairpin stability involve more subtle peptide backbone modifications. For example, Del Valle *et al.* demonstrated that *N*-amination of amino acid residues at the non-hydrogen-bonded (NHB) face of a β-hairpin model system increased the stability of the structures from 75% to up to 96% folded population in analogs containing two *N*-aminated residues (Table 1.1).[23d]

**Table 1.1.** Effects of *N*-amination and *N*-methylation substitutions on folding and stability in model β-hairpin peptides.[23d]

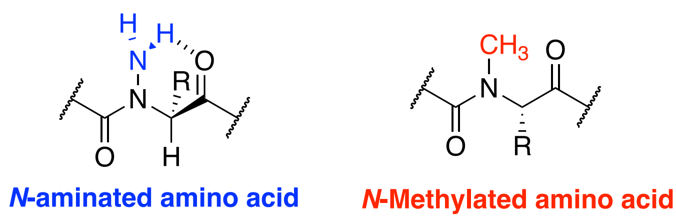


| Peptide[a] | Avg percent folding[b] | Avg ΔΔG kcal $mol^{-1}$ |
|---|---|---|
| **1** H-Arg-Tyr-Val-Glu-Val-pro-Gly-Orn-Lys-Ile-Leu-Gln-$NH_2$ | 75 | - |
| **2** H-Arg-aTyr-Val-Glu-Val-pro-Gly-Orn-Lys-Ile-Leu-Gln-$NH_2$ | 77 | ±0.09 |
| **3** H-Arg-Tyr-Val-Glu-Val-pro-Gly-Orn-aLys-Ile-Leu-Gln-$NH_2$ | 90 | −1.07 |
| **4** H-Arg-Tyr-Val-Glu-Val-pro-Gly-Orn-Lys-Ile-aLeu-Gln-$NH_2$ | 78 | ±0.09 |
| **5** H-Arg-Tyr-Val-Glu-Val-pro-Gly-Orn-aLys-Ile-aLeu-Gln-$NH_2$ | 96 | −1.33 |
| **6** H-Arg-Tyr-Val-Glu-Val-pro-Gly-Orn-Lys-Ile-(N-Me)Leu-Gln-$NH_2$ | 52 | +0.56 |

[a]aTyr = Nα-aminotyrosine, aLys = Nα-aminolysine, aLeu = Nα-aminoleucine, (N-Me)Leu = Nα methylleucine.[b]Percent folding is an average of values obtained from αCH chemical shifts for Val[3], Val[5], Orn[8], and Ile[10] residues.

*N*-amino peptides (NAP) stabilize β-hairpins *via* an additional hydrogen bond between the amino group and the amide functional group of the neighboring residue, enforcing a *trans*-amide bond geometry (ω = 180°) and restricting backbone phi (ϕ) and psi (φ) torsion angles. This linearity assists in forming a template for the complementary strand to associate with. As a direct comparison, *N*-amination *vs* *N*-methylation of the Leu[11] residue resulted in 78% and 52% folding, respectively (Table 1.1, entries 4 and 6).

Interestingly, imposing additional cyclic constraints using pyrazolidinone and tetrahydropyridazinone dipeptide scaffolds (see Figure 1.3) did not have further stabilizing effects.[33] To the contrary, it was found that, even though cyclization makes for more rigid systems, this rigidity does not necessarily induce the proper dihedral angles required for β-sheet formation.

### 1.4 Azapeptides

Azapeptides are peptidomimetics in which the α–carbon of one or more residues is replaced by a nitrogen (Figure 1.6).[34] This backbone substitution leads to increased protease and chemical stability, in addition to imposing new local conformational restrictions and leading to the loss of a defined chiral center.[35] The distinct hydrogen-bonding properties of the semicarbazide unit is also unique in aza-amino acids, but has been exploited to a lesser extent.

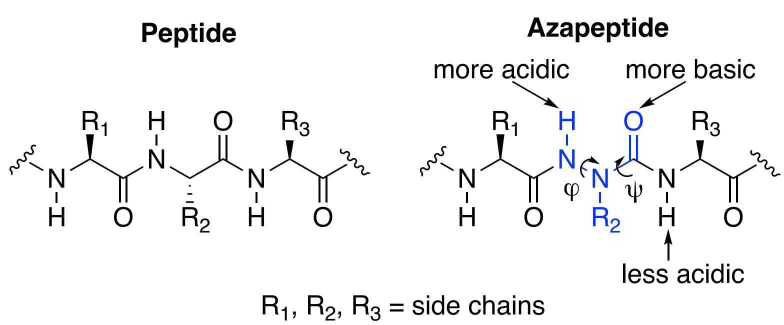


**Figure 1.6.** Comparative structure of a peptide (left) and azapeptide (right).

Aza-amino acid substitution has proven to be a useful tool in the study and, potentially, improvement of biologically active compounds through structure-activity-relationship (SAR) studies. Due in part to their protease stability, azapeptides have been pursued as both enzyme inhibitors and receptor ligands.[34] For example, Zoladex is an FDA approved luteinizing hormone releasing hormone (LHRH) agonist used for the treatment of breast and prostate cancer that contains a *C*-terminus aza-glycine residue.[36] In a recent example, an aza-glycine residue was incorporated at the P1 position of known peptide substrates of human cathepsins (Cat) S and K. The azapeptide derivatives exhibited inhibitory constants (Ki) in the nanomolar range and selectivity for the respective cysteine proteases.[37] Aza-amino acid scanning has also proven to be effective in the discovery of receptor ligand with improved selectivity, likely due to the conformational attributes they impart on short peptide sequences (*vide infra*). One such example is the substitution of Trp[4] for azaPhe[4] in the growth hormone releasing peptide GHRP-6 (His-D-Trp-Ala-Trp-D-Phe-Lys-$NH_2$).[38,39] The singular aza-substitution in the hexamer sequence is believed to nucleate a β-turn, as demonstrated by circular dichroism spectroscopy.[38,39] While the native GHRP-6 peptide binds to two receptors, CD36 and GHS-R1a, the azapeptide analog maintains a similar binding affinity to the CD36 receptor while exhibiting a 1000-fold loss of affinity for GHS-R1a.

### 1.4.1 Conformational properties of azapeptides

The planarity of the urea moiety and lone pair–lone pair repulsion between the two adjacent nitrogen atoms in the semicarbazide unit (Figure 1.6) provides a vastly different conformational landscape compared to a natural peptides. Serving as a simple model system for aza amino acids (azaGly), a theoretical study of the conformational properties of *N,N*'-diformylhydrazine found that the *Z,Z* configuration was the most stable with a 90° angle between the two lone pairs (Figure 1.7).[40]

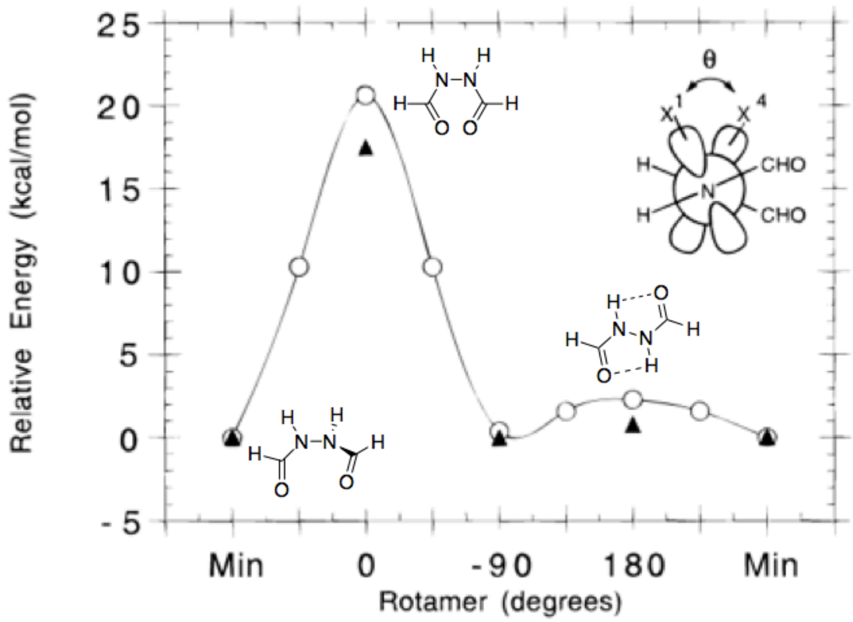


**Figure 1.7.** Calculated potential energy surface for the Z,Z configuration of diacylhydrazine.[40]

Albeit higher in energy relative to the twisted conformer, intramolecular hydrogen bonding opportunities were found to stabilize the conformational isomer with the lone pairs in an anti-configuration (180°). As a result, the energetic threshold from the energetic well at 90° only reaches a maximum of 3.2 kcal/mol. This may allow for alternative ϕ and φ torsional angles in aza-amino acids, which could accommodate extended as opposed to twisted (turn) conformations in certain azapeptide sequences. However, substitution of one of the two nitrogen atoms with a methyl group leads to the loss of an intramolecular hydrogen bond and increases the energy of the 180$^{o}$ rotamer by up to 5 kcal/mol.[40]

Other model compounds containing aza-amino acids have been investigated using computational methods and crystallographic analyses, as well as NMR, IR, and CD spectroscopy. Various substitutions of aza-amino acids, particularly azaGly[41], azaAla,[42] azaLeu[43], and azaPhe[44] were embedded in model di- and tripeptide sequences and found to exhibit similar dihedral angles in computational analyses, with $\phi$ = 90 ° ± 30 ° or -90 ° ± 30 °, and $\psi$ = 0 ± 30 ° or 180 ° ± 30 °. Such dihedral angles fall into the realm of 1) the polyproline type II helix, and 2) the $i$ + 1 and $i$ + 2 positions of β-turn secondary structures.[44,45] In addition to computational studies, several X-ray crystal structures of azapeptides have also been obtained, with many adopting turn-like secondary structures in the solid state. However, these short azapeptide sequences often contain other structure-inducing residues, such as proline, or include additional covalent constraint in the aza-amino acid itself (*e.g.* azaPro, aza-pipecolic acid (azaPip)).[46]

In terms of stereochemistry, the α-nitrogen in azapeptides can be described as having adaptive chirality, in which the side chain can invert between mirror images through a planar intermediate. Whether the aza-amino acid adopts an L or D-like chirality is contingent factors such as the α-nitrogen participating in hydrogen bonding events and overall stability of the peptide, *i.e.* location of the aza-amino acid residue and nature of the neighboring amino acid residues.

### 1.4.2 Other applications of azapeptides

The preference for aza amino acids to adopt a type II polyproline helix conformation (*vide supra*) and the opportunity for additional hydrogen bonding in aza-glycine residues inspired Chenoweth *et al.* to pursue azapeptide analogs of a 21mer collagen model peptide (CMP) (Table 1.2, Fig. 1.8).[47] Collagen is a right-handed triple helix, with three peptide chains often composed of a repeating tripeptide sequence: Pro-Hyp-Gly, where Hyp = (2*S*, 4*R*)-hydroxyproline. Remarkably, in substituting a single glycine for an aza-glycine in the center of the CMP peptide sequence (Table 1.2, entry 5), the stability of the collagen triple helix increased significantly, exhibiting a melting temperature of 51 °C *vs* 40 °C for the control CMP peptide (Table 1.2, entry 1).[47]

**Table 1.2.** Effect of azaGly substitutions in collagen model peptides on melting temperatures. P = (2S)-proline, O = (2S,4R)-hydroxyproline, and azG = aza-glycine.

| Entry | Peptide | $T_m$ | $\Delta T_m$ |
|---|---|---|---|
| 1 | Ac-POG-POG-POG-POG-POG-POG-POG-$NH_2$ | 40 | - |
| 2 | Ac-POazG-POG-POG-POG-POG-POG-POG-$NH_2$ | 46 | +6 |
| 3 | Ac-POG-POazG-POG-POG-POG-POG-POG-$NH_2$ | 48 | +8 |
| 4 | Ac-POG-POG-POazG-POG-POG-POG-POG-$NH_2$ | 50 | +10 |
| 5 | Ac-POG-POG-POG-POazG-POG-POG-POG-$NH_2$ | 51 | +11 |
| 6 | Ac-POG-POG-POG-POG-POazG-POG-POG-$NH_2$ | 49 | +9 |
| 7 | Ac-POG-POG-POG-POG-POG-POazG-POG-$NH_2$ | 47 | +7 |
| 8 | Ac-POG-POazG-POG-POG-POG-POazG-POG-$NH_2$ | 57 | +17 |
| 9 | Ac-POG-POG-POazG-POG-POazG-POG-POG-$NH_2$ | 59 | +19 |
| 10 | Ac-POG-POG-POG-POazG-POazG-POG-POG-$NH_2$ | 61 | +21 |
| 11 | Ac-POG-POazG-POG-POazG-POG-POazG-POG-$NH_2$ | 69 | +29 |
| 12 | Ac-POG-POG-POazG-POazG-POazG-POG-POG-$NH_2$ | 74 | +34 |
| 13 | Ac-azG-POazG-POazG-PO-$NH_2$ | - | - |
| 14 | Ac-azG -POazG-POazG-POazG-PO-$NH_2$ | 36 | -4 |
| 15 | Ac-azG-POazG-POazG-POazG-POazG-PO-$NH_2$ | 78 | +38 |

Further analysis showed that aza-glycine substitution closer to the terminus of the sequence also increased thermal stability, albeit to a lesser extent presumably due to fraying of the triple helix (Table 1.2, entries 2-4 and 6-7). Addition of a second or third azaGly led to additive effects on the thermal stability (Table 1.2, entries 8-12), with a maximum melting temperature of 74 °C when the three central repeat units possess azaGly residues (Table 1.2, entry 12).[47] To test the limits of azaGly substitution in collagen model peptides, all azaGly-substituted CMPs were created with 9, 12 and 15 residues in total, respectively (Table 1.2, entries 13-15). The 9-mer was unable to form the triple helix structure. While the 12-mer was still able to form the triple helix tertiary structure and constitutes the shortest peptide mimic capable of doing so, it proved to not be as robust as the larger 21mer natural sequence with a $T_m$ decrease of 4 °C (Table 1.2, entry 14). The 15-mer, however, is the most stable self-assembled collagen peptide reported to date with an increased melting point 38 °C above the natural model (Table 1.2, entry 15).[47]

This increase in thermal stability has been attributed to the dihedral angle preferences of the aza-glycine and the strengthened hydrogen bonding network from the C to N substitution, which can be seen in the X-ray crystal structure of (Pro-Hyp-Gly)$_3$-Pro-Arg-azGly-(Pro-Hyp-Gly)$_4$-NH$_2$ (Fig. 1.8). The $T_m$ values for this azapeptide analog also exhibited a marked increase from 42 °C in the control peptide to 51 °C for the aza-derivative.[47]

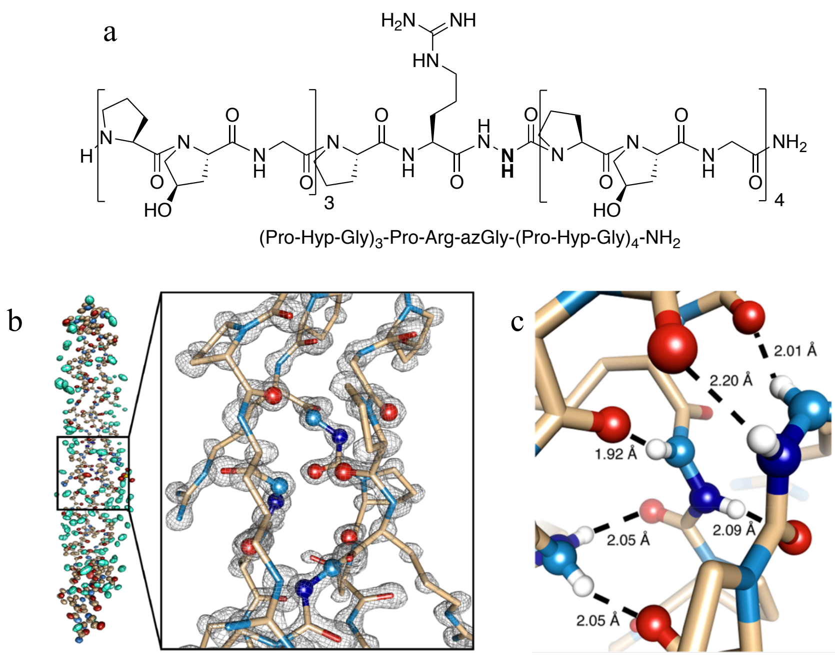


**Figure 1.8.** a) Chemical structure of the peptide sequence with singular azaGly substitution in the center of collagen. b) X-ray crystal structure of azaGly substituted collagen triple helix (red = oxygen, tan = carbon, light blue = nitrogen, dark blue = nitrogen from azaGly.) c) Canonical hydrogen bonding network with the additional hydrogen bonds formed by aza-Gly substitution shown with dashed lines.[47]

## 1.5 Summary of thesis: incorporation of aza-amino acids into β-hairpin model systems

The purpose of this research is to interrogate the structural effects of aza-amino acid incorporation into the β−strand segment of β-hairpin model systems. It is now known that aza-amino acids can be used as β-turn inducing agents through the twisting of the semicarbazide backbone, and that the additional hydrogen bonding opportunities of azaGly can create hyperstability when substituted into collagen triple helix model peptides. Understanding the "folding rules" of aza-amino acids beyond turns and helices is important to expand their use in peptide mimicry. Past research based on computational analyses has explicitly stated that the backbone conformation of azapeptides will not allow for extended β−sheet conformation (see section 1.4.1), but with the caveat that the azapeptide model compounds tested were small. Embedding an aza-amino acid residue in one of the β-strands of a β-hairpin, however, could in principle be tolerated considering the hydrogen bonding properties of semicarbazide residues. Indeed, much like the Hao template (see section 1.3.1), aza-amino acids exhibit one face with enhanced hydrogen-bonding properties while decreasing the hydrogen-bonding strength of the solvent exposed face (Figure 1.6).

In order to properly analyze the ability of aza-amino acid residues to adopt extended conformations, this thesis will explore the effects of aza-substitution on the stability of β−hairpin model peptides. Specifically, the aza-amino acids will be placed away from the turn sequence within the β-strand segment and away from the termini to prevent complications from hairpin fraying. Additionally, the aza-amino acid residues will be placed in the hydrogen bonded (HB) region of the β-hairpin, in order to properly utilize the differential faces of the aza-residue and have the reactive face (stronger H-bond donors/acceptors) of the residue available for intramolecular hydrogen-bonding. To best meet these criteria, the substitutions location has been chosen to be the third residue in model (12-residue) β-hairpin peptides (Figure 1.9).

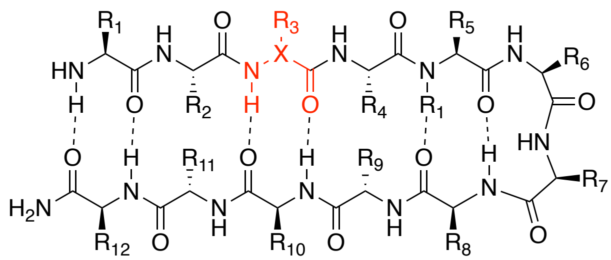


**Figure 1.9.** 12-residue β-hairpin model system with residue 3 highlighted as the substitution position.

## 1.6 REFERENCES

[1] Snyder, S. H. Brain Peptides as Neurotransmitters. *Science* **1980**, *209*, 976-983.

[2] McGonigle, P. Peptide therapeutics for CNS indications. *Biochem. Pharm.* **2012**, *83*, 559-566.

[3] Henninot, A.; Collins, J. C.; Nuss, J. M. The Current State of Peptide Drug Discovery: Back to the Future? *J. Med. Chem.* **2018**, *61*, 1382-1414.

[4] Craik, D. J.; Fairlie, D. P.; Liras, S.; Price, D. The Future of Peptide-based Drugs. *Chem. Biol. Drug. Des.* **2013**, *81*, 136-147.

[5] McGregor, D. P. Discovering and Improving Novel Peptide Therapeutics. *Curr. Op. Parm.* **2008**, *8*, 616-619.

[6] Fosgerau, K.; Hoffmann, T. Peptide therapeutics: current status and future directions. *Drug Disc. Today* **2015**, *20*, 122-128.

[7] Kaiser, E. T.; Kezdy, F. J. Secondary structures of proteins and peptides in amphiphilic environments (A Review). *Proc. Natl. Acad. Sci.* **1983**, *80*, 1137-1143.

[8] Bordo, D.; Argos, P. The Role of Side-chain Hydrogen Bonds in the Formation and Stabilization of Secondary Structure in Soluble Proteins. *J. Mol. Biol.* **1994**, *243*, 504-519.

[9] Kanehisa, M. I. Local Hydrophobicity Stabilizes Secondary Structures in Proteins. *Biopolymers* **1980**, *19*, 1617-1628.

[10] Baldauf, C.; Rossi, M. Going clean: structure and dynamics of peptides in the gas phase and path to solvation. *J. Phys.: Condens. Matter* **2015**, *27*, 493002.

[11] Obrecht, D.; Chevalier, E.; Moehle, K.; Robinson, J. β-Hairpin protein epitope mimetic technology in drug discovery. *Drug Discovery Today: Technologies* **2012**, *9*, e63-e69.

[12] Cheng, P.; Pham, J.; Nowick J. The Supramolecular Chemistry of β-sheets. *J. Am. Chem. Soc.* **2013**, *135*, 5477-5492.

[13] Chiti, F.; Dobson, C. M. Protein Misfolding, Functional Amyloid, and Human Disease. *Annu. Rev. Biochem.* **2006**, *75*, 333-336.

[14] Aguzzi, A.; O'Connor, T. Protein aggregation diseases: pathogenicity and therapeutic perspectives. *Nature Rev. Drug Discov.* **2010**, *9*, 237-248.

[15] Bartolini, M.; Andrisano, V. Strategies for the inhibition of protein aggregation in human diseases. *ChemBioChem.* **2010**, *11*, 1018-1035.

[16] Murphy, R. Peptide Aggregation in Neurodegenerative Disease. *Annu. Rev. Biomed. Eng.* **2002**, *4*, 155-174.

[17] Ramirez-Alvarado, M.; Blanco, F. J.; Serrano, L. *De novo* design and structural analysis of a model β-hairpin peptide system. *Nat. Struct. Biol.* **1996**, *3*, 604-612.

[18] Kim, C.; Berg, J. Thermodynamic β-sheet propensities measured using a zinc-finger host peptide. *Nature* **1993**, *362*, 267-270.

[19] Haque, T. S.; Little, J. C.; Gellman, S. H. Stereochemical Requirements for β-Hairpin Formation; Model Studies with Four-Residue Peptides and Depsipeptides. *J. Am. Chem. Soc.* **1996**, *118*, 6975-6985.

[20] Richardson, J. S.; Richardson, D. C. Natural β-sheet proteins use negative design to avoid edge-to-edge aggregation. *PNAS*, **2002**, *99*, 2754-2759.

[21] Blanco, F.; Jimenez, A.; Herranz, J.; Rico, M. Santoro, J. Nieto, J. NMR Evidence of a Short Linear Peptide That Folds into a β-Hairpin in Aqueous Solution. *J. Am. Chem. Soc.* **1993**, *115*, 5887-5888.

[22] Stanger, H.; Gellman, S. Rules for Antiparallel β-Sheet Design: D-Pro-Gly Is Superior to L-Asn-Gly for β-Hairpin Nucleation. *J. Am. Chem. Soc.* **1998**, *120*, 4236-4237.

[23] For selected examples, see: A) Kiehna, S. E.; Waters, M. L. Sequence dependence of β-hairpin structure: Comparison of a salt bridge and an aromatic interaction. *Protein Science* **2003**, *12*, 2657-2667. B)Colombo, G.; De Mori, G.; Roccatano, D. Interplay between hydrophobic cluster and loop propensity in β-hairpin formation: A mechanistic study. *Protein Sci.* **2003**, *12*, 538-550. C) Kuo. H. T.; Liu, S. L.; Chiu, W. C.; Fang, C. J.; Chang, H. C.; Wang, W. R.; Yang, P. A.; Li, J. H.; Huang, S. J.; Huang, S. L.; Cheng, R. P. Effect of charged amino acid side chain length on lateral crosss-strand interactions between carboxylate- and guanidinium-containing residues in a β-hairpin. *Amino Acids* **2015**, *47*, 885-898. D)Sarnowski, M. P.; Kang, C. K.; Elbatrawi, Y. M.; Wojtas, L.; Del Valle, J. R. Peptide N-Amination Supports β-sheet conformations. *Angew. Chem. Int. Ed.* **2017**, *56*, 2083-2086.

[24] Hutchinson, G. E.; Thronton, J. M. A revised set of potentials for β-turn formation in proteins. *Protein Science* **1994**, *3*, 2207-2216.

[25] Syud, F. A.; Espinosa, J. F.; Gellman, S. H. NMR-Based Quantification of *β*-Sheet Populations in Aqueous Solution through Use of Reference Peptides for the Folded and Unfolded States. *J. Am. Chem. Soc*. **1999**, *121*, 11577-11578.

[26] Tatko, C. D.; Waters, M. L. Selective Aromatic Interactions in β-Hairpin Peptides. *J. Am. Chem. Soc.* **2002**, *124*, 9372-9373.

[27] Vagner, J.; Qu, H.; Hruby, V. Peptidomimetics, a synthetic tool of drug discovery. *Curr. Op. Chem. Bio.* **2008**, *12*, 292-296.

[28] Nowick, J. S.; Tsai, J. H.; Bui, Q. D.; Maitra, S. A Chemical Model of a Protein β-Sheet Dimer. *J. Am. Chem. Soc.* **1999**, *121*, 8409-8410.

[29] For recent examples, see: A) Spencer, R.; Li, H.; Nowick, J. S. X-ray Crystallographic Structures of Trimers and Higher-Order Oligomeric Assemblies of a Peptide Derived from $A\beta_{17-36}$. *J. Am. Chem. Soc.* **2014**, *136*, 5595-5598. B) Pham, J. D.; Spencer, R. K.; Chen, K. H.; Nowick, J. S. A Fibril-like Assembly of Oligomers of a Peptide Derived from b-Amyloid. *J. Am. Chem. Soc.* **2014**, *136*, 12682-12690. C) Truex, N. L.; Nowick, J. S. Coassembly of Peptides Derived from b-sheet Regions of b-Amyloid. *J. Am. Chem. Soc.* **2016**, *138*, 13891-13900. D) Wang, Y.; Kreutzer, A. G.; Truex, N. L.; Nowick, J. S. A Tetramer Derived from Islet Amyloid Polypeptide. *J. Org. Chem.* **2017**, *82*, 7905-7912. E) Wang, Y.; Truex, N. L.; Vo, N. D. P.; Nowick, J. S. Effects of Charge and Hydrophobicity on the Oligomerization of Peptides Derived from IAPP. *Bioorganic Med. Chem.* **2018**, *26*, 1151-1156. F) Kreutzer, A. G.; Nowick, J. S. Elucidating the Structures of Amyloid Oligomers with Macrocyclic b-Hairpin Peptides: Insights into Alzheimer's Disease and other Amyloid Diseases. *Acc. Chem. Res.* **2018**, *51*, 706-718.

[30] Nowick, J. S.; Chung, M.; Maitra, K.; Stigers, K. D.; Sun, Y. An unnatural amino acid that mimics a tripeptide β-strand and forms β-sheetlike hydrogen-bonded dimers. *J. Am. Chem. Soc.* **2000**, *122*, 7654-7661.

[31] Liu, C.; Sawaya, M. R.; Cheng, P. N.; Zheng, J.; Nowick, J. S.; Eisenberg, D. Characteristics Of Amyloid-Related Oligomers Revealed by Crystal Structures of Macrocyclic β-Sheet Mimics. *J. Am. Chem. Soc.* **2011**, *133*, 6736-6744.

[32] Cheng, P. N.; Liu, C.; Zhao, M.; Eisenberg, D.; Nowick, J. S. Amyloid β-Sheet Mimics that Antagonize Protein Aggregation and Reduce Amyloid Toxicity. *Nat. Chem.* **2012**, *4*, 927-933.

[33] Sarnowski, M.; Pedretty, K.; Giddings, N.; Woodcock, L.; Del Valle, J. Synthesis and β-sheet propensity of constrained N-amino peptides. *Bioorg. Med. Chem.* **2018**, *26*, 1162-1166.

[34] Proulx, C. Sabatino, D.; Hopewell, R.; Spiegel, J.; Ramos, Y. G.; Lubell, W. D. Azapeptides and their therapeutic potential. *Future Med. Chem.* **2011**, *3*, 1139-1164.

[35] Dutta, A. S.; Giles, M. B. Polypeptides. Part XIV.[1] A Comparative Study of the Stability towards Enzymers of Model Tripeptides containing α-Aza-amino-acids, L-Amino-acids, and D-Amino-acids. *Chem Soc [Perkin 1]* **1976**, *2*, 244-248.

[36] Ahmann, F.; Citrin, D.; deHaan, H.; Guinan, P.; Jordan, V.; Kreis, W.; Scott, M.; Trump D. Zoladex: a sustained-release, monthly luteinizing hormone-releasing hormone analogue for the treatment of advanced prostate cancer. *J. Clin. Oncology* **1987**, *5*, 912-917.

[37] Galibert, M.; Wartenberg, M.; Lecaille, F.; Saidi, A.; Mavel, S.; Joulin-Giet, A.; Korkmaz, B.; Bromme, D.; Aucagne, V.; Delmas, A.; Lalmanach, G. Substrate-derived triazolo- and azapeptides as inhibitors of cathepsins K and S. *Eu. J. Med. Chem.* **2018**, *144*, 201-210.

[38] Proulx, C.; Picard, E.; Boeglin, D.; Pohankova, P.; Chemtob, S.; Ong, H.; Lubell, W. D. Azapeptide analogues of the growth hormone releasing peptide 6 as cluster of differentiation 36 receptor ligands with reduced affinity for the growth hormone secretagogue receptor 1a. *J. Med. Chem.* **2012**, *55*, 6502-6511.

[39] Sabatino, D.; Proulx, C.; Klocek, S.; Bourguet, C.; Boeglin, D.; Ong, H.; Lubell, W. D. Exploring side-chain diversity of submonomer solid-phase aza-peptide synthesis. *Org. Lett.* **2009**, *11*, 3650-3653.

[40] Reynolds, C.; Hormann, R. Theoretical study of the structure and rotational flexibility of diacylhydrazines: Implications for the structure of nonsteroidal ecdysone agonists and azapeptides. *J. Am. Chem. Soc.* **1996**, *118*, 9395-9401.

[41] Lee, H.; Jung, H.; Kim, J.; Park, H.; Lee, K. Conformational preference of azaglycine-containing dipeptides studied by PCM and IPCM methods. *Chem. Phys.* **2003**, *294*, 201-210.

[42] Lee, H. J.; Choi, K. H.; Ahn, I. A., The β-turn preferential solution conformation of a tetrapeptide containing an azaamino acid. *J. Mol. Struct.* **2001**, *569*, 43-54.

[43] Lee, H.; Lee, K.; Ahn, I.; Ro, S.; Choi, K.; Choi, Y. Role of azaamino acid residue in β-turn formation and stability in designed peptide. *J. Pept. Res.* **2000**, *56*, 35-46.

[44] Lee, H.; Park, H.; Lee, K. The β-turn scaffold of tripeptide containing an azapehenylalanine residue. *Biophys. Chem.* **2007**, *125*, 117-126.

[45] Thormann, M.; Hoffmann, H. Conformational properties of azapeptides. *Theochem.* **1999**, *469*, 63-76.

[46] For selected examples, see: A) Benatalah, Z.; Aubry, A.; Boussard, G.; Marraud, M. Evidence for a β-turn in an azadipeptide sequence: Synthesis and crystal structure of $Bu^tCO$-Pro-AzaAla-$NHPr^i$. *Int. J. Pept. Protein. Res*. **1991**, *38*, 603–605. B) Marraud, M.; Aubry, A. Crystal structures of peptides and modified peptides. *Pept. Sci.* **1996**, *40*, 45–83. C) Lecoq, A.; Boussard, G.; Marraud, M.; Aubry, A. Crystal state conformation of three azapeptides containing the azaproline residue, a β-turn regulator *Biopolymers* **1993**, *33*, 1051–1059. D) Didierjean, C.; Aubry, A.; Wyckaert, F.; Boussard, G. Structural features of the pip/azpip couple in the crystalline state: influence of the relative azpip location in an azadipeptide sequence upon the induced chirality and conformational characteristics. *J. Pept. Res.* **2000**, *55*, 308-317. E) Che, Y.; Marshall, G. R. Impact of azaproline on peptide conformation. *J. Org. Chem.* **2004**, *69*, 9030-9042.

[47] For aza-Glycine substitution inducing collagen hyperstability, see: A) Zhang, Y.; Malamakal, R.; Chenoweth, D. Aza-glycine induces collagen hyperstability. *J. Am. Chem. Soc.* **2015**, *137*, 12422-12425. B) Zhang, Y.; Herling, M.; Chenoweth, D. General solution for stabilizing triple helical collagen. *J. Am. Chem. Soc.* **2016**, *138*, 9751-9754. C) Kasznel, A.; Zhang, Y.; Hai, Y.; Chenoweth, D. Structural basis for aza-glycine stabilization of collagen. *J. Am. Chem. Soc.* **2017**, *139*, 9427-9430.

**CHAPTER 2**

# Synthesis of azapeptide model systems

## 2.1 Choosing the model systems and substitutions to analyze

Since the structural effects of aza-amino acid substitutions in β-hairpins are unknown, it was important to have a series of model systems varying in stability to study the (de)stabilizing effects of the aza-substitution. It was also our intention to choose a model system that allowed quick analysis using 1D NMR analysis. We also wanted to be able to easily synthesize the required aza-amino acid building block (*N*-Fmoc-*N*'-alkyl carbazate) of the residue at the third position of the model peptide(s).

With that in mind, three sequences were selected as starting points, previously studied by Waters *et al.* (Figure 2.1a, peptides **1a**, **2a**, and **3a**). [1-2] In these systems, an Asn-Gly turn motif is utilized to allow for easy and reliable hairpin formation calculations using glycine-splitting measurements. Through a single modification at the 2 position, the peptide β-hairpin stability was found to go from a 51% folded state (Figure 2.1a, peptide **1a**, $Phe^2$) to 77% folded (Figure 2.1a, peptide **2a**, $Trp^2$).[1] In a separate study aimed at creating β-hairpin peptides that recognize and bind ATP, Waters *et al.* was able to increase β-hairpin stability to 96% in solution by enhancing diagonal side-chain cation-π interactions (Figure 2.1a, peptide **3a**).[2] Between these three systems, we have a series of comparable models that are 51%, 77%, and 96% folded through minor structure modifications. The final model peptide (Figure 2.1a, peptide **4a**) is the original β-hairpin model system proposed by Gellman *et al.* that incorporates a D-Pro-Gly turn sequence.[3] This sequence exhibits a folding state of 75%. Additionally, valine is found in the 3 position of all peptides, and the corresponding *N*'-

isopropyl-fluorenylmethyl carbazate building block required to access aza-Val is synthetically simple compared to other side-chains (Scheme 2.2).

Aza-valine was thus incorporated into all peptide sequences at the third position, situated in the middle of the upper β-strand at a hydrogen-bonded site, to give peptides **1b**, **2b**, **3b,** and **4b** (Figure 2.1a). In order to separately analyze the effects of aza-valine's adaptive chirality and hydrogen-bonding properties, further control sequences were synthesized for peptides **2a** and **4a**, each exhibiting 75-77% folding states. D-Valine[3] analogs were pursued to gain an understanding on the effects of amino acid chirality on β-hairpin stability (Figure 2.1a, peptides **2c**, **4c**). Removal of the isopropyl group eliminates the steric effects in aza-glycine analogs (Figure 2.1a, peptides **2d**, **4d**). It also introduces an additional hydrogen-bonding partner (NαH), which was previously shown to lead to hyperstable collagen mimetics,[4] as well as stabilize the 180$^{o}$ rotamer in diformylhydrazine *via* intramolecular hydrogen-bonding.[5] However, potentially important cross-strand side-chain interactions are lost.[6] As a direct comparison, the azaGly[3] analogs required to be tested against their natural controls, possessing a glycine residue at the third position (Figure 2.1a, peptides **2e**, **4e**). In all cases, it is important to note that the hydrogen bonding properties of the semicarbazide may not be able to compensate for the preferred twisted backbone conformation observed in many previously studied azapeptides.[7] Finally, appropriate negative controls were also synthesized (Figure 2.1b, peptides **5a-b**, **6**, **7a–b**, **8**), which contain heptamers corresponding to the upper and bottom β-strands and an analog with an L-Pro-Gly turn motif.

a) β-hairpin peptides and azapeptides under study

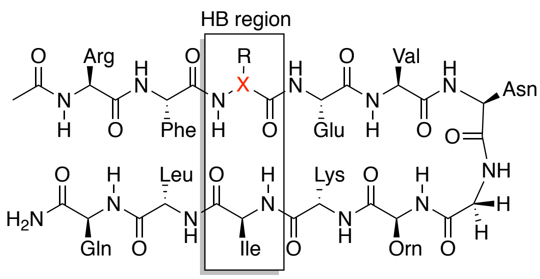


**1a:** X= CH, R = *i*Pr (L-Val)
**1b:** X = N, R = *i*Pr (aza-Val)

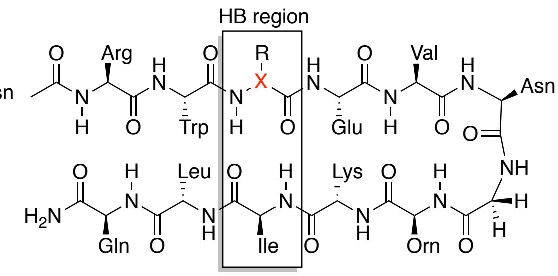


**2a:** X= CH, R = *i*Pr (L-Val)
**2b:** X = N, R = *i*Pr (aza-Val)
**2c**: X =CH, R = *i*Pr (D-Val)
**2d:** X = N, R = H (aza-Gly)
**2e:** X = C, R= H (Gly)

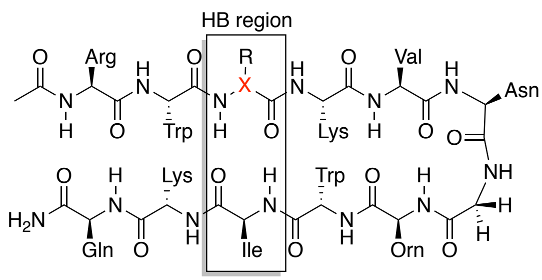


**3a:** X= CH, R = *i*Pr (L-Val)
**3b:** X = N, R = *i*Pr (aza-Val)

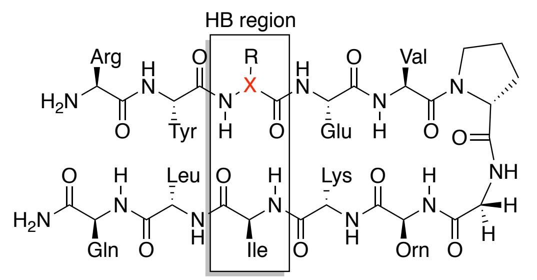


**4a:** X= CH, R = *i*Pr (L-Val)
**4b:** X = N, R = *i*Pr (aza-Val)
**4c:** X= CH, R = *i*Pr (D-Val)
**4d:** X = N, R = H (aza-Gly)
**4e:** X = C, R= H (Gly)

b) Control sequences synthesized

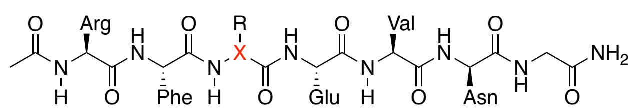


**5a:** X= CH, R = *i*Pr (L-Val)
**5b:** X = N, R = *i*Pr (aza-Val)

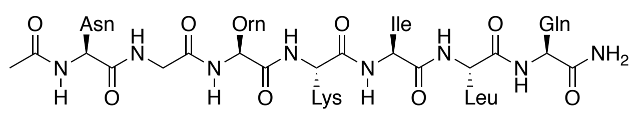


**6**

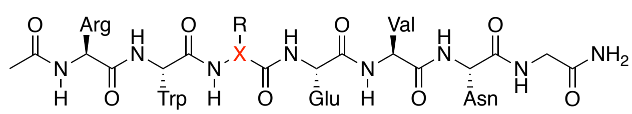


**7a:** X= CH, R = *i*Pr (L-Val)
**7b:** X = N, R = *i*Pr (aza-Val)

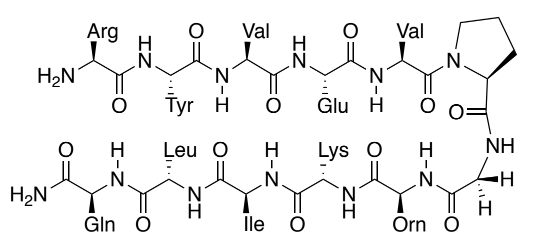


**8**

**Figure 2.1.** Peptide library created for the analysis of aza-substitution in model β-hairpin systems.

## 2.2 Solid Phase Peptide Synthesis (SPPS) of "difficult peptides"

Since the development of solid phase peptide synthesis by Merrifield in 1963,[8] considerable research has gone into improving and expediting the synthetic process.[9] Alternative activating reagents,[10] more effective protecting groups,[11] various solid supports,[12] and even automation of the synthesis[13] has expedited the process significantly. While the majority of advancements are focused on the synthetic process of amino acid coupling reactions, sequence effects and on-resin secondary structure formation/aggregation has been studied far less. The formation of secondary structures or growth of sequences prone to aggregation can stunt reaction progress and lead to incomplete couplings and heterogeneous sequences on solid support. Such sequences are referred to as 'difficult sequences.'[14] In particular, β-sheet and β–hairpin structures have historically shown to be especially prone to self-association and aggregation in solution, and such tendencies can hinder their synthesis on solid support.[15] In this thesis, the synthesis of β-hairpin model systems and their azapeptide derivatives required optimization of nearly every step of synthesis to accommodate for the slowed reactivity due to steric hindrance and inter-strand association on solid support.

## 2.3 Synthesis and incorporation of aza-amino acids

The synthesis of azapeptides involves hydrazine chemistry. Typically, hydrazine is first subjected to protecting group installation on one of the two nitrogen, followed by reductive amination chemistry to install the desired side-chain functional group and give an *N*'-alkyl carbazate building block such as **11** (Scheme 2.1).[16] This building block is then either a) activated with a "carbonyl donor" such as carbonyldiimidazole (CDI), bistrichloromethyl carbonate (BTC), or phosgene to give an acylated reactive species **12** that is added to the resin-bound growing peptide **9** (Figure 2.2a), or b) directly added to a pre-activated resin-bound carbamyl chloride (**14**) or isocyanate (**15**) intermediate, obtained *via* on-resin activation of the peptide *N*-terminus using similar "carbonyl donor" reagents (Figure 2.2b).[17]

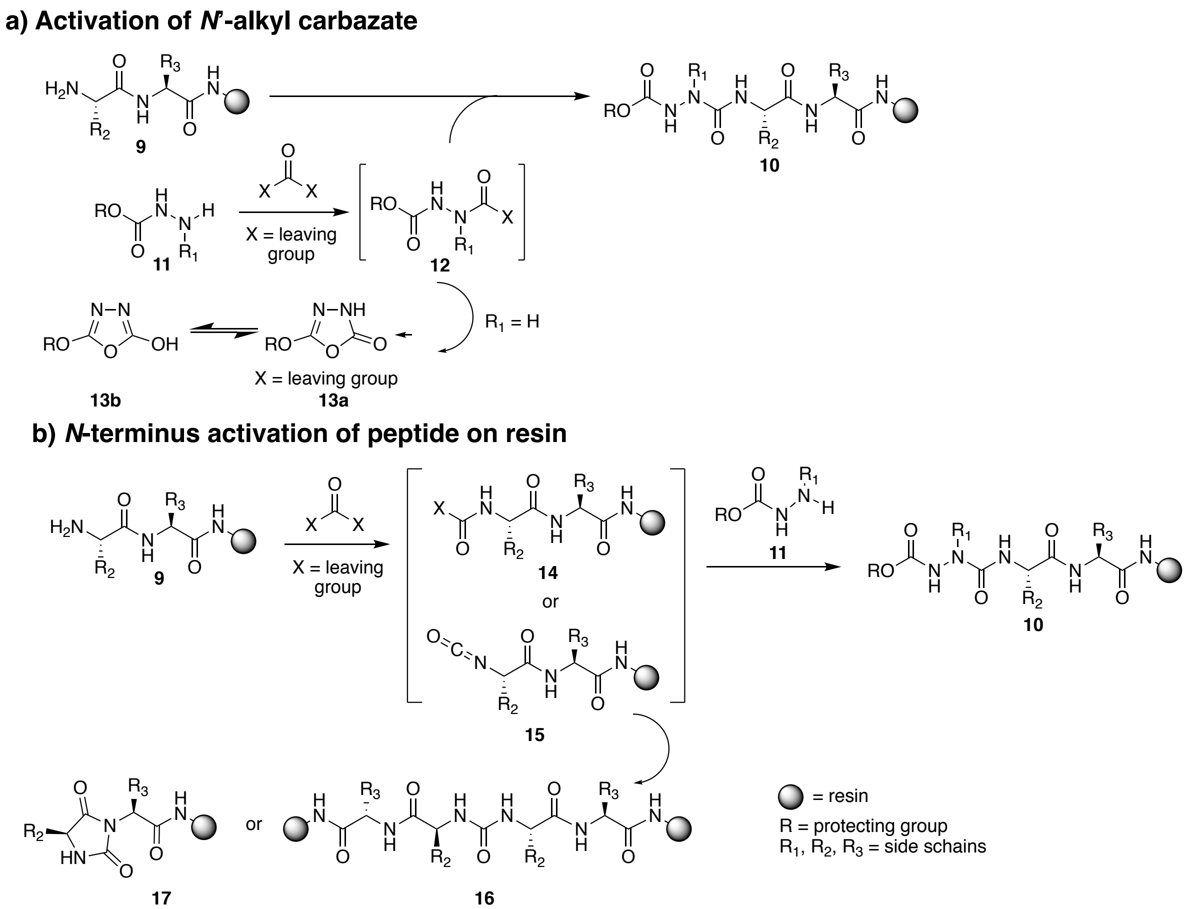


**Scheme 2.1.** Azapeptide synthesis methods through a) solution phase activation of *N*'-alkyl carbazate building blocks, and b) *N*-terminus peptide activation followed by addition of *N*'-alkyl carbazates.

Activation of the *N*-terminus of a peptide on solid phase has inherent complications (Figure 2.2b). For example, side products such as hydantoin **17** and symmetric urea **16** are often formed *via* an intramolecular nucleophilic attack by the preceding amide residue and an adjacent peptide strands, respectively. The latter byproduct happens more frequently on high-loading resin (> 0.4 mmol/g). Solution phase activation of the protected hydrazide building block (**11**) prevents the formation of these byproducts; however, in the case of aza-glycine synthesis in particular, formation of oxadiazolone **13 a** and **b** has been observed.[18,19] For this thesis, method A in Figure 2.2 proved to be the most reliable method for the incorporation of aza-valine onto the resin-bound peptide.

### 2.4 *N*'-isopropyl-fluorenylmethyl carbazate synthesis

In order to couple aza-valine using Fmoc-based solid phase peptide chemistry, the *N*'-isopropyl-fluorenylmethyl carbazate (**21**) precursor needed to be made (Scheme 2.2). Synthesis of the hydrazide proceeded through the treatment of hydrazine hydrate with Fmoc-chloride to first form *N*-Fmoc-hydrazine **20** in 98% yield after precipitation and filtration. Condensation with acetone followed by reduction of the imine intermediate with sodium cyanoborohydride gave the desired *N*'-isopropyl-fluorenylmethyl carbazate **21** in 59% yield in gram scale (Scheme 2.2).

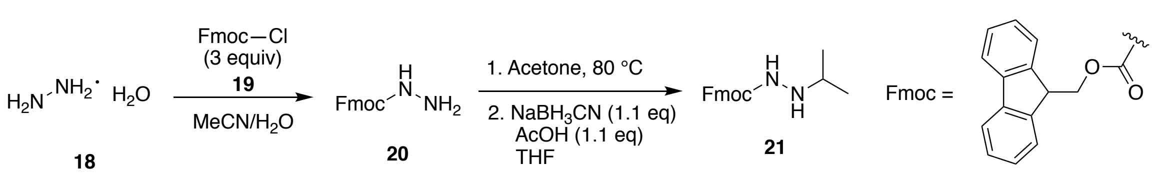


**Scheme 2.2.** Synthesis of *N*'-isopropyl-fluoren-9-ylmethyl carbazate **21.**

For the condensation step, literature protocols generally call for one equivalent of aldehyde or ketone.[16] While cost and solubility may be limiting the use of excess reagents, acetone in this case is a cheap reagent that the hydrazide solvated in readily. In order to maximize the yield of the reaction, it was thus used as the solvent.

## 2.5 Optimization of aza-amino acid incorporation

*Aza-Valine addition*

Historically, reagents such as carbonyldiimidazole (CDI),[20] phosgene,[21] BTC,[22] and *bis*(pentafluorophenyl) carbonate[23] have been utilized to activate *N*'-alkyl carbazate building blocks prior to adding them to a pre-swelled resin-bound peptide. For example, aza-valine in particular was incorporated in a Cilengitide analog, *cyclo*[R-G-D-f-azaV], using phosgene to activate *N*'-isopropyl-fluorenylmethyl carbazate.[24]

For this research, to optimize the incorporation of aza-valine onto our β-hairpin mimetic sequences, three activating agents were screened: CDI[4b,20], *bis*(trichloromethyl) carbonate (BTC, triphosgene)[16,22], and *p*-nitrophenyl chloroformate[25] (Table 2.1). Procedures of carbazate activation with the selected activating agents were based off of past literature. BTC was used in place of phosgene for safety and ease of handling. To avoid issues with on-resin aggregation in longer sequences, we first chose to optimize the introduction of aza-valine onto a tetramer (**22**), which would undergo further elongation to give the random coil negative control peptides **5b** and **7b** (Figure 2.1).

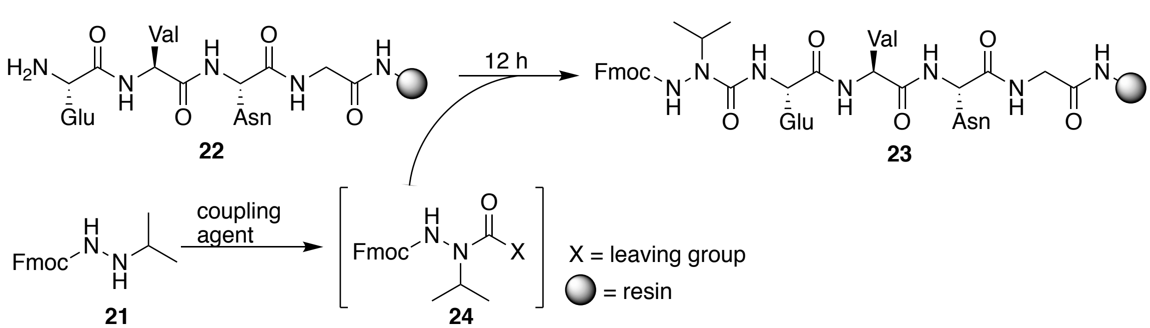


**Scheme 2.3.** Coupling aza-Valine on tetramer, EVNG, with varying activating agents.

**Table 2.1.** Optimization of of *N'*-isopropyl-Fmoc carbazate activation and coupling.

| Activating agent | Equivalents of activating agent | Base | Temperature of activation | Percent coupling |
|---|---|---|---|---|
| BTC | 1 | DIEA | 0 °C to RT | 83 |
| *p*-nitrophenyl chloroformate | 3 | DIEA | 0 °C to RT | 0[a] |
| CDI | 3 | NA | RT | 25[a] |

[a]the major by-products were isocyanate and symmetric urea (dimerization) formation.

Using LCMS analysis to monitor the progress of the reactions, BTC was found to be the best coupling agent, giving 83% conversion to the aza-valine-coupled product through a single overnight coupling. Upon a second overnight coupling reaction, near complete conversion to the desired aza-pentapeptide (**23**) was observed with minimal (< 10%) formation of side products. In contrast, coupling with CDI gave many side reactions and a low overall yield (25%) to the desired product, and *p*-nitrophenyl chloroformate showed no aza-valine incorporation. Both CDI and *p*-nitrophenyl chloroformate led to the formation of hydantoin (**27**) and symmetric urea (**28**) as major by-products characteristic of on-resin, *N*-terminus peptide activation (Schemse 2.1b and 2.4). This indicates a lack of reactivity between *N*'-isopropyl-fluoren-9-ylmethyl carbazate **21** and these coupling agents in solution. Beyond the test EVNG tetrapeptide sequence used for our optimization studies, this method was successfully applied for aza-valine incorporation in azapeptide sequences **1b**, **2b**, **3b**, and **4b**.

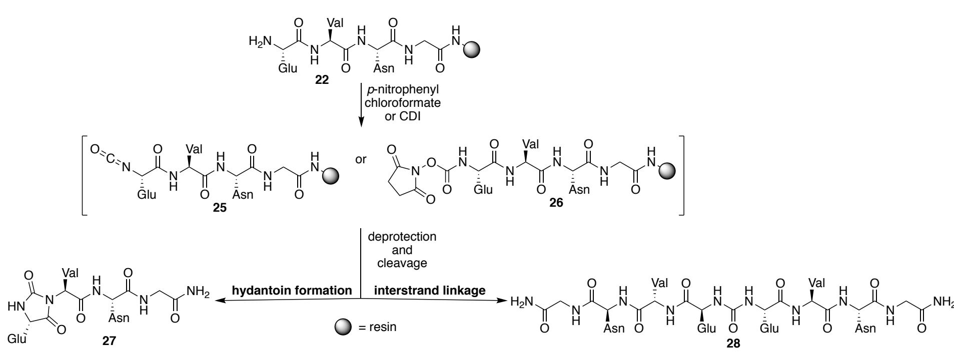


**Scheme 2.4.** Side reactions observed during aza-Val coupling with CDI and *p*-nitrophenyl chloroformate.

*Aza-Glycine addition*

The incorporation of aza-glycine on resin required alternative coupling methods compared to aza-valine. While BTC was found to be optimal for azaVal addition, the use of BTC while incorporating azaGly led to significant production of side reactions. It was previously shown that activation of Fmoc-hydrazine with phosgene leads to the formation of a unique oxadiazalone intermediate (Scheme 2.1, compound **13**), which is not observed upon activation of other *N*'-substituted aza-amino acid precursors.[18,19] In earlier studies, this heterocycle was found to readily ring-open during coupling to the *N*-terminus of resin-bound peptides to provide azaGly-terminated peptides in good conversions.[19] In later studies, however, ring-opening of this oxadiazalone proved to be sluggish,[18] demonstrating that this reaction is likely sequence-dependent.

Recently, a series of azaGly-containing peptides were synthesized *via* the activation of a growing-peptide chain on solid support with disuccinimidyl carbonate (DSC), followed by treatment of the resin with a solution of 60% hydrazine hydrate in DMF (Scheme 2.5). This simplified method was appealing because of the commercial availability of the DSC activating agent and hydrazine. The lack of the Fmoc-protecting group also removes the need for synthetic protection/deprotection procedures both in solution and on solid-phase, respectively. Surprisingly, the authors reported complete suppression of the hydantoin byproducts using this method, which inspired us to try this procedure for aza-glycine incorporation into our β-hairpin model peptides.[26]

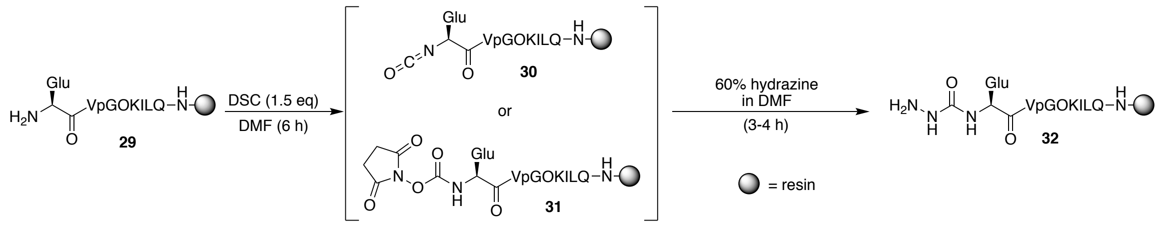

**Scheme 2.5.** DSC activation of solid phase peptide and hydrazine condensation to create N terminal azaGly.

Unfortunately, using EVpGOKILQ as a test peptide sequence, we observed significant amounts of side-products as well as reproducibility issues using this method. Ultimately, we abandoned this route and went back to a more traditional approach involving activation of an Fmoc-protected hydrazine building block. We did, however, adopt the use of DSC as activating agent to obtain our desired azaGly-containing peptides in good (80-90%) conversions (Scheme 2.6), eventually yielding unacetylated azapeptides **2d** and **4d**. Of note, it is unknown whether activation of Fmoc-carbazate with DSC in this manner also leads to the formation of an oxadiazalone intermediate, similarly to what has been observed using phosgene as the activating agent.

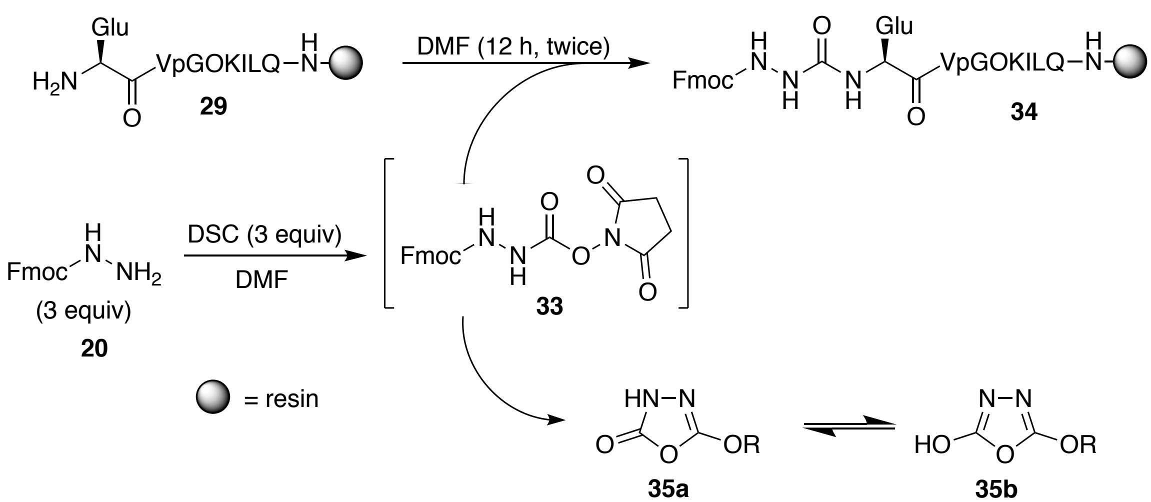

**Scheme 2.6.** Fmoc protected hydrazide activation with DSC and coupling onto solid phase.

## 2.6 Optimization of amino acid coupling onto terminal aza-residues

The decreased nucleophilicity of aza-amino acid residues, coupled with slower coupling rates due to aggregating peptides on solid phase, caused coupling onto aza-amino acids to be sluggish and gave opportunity for the accumulation of side products during coupling. Optimization of this coupling procedure was therefore also required to expedite the coupling process and minimize side reactions (Table 2.2). To do so, rather than focusing on shorter negative control sequences, we tackled the more challenging synthesis of Fmoc-F-aza-V-EVNGOKILQ, one residue away from the completed β-hairpin model 12-mer **1b**.

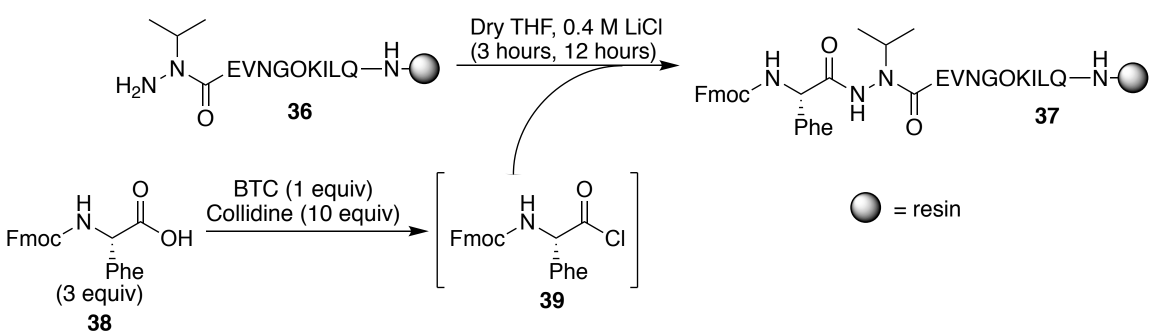


**Scheme 2.7.** Coupling Phe onto an N-terminal aza-Val.

**Table 2.2.** Optimization of phenylalanine coupling to aza-V-EVNGOKILQ.[a]

| Entry | # of base equiv. | Activation temp. | LiCl (0.4 M) additive | Time of LiCl addition | % coupling | % uncoupled | % isocyanate formation | % impurities before coupling[b] |
|---|---|---|---|---|---|---|---|---|
| 1 | 14 | RT | No | - | 19 | 31 | 8[c] | 18 |
| 2 | 10 | 0 °C to RT | No | - | 20 | 62 | 8 | 10 |
| 3 | 10 | 0 °C to RT | Yes | During activation | 0 | 54 | 0 | 46 |
| 4 | 10 | 0 °C to RT | Yes | After activation | 45 | 37 | 6 | 12 |
| 5 | 10 | 0 °C to RT | Yes[d] | After Activation | 62 | 5 | trace | 33 |

[a]Coupling proceeded for 3 hours, then the resin was drained and washed to remove reagent, and the coupling was repeated for 12 hours. [b]Coupling was performed on crude material in separate batches of resin. Percentages based off of absorbance at 214 nm in crude LCMS traces. [c]Further production of side products were found, but not identifiable. [d]Resin was pre-saturated with 0.4 M LiCl.

BTC has been used successfully in the past[16] to give *N*-Fmoc-amino acid chlorides *in situ* in the presence of excess base (2,4,6-collidine) in THF, which coupled onto resin-bound *N*-terminal aza-amino acid residues in good conversions. In our case, it proved to be an effective activating agent, but side reactions developed when activating the Fmoc-amino acid at room temperature (Table 2.2, entry 1), which was consistent with previous reports.[24] The activation method was adjusted to activate the amino acid at 0 °C and side reactions were reduced significantly (Table 2.2, entry 2). In order to increase the rate of coupling, LiCl was added to the coupling solution. Chaotropic salts have been proven to disrupt the secondary structure and decrease aggregation on solid phase to allow couplings to proceed more efficiently.[27] Interestingly, we found that the order of addition is crucial. When LiCl was added to the Fmoc-Phe-OH solution during the preactivation with BTC, no product was detected (Table 2.2, entry 3). In contrast, when LiCl was added to the resin after the preformed Fmoc-Phe-Cl had been added to the resin, the coupling proceeded as expected (Table 2.2, entry 4). Pre-swelling the resin in 0.4 M LiCl in THF proved to be beneficial to the coupling of Fmoc-Phe-OH as well (Table 2.2, entry 5).

*Sequence effects during coupling onto aza-amino acid residues*

The synthesis of azapeptide analogs **2b** and **3b** required coupling of an Fmoc-Trp(Boc)-OH amino acid onto a resin-bound, *N*-terminal aza-valine residue. In a recent study, the coupling kinetics of a series of natural amino acids (Gly, Ala, Leu, Val, Ile, Phe, Arg) onto an aza-alanine residue were monitored, using COMU as the activating agent.[28] This study reported that coupling of a more sterically hindered isoleucine residue was ~28 fold slower than the coupling of glycine onto resin-bound azaAla-Phe-$NH_2$. In our hands, we found the steric bulk of the amino acid to be coupled onto the aza-amino acid to greatly impact of the rate of coupling as well, with noticeable differences when coupling Fmoc-Phe-OH *vs* Fmoc-Trp(Boc)-OH onto azaV-EVNGOKILQ-$NH_2$ (Table 2.2, entry 4 vs Table 2.3, entry 1). In addition, when Fmoc-Trp(Boc)-OH was coupled to an aza-Val *vs* aza-Gly residues, the amino acid coupling to aza-Gly consistently afforded the desired product in greater conversions (Table 2.3). Moreover, sequence length affected overall conversions, where the formation of secondary structure on resin was likely responsible for decreased coupling efficiencies in longer sequences. When comparing identical coupling reactions performed on pentapeptides *vs* decapeptides containing a turn sequence to induce hairpin formation, couplings were much more efficient on the shorter sequences (71 and 87%, Table 2.3, entries 2 and 4) compared to the elongated strands (32 and 76%, Table 2.3, entries 1 and 3).

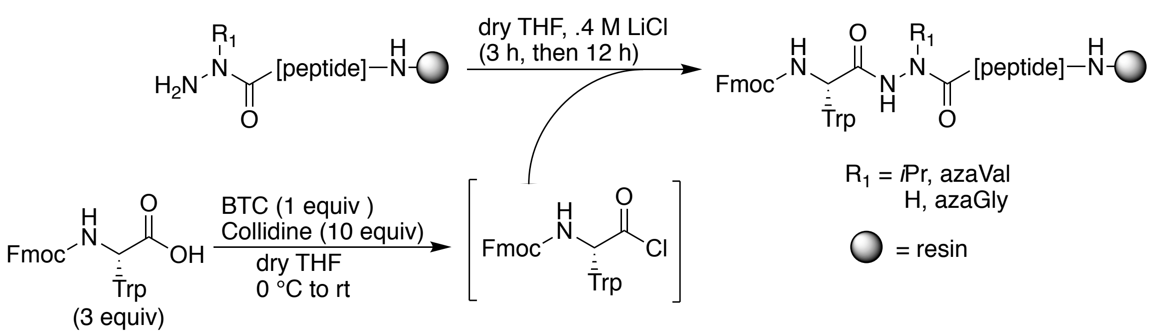


**Scheme 2.8.** General protocol of coupling Trp onto a terminal aza-residue (aza-Val or aza-Gly) with various peptide sequences (see table 2.3).

**Table. 2.3.** Comparative coupling conversions of Fmoc-Trp(Boc)-OH onto azaVal- and azaGly-terminated peptides.

| Entry | Peptide | % coupling[a] | % uncoupled | % side products | % impurities before coupling |
|---|---|---|---|---|---|
| 1 | $H_2N$-[azaV]EVNGOKILQ-$NH_2$ | 32[b] | 33 | 35 | 23 |
| 2 | $H_2N$-[azaV]EVNG-$NH_2$ | 71 | 14 | 15 | 17 |
| 3 | $H_2N$-[azaG]EVNGOKILQ-$NH_2$ | 76 | trace[c] | 24 | 19[d] |
| 4 | $H_2N$-[azaG]EVNG-$NH_2$ | 87 | trace[c] | 13 | 11[d] |

[a]Coupling method performed with LiCl(.4 M) additive for 3h, then repeated overnight. [b]After two additional nights of coupling, the reaction would not proceed beyond 52%. [c]N-terminal aza-glycine was found to degrade upon purification. Artifacts of degradation may be counted in side products. [d]Analysis for the purity of starting material in terminal aza-Gly analogs required the Fmoc group to protect the N-terminal aza-Gly from degredation.

## 2.7 Further complications in synthetic procedures

*Further peptide elongation*

While coupling of the last amino acid (Fmoc-Arg(pbf)-OH), was performed using standard solid phase peptide synthesis procedures (HBTU, DIEA), the effects of peptide aggregation were still present and coupling of the final amino acid occasionally required an additional coupling to ensure complete amino acid addition. LiCl was also consistently added to the amino acid coupling reactions after the aza-amino acid incorporation in attempts to improve overall yields in the synthesis of these difficult sequences.

*Fmoc deprotection on aggregating peptides*

20% Piperidine in DMF is commonly used for Fmoc deprotection on solid phase to expose the primary *N*-terminus for elongation.[29] It has, however, been proven that piperidine is not always the ideal base to remove the Fmoc group in aggregating peptide sequences.[30] Bases such as piperazine, 1-hydroxypiperidine, 1,8-diazabicyclo-[5.4.0]undec-7ene (DBU), and tetra-n-butylammonium fluoride (TBAF) have been shown to function as alternative bases to remove the Fmoc protecting group, but sometimes at the cost of side reactions, especially when the peptide is in the presence of base for extended periods.[31,32] For my synthesis, difficulties in Fmoc deprotections would happen sporadically after the incorporation of the β-turn motif. In order to counteract incomplete deprotection, DBU was incorporated into the deprotection solution along with piperidine to give a 2:2:96 v/v/v solution of DBU/piperidine/DMF.[33] In conjugation, the combined bases were able to deprotect the Fmoc groups completely.

However, due to the incorporation of a stronger base, the peptide became susceptible to base-catalyzed side reactions, such as intramolecular backbone *N*H cyclization onto asparagine and glutamic acid side-chains to form succinimide and pyroglutamate by-products, respectively (Figure 2.2).[34] Although slow, peptides in the presence of base for extended times will gradually cyclize in an irreversible reaction, ultimately lowering the purity of the crude peptide and complicating purification becuause these side products often co-elute with the desired peptide during HPLC analysis.

Both side reactions were seen during the synthesis of peptides containing these amino acids while using DBU as an Fmoc deprotecting agent. Using standard resin washing procedures (3 x 1 mL DMF), DBU was found to remain in the resin matrix in trace amounts as detected by LCMS analysis, and slowly cause cyclization events to occur on the peptide. Succinimide formation would occur at any point after asparagine incorporation, but pyroglutamate formation was only seen as the glutamic acid was deprotected as the N-terminus residue.

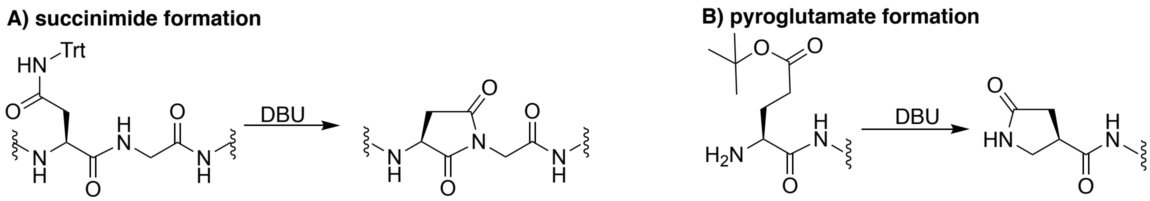


**Figure 2.2.** The formation of succinimide from asparagine (left) and the formation of pyroglutamate from glutamic acid (right).

While the final peptides could not be separated from these by-products using HPLC, washing the resin more thoroughly (2 x 1 mL DMF, MeOH, then DCM) following DBU treatment was found to suppress these cyclization reactions. The use of DBU to completely remove the Fmoc Protecting group before each coupling step is a powerful and important tool to ensure the entire coupling of each amino acid, but care has to be taken to remove all DBU from the resin after each Fmoc deprotection to ensure that lingering base will not compromise the final peptide purity.

For the synthesis of the peptide library, the Fmoc deprotection procedure utilizing only piperidine was used for peptide models **1** and **2**, but the use of DBU was incorporated for all Fmoc deprotections on model systems **3** and **4**, with thorough resin washing after each DBU treatment.

*Acetylation of azaGly containing peptides*

The synthesis of peptides **1a-b**, **2a-e**, **3a-b**, and the corresponding negative controls required acetylation of the *N*-terminus. Surprisingly, while acetylation of the natural and azaVal variants of these peptide analogs proceeded without issue, every attempt to acetylate azaGly-containing peptides failed to provide the expected products and we were unable to make azapeptide **2d**. Model peptide **4a**, with the D-Pro-Gly turn motif reported by Gellman *et* *al.*, lacks an acetyl group at the *N*-terminus. This allowed the synthesis, purification, and comparative analysis of its aza-glycine-containing analog, azapeptide **4d**.

*Failures of select sequences*

During the synthesis of the peptide library, no two analogs behaved the same. For some sequences, difficulties in synthesis or purification led to failure. As stated before, the acetylation of aza-Gly containing peptides failed (**2d**). With that, synthesis and analysis of peptide **2e** was also deemed unnecessary.

Further issues came about with co-eluents contaminating the product peptide during purification steps. During the synthesis of the 96% folded model system and its aza variant, (peptides **3a** and **b**) slowed and incomplete couplings caused by the aggregating peptides caused an accumulation of side products and ultimately led to byproducts eluting with the desired peptide, giving the final product in 47% purity (**3b**), or leading to purification with no discernable yield or purity (**3a**).

A final issue to be acknowledged was the varying solubility of the different peptides. While the overall peptide was designed to be optimal for solubility and prevent aggregation, the truncated strand segments (**5a**-**b**, **6, 7a-b**) did not maintain the same characteristics. Peptide **5a** and **b** proved to be exceedingly difficult to solvate in acetonitrile/water mixtures required for HPLC purification. While the aza-variant (**5b**) ultimately was able to go into solution for purification steps, the natural variant **5a** proved impossible and was left in its crude state.

## 2.8 Characterization of the peptide/azapeptide library

The synthesis of peptides analyzed in this thesis can be summarized in Table 2.4 in which all peptides are characterized with yields in their crude and purified forms.

**Table 2.4.** Characterization of peptide library.

| peptide | crude yield[a] | crude purity[a] | yield[a] | purity | m/z (cald) $[M+1]^+$ | m/z (obsd) $[M+1]^+$ | retention time[b] (min) |
|---|---|---|---|---|---|---|---|
| **1a** Ac-RFVEVNGOKILQ-$NH_2$ | 70.1 | 38.7 | 27.4 | >99 | 1457.9 | 1458.1 | 8.36 |
| **1b** Ac-RF**azaV**EVNGOKILQ-$NH_2$ | 40.7 | 35.5 | 7.4 | 84.9 | 1458.9 | 1459.1 | 8.69 |
| **2a** Ac-RWVEVNGOKILQ-$NH_2$ | 63 | 43 | 4.5 | >99 | 1496.9 | 1497.1 | 8.47 |
| **2b** Ac-RW**azaV**EVNGOKILQ-$NH_2$ | 46 | 34 | 2.2 | 96 | 1497.9 | 1497.8 | 8.69 |
| **2c** Ac-RW**v**EVNGOKILQ-$NH_2$ | 53 | 61 | 12 | >99 | 1496.9 | 1497.1 | 8.81 |
| **3a** Ac-RWVKVNGOWIKQ-$NH_2$ | 57 | 59 | - | - | 1568.9 | 1569.1 | 7.687 |
| **3b** Ac-RW**azaV**KVNGOWIKQ-$NH_2$ | 42 | 24 | 3 | 47 | 1569.9 | 1570.2 | 8.437 |
| **4a** H-RYVEVpGOKILQ-$NH_2$ | 54 | 68 | 8.3 | >99 | 1414.9 | 1415.1 | 7.95 |
| **4b** H-RY**azaV**EVpGOKILQ-$NH_2$ | 58 | 36 | 7.4 | 95 | 1415.9 | 1416.2 | 8.19 |
| **4c** H-RYvEVpGOKILQ-$NH_2$ | 67.0 | 74.1 | 28.4 | >99 | 1414.9 | 1415.1 | 8.27 |
| **4d** H-RY**azaG**EVpGOKILQ-$NH_2$ | 53 | 43 | 7.6 | 89 | 1373.8 | 1374.2 | 7.80 |
| **4e** H-RY**G**EVpGOKILQ-$NH_2$ | 61.8 | 73.4 | 24.9 | >99 | 1372.8 | 1373.1 | 7.82 |
| **5a** Ac-RFVEVNG-$NH_2$ | 85 | 81 | - | - | 861.46 | 861.6 | 7.889 |
| **5b** Ac-RF**azaV**EVNG-$NH_2$ | 44.8 | 55.4 | 13.8 | >99 | 862.5 | 862.7 | 8.40 |
| **6** Ac-NGOKILQ-$NH_2$ | 78.8 | 77.0 | 29.5 | >99 | 827.5 | 827.7 | 7.27 |
| **7a** Ac-RWVEVNG-$NH_2$ | 87 | 30 | 9.2 | >99 | 900.5 | 900.7 | 8.38 |
| **7b** Ac-RW**azaV**EVNG-$NH_2$[c] | 64 | 58 | - | - | 901.46 | 901.7 | 8.351 |
| **8** H-RYVEVPGOKILQ-$NH_2$ | 64 | 64 | 12.8 | >99 | 1414.9 | 1415.1 | 7.94 |

[a]Yields are calculated based on resin loading. [b]Unless otherwise noted, analytical LCMS analyses were performed on a 5 µM, 150 x 4.6 mm C18 Vydac column from Mac-Mod Analytical, Inc (cat#218TP5415)with a flow rate of 0.5 mL/min using a 12 min 5-95% linear gradient of MeCN (0.1% TFA) in water(0.1% TFA). The purity at 214 nm wavelength is reported in all cases. [c]Product mass could not be found after purification.

## 2.9 REFERENCES

[1] Tatko, C. D.; Waters, M. L. Comparison of C-H•••π and Hydrophobic Interactions in a β-Hairpin Peptide: Impact on Stability and Specificity. *J. Am. Chem. Soc*. **2004**, *126*, 028-2034.

[2] Butterfield, S. M.; Waters, M. L. A Designed β-Hairpin Peptide for Molecular Recognition of ATP in Water. *J. Am. Chem. Soc.* **2003**, *125*, 9580-9581.

[3] Syud, F. A.; Espinosa, J. F.; Gellman, S. H. NMR-Based Quantification of β-Sheet Populations in Aqueous Solution through Use of Reference Peptides for the Folded and Unfolded States. *J. Am. Chem. Soc.* **1999**, *121*, 11577-11578.

[4] For aza-Glycine substitution inducing collagen hyperstability, see: A) Zhang, Y.; Malamakal, R.; Chenoweth, D. Aza-glycine induces collagen hyperstability. *J. Am. Chem. Soc.* **2015**, *137*, 12422-12425. B) Zhang, Y.; Herling, M.; Chenoweth, D. General solution for stabilizing triple helical collagen. *J. Am. Chem. Soc.* **2016**, *138*, 9751-9754. C) Kasznel, A.; Zhang, Y.; Hai, Y.; Chenoweth, D. Structural basis for aza-glycine stabilization of collagen. *J. Am. Chem. Soc.* **2017**, *139*, 9427-9430.

[5] Reynolds, C.; Hormann, R. Theoretical study of the structure and rotational flexibility of diacylhydrazines: Implications for the structure of nonsteroidal ecdysone agonists and azapeptides. *J. Am. Chem. Soc.* **1996**, *118*, 9395-9401.

[6] Wouters, M. A.; Curmi, P. M. An Analysis of Side Chain Interactions and Pair Correlations Within Antiparallel β-Sheets: The Differences Between Backbone Hydrogen-Bonded and Non-Hydrogen-Bonded Residue Pairs. *Proteins: Struct, Funct., Gen.* **1995**, *22*, 119-131.

[7] Thormann, M.; Hoffmann, H. Conformational properties of azapeptides. *Theochem.* **1999**, *469*, 63-76.

[8] Merrifield, R. B. Solid Phase Peptide Synthesis I. The Synthesis of a Tetrapeptide. *J. Am. Chem. Soc.* **1963**, *85*, 2149-2154.

[9] Chandrudu, S.; Simerska, P.; Toth, I. Chemical Methods for Peptide and Protein Production. *Molecules*. **2013**, *18*, 4373-4388.

[10] El-Faham, A.; Albericio, F. Peptide Coupling Reagents, More than a Letter Soup. *Chem. Rev.* **2011**, *111*, 6557-6602.

[11] Isidro-Llobet, A.; Alvarez, M.; Albericio, F. Amino Acid-Protecting Groups. *Chem. Rev.* **2009**, *109*, 2455-2504.

[12] Gongora-Benitez, M.; Tulla-Puche, J.; Albericio, F. Handles for Fmoc Solid-Phase Synthesis of Protected Peptides. *ACS Comb. Sci.* **2013**, *15*, 217-228.

[13] Made, V.; Els-Heindl, S.; Beck-Sickinger, A. G. Automated Solid-Phase Peptide Synthesis to obtain Therapeutic Peptides. *Beilstein J. Org. Chem.* **2014**, *10*, 1197-1212.

[14] Paradis-Bas, M.; Tulla-Puche, J.; Albericio, F. The Road to the Synthesis of "Difficult Peptides". *Chem. Soc. Rev.* **2016**, *45*, 631-654.

[15] Milton, R. C.; Milton, S. C.; Adams, P. A. Prediction of Difficult Sequences in Solid-Phase Peptide Synthesis. *J. Am. Chem. Soc.* **1990**, *112*, 6039-6046.

[16] Boeglin, D.; Lubell, W. D. Aza-Amino Acid Scanning of Secondary Structure Suited for Solid-Phase Peptide Synthesis with Fmoc Chemistry and Aza-Amino Acids with Heteroatomic Side Chains. *J. Comb. Chem.* **2005**, *7*, 864-878.

[17] Proulx, C.; Sabatino, D.; Hopewell, R.; Spiegel, J.; Ramos, Y. G.; Lubell, W. D. Azapeptides and their Therapeutic Potential. *Future Med. Chem.* **2011**, *3*, 1139-1164.

[18] Bourguet, C. B.; Sabatino, D.; Lubell, W. D. Benzophenone Semicarbazone Protections Strategy for Synthesis of Aza-Glycine Containing Aza-Peptides. *Biopolymers* **2008**, *90*, 824-831.

[19] Gibson, C.; Goodman, S. L.; Hahn, D.; Holzemann, G.; Kessler, H. Novel Solid-Phase Synthesis of Azapeptides and Azapeptoides via Fmoc-Strategy and its Application in the Synthesis of RGD-Mimetics. *J. Org. Chem.* **1999**, *64*, 7388-7394.

[20] Mhidia, R.; Melnyk, O. Selective Cleavage of an azaGly Peptide Bond by Copper (II). Long-Range Effect of Histidine Residue. *J. Pept. Sci.* **2010**, 16**,** 141-147.

[21] Freeman, N. Hurevich, M.; Gilon, C. Synthesis of N'-Substituted Ddz-Protected Hydrazines and their Application in Solid Phase Synthesis of aza-Peptides. *Tetrahedron* **2009**, *65*, 1737-1745.

[22] Frochot, C.; Vanderesse, R.; Driou, A.; Linden, G.; Marraud, M.; Cung, M. T. A Solid-Phase Synthesis of Three aza-, iminoaza- and Reduced aza-Peptides from the same Precursor. *Lett. Pept. Chem.* **1997**, *4*, 219-225.

[23] Han, H.; Janda, K. D. Azatides: Solution and Liquid Phase Syntheses of a New Peptidomimetic. *J. Am. Chem. Soc.* **1998**, *118*, 2539-2544.

[24] Spiegel, J.; Mas-Moruno, C.; Kessler, H.; Lubell, W. D. Cyclic aza-Peptide Integrin Ligand Synthesis and Biological Activity. *J. Org. Chem.* **2012**, *77*, 5271-5278.

[25] Sabatino, D.; Proulx, C.; Klocek, S.; Bourguet, C. B.; Boeglin, D.; Ong, H.; Lubell, W. D. Exploring Side-Chain Diversity by Submonomer Solid-Phase Aza-Peptide Synthesis. *Org. Lett.* **2009**, *11*, 3650-3653.

[26] Singh, S.; Shrivastava, R.; Singh, G.; Ali,; Ampapathi, R. S.; Bhadhuria, S.; Haq, W. AzaGly-Appended Peptidomimetics Structurally Related to PTR6154 as Potential PKB/Akt Inhibitors. *ChemBioChem.* **2017**, *18*, 1061-1065.

[27] Thaler, A.; Seebach, D. Lithium-Salt Effects in Peptide Synthesis. Part I. Conditions for the Use of Lithium-Salts in Coupling Reactions. *Helv. Chim. Acta.* **1991**, *74*, 617-627.

[28] Arujoe, M.; Ploom, A.; Mastitski, A.; Jarv, J. Influence of Steric Effects in Solid-Phase aza-Peptide Synthesis. *Tet. Lett.***2018**, *59*, 2010-2013.

[29] Luna, O. F.; Gomex, J.; Cardenas, C.; Albericio, F.; Marshall, S. H.; Guzman, F. Deprotection Reagents in Fmoc Solid Phase Peptide Synthesis: Moving Away from Piperidine? *Molecules* **2016**, *21*, 1542-1554.

[30] Dettin, M.; Pegoraro, S.; Rovero, P.; Bicciato, S.; Bagno, A.; Bello, C. SPPS of Difficult Sequences: A Comparison of Chemical Conditions, Synthetic Strategies and on-line Monitoring. *J. Pep. Res.* **1997**, *49*, 103-111.

[31] Wade, J. D.; Mathieu, M. N.; Macris, M; Tregear, G. W. Base-Induced Side Reactions in Fmoc-Solid Phase Peptide Synthesis: Minimization by use of Piperazine as $N^{\alpha}$-Deprotection Reagent. *Lett. Pept. Sci.* **2000**, *7*, 107-112.

[32] Enjalbal, C.; Maux, D.; Subra, G.; Martinez, J.; Combarieu, R.; Aubagnac, J. L. Monitoring and Quantification on Solid Support of a by-product Formation During Peptide Synthesis by Tof-SIMS. *Tet. Lett.* **1999**, *40*, 6217-6220.

[33] Park, J. H.; Waters, M. L. Positional Effects of Click Cyclization on β-Hairpin Structure, Stability, and Function. *Org. Biomol. Chem.* **2013**, *11*, 69-77.

[34] Wade, J.; Mathieu, M. N.; Macris, M.; Tregear, G. W. Base-induced side reactions in Fmoc-solid phase peptide synthesis: Minimization by the use of piperazine as $N^{\alpha}$-deprotection reagent. *Lett. Pep. Sci.* **2000**, *7*, 107-112.

## CHAPTER 3

# Conformational Analysis of Azapeptide Model Systems

### 3.1 Conformational analysis of azapeptides

In this thesis, the conformational analysis of the model systems are primarily based off of 1D NMR analysis, including Cα-proton downfield shifting (see equation 1, p. 4) in response to β-hairpin formation, and glycine's diastereotopic proton splitting (see equation 2, p. 5). The $\delta_{100}$ and $\Delta\delta_{Gly100}$ values used for our calculations were taken from previously reported, fully folded (cyclic) positive controls.[1,2] 1D NMR spectra can be found in Appendix A, and information on sample preparation and acquisition parameters can be found in the experimental section.

#### 3.1.1 Model peptides 1a-b, 2a-c.

A comparative analysis began using control peptide **1a**, which had previously been shown to exhibit 51% folding by Water *et al.* using glycine splitting analysis, and its azaVal$^3$-derivative **1b**. In our hands, the glycine splitting values observed for **1a** ($\Delta\delta_{GlyObs}$ = 0.23 ppm, 51% folding) closely matched the literature (Figure 3.1a).[2] Upon witnessing no glycine splitting in the 1D NMR spectrum for **1b** (Figure 3.1b), it was determined that aza-valine substitution at position 3 completely disrupted β-hairpin formation. With this preliminary data in hand, it was likely that azaVal$^3$ substitution on all other model peptides was going to have disruptive effects. However, to quantify the destabilizing effect, we needed to evaluate the impact of azaVal$^3$ substitutions in model peptides that exhibited higher (> 51%) β-hairpin stability in control sequences.

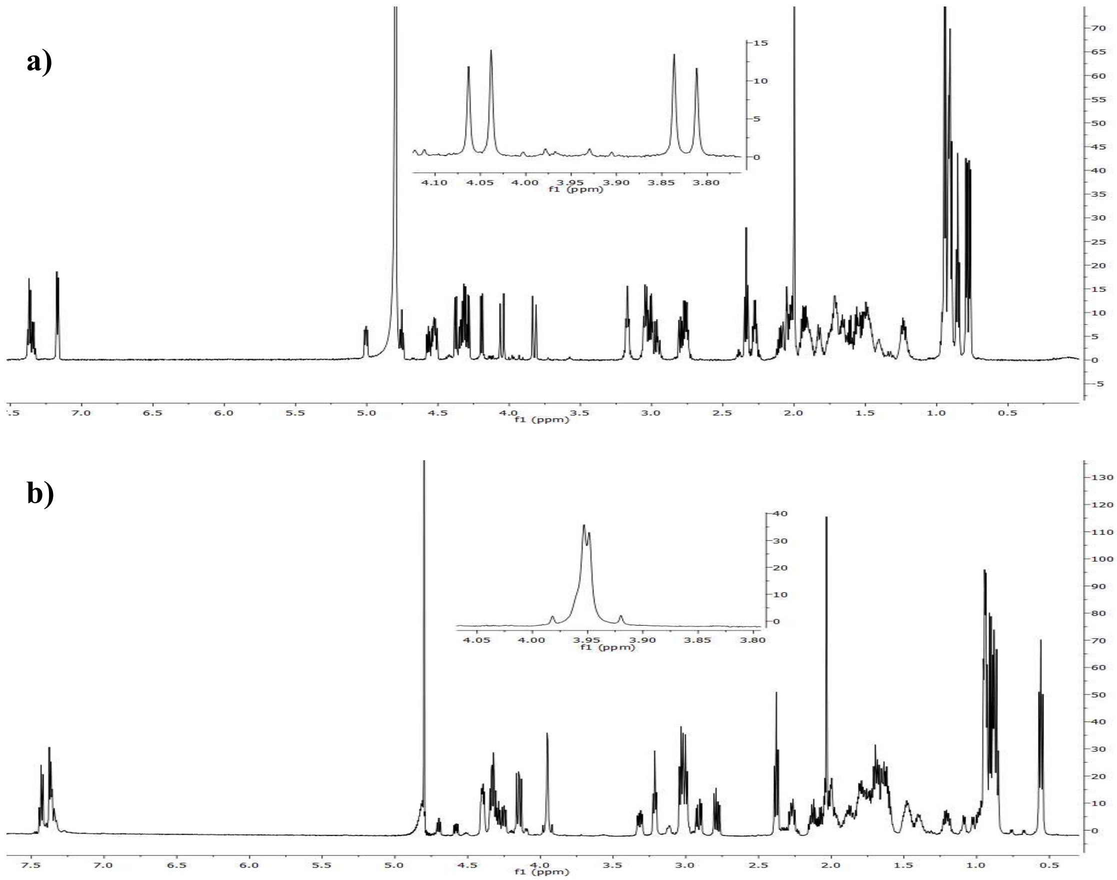


**Figure 3.1.** NMR analysis of a) peptide **1a** and b) peptide **1b**. Full spectra are shown with magnification on glycine peak. **1a** shows the splitting of the two α-hydrogens consistent with literature, while **1b** shows no separation.

NMR spectra for peptides **2a-c** were next obtained, with glycine splitting of the natural peptide derivative **2a** in accordance with the literature ($\Delta\delta_{GlyObs}$ = 0.34 ppm, 77% folding).[2] While it was found that the D-Val substitution in **2c** retained some – but a significant loss in – β-hairpin population ($\Delta\delta_{GlyObs}$ = 0.085 ppm, 19% folding), the aza-valine[3] substitution was found to once again completely disrupt the β-hairpin structure with no observed glycine splitting (Figure 3.2).

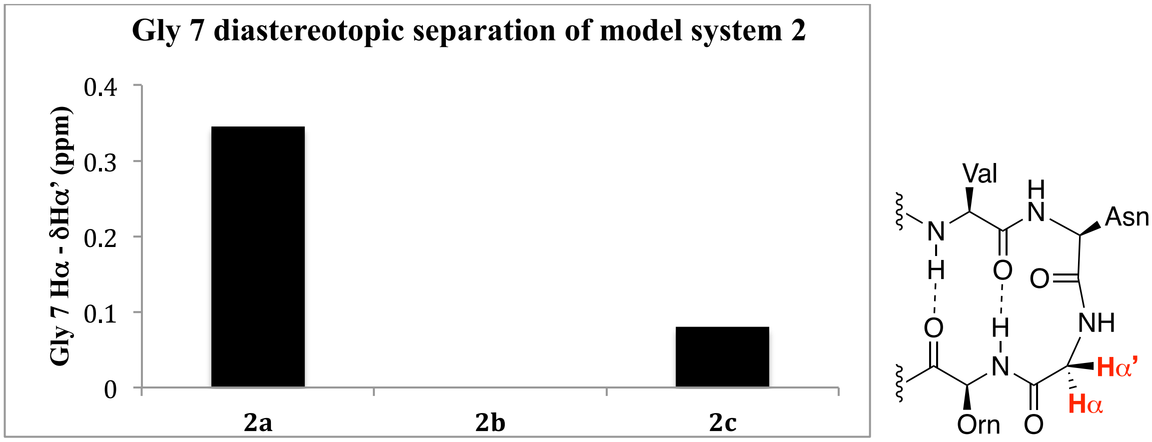


**Figure 3.2.** NMR analysis of glycines diastereotopic splitting (left) displays the extent of separation (in ppm) of the two glycine peaks (right) and serves as a direct representation of β-hairpin formation.

While the beneficial effects of D-amino acids in the turn region of β-hairpins are well known,[3] the effects of D-amino acid substitution in the β-strand segments have not been as rigorously studied. It has been shown that D-amino acid substitution in cyclic peptides displaying β-sheet formation disrupts the secondary structure in aqueous solution,[4] but little is known about the extent of secondary structure destabilization or the varying effects of different amino acids and their position within the β-sheet structure. Here we have shown and quantified the destabilizing effects of the stereo-inversion of valine in the β-strand segment of a β-hairpin. The destabilizing effects are presumably due to the loss of cross-strand side chain interactions between the valine[3] and cross-strand isoleucine[10], commonly seen in β-sheet formation.[5]

The adaptive chirality of the aza-amino acid means that it could adopt either L- or D-like chirality. However, the complete disruption of β-hairpin folding in aza-valine[3] analogs suggests that the destabilizing effect of aza-substitution goes beyond the loss of a defined chiral center. While the aza-residue may be stabilized by enhanced cross-strand hydrogen bonding interactions in the extended conformation, the local energetic penalty of eclipsing lone pairs may prevent aza-valine from adopting the necessary dihedral angles for β-hairpin formation. This penalty is greater than that of diacylhydrazine, or aza-glycine, since the substitution of the isopropyl side chain prevents additional hydrogen-bonding to occur and reduce the energy threshold of the extended conformation (Figure 3.2).

As previously discussed in Chapter 2, attempts to acetylate aza-Glycine-containing peptide analogs were unsuccessful. Thus, we were unable to compare the conformational impact of azaVal$^3$ *vs* azaGly$^3$ in this series. In addition, attempts to make peptide **3a**, which was previously shown to adopt a > 99% folded state by other groups,[6] as well its aza-Val$^3$ derivative (**3b**) failed to produce the desired peptides in good purity, which prevented NMR analyses.

### 3.1. 2 Model peptide 4a-e

Model peptide **4** was next analyzed, which contains a stronger D-Pro-Gly β-hairpin inducer and a free, unacetylyated *N*-terminus. With the accessibility of azaGly$^3$ substitution to give azapeptide **4d**, the electronic and steric contributions of the aza-amino acid substitution could more rigorously be analyzed with a larger library of analogs. With this model system using a D-Pro-Gly in the turn region, the system was theorized to be more resilient to the disruptive nature of the aza substitution in the β-strand segment. Figure 3.3 shows the glycine splitting among the various substitutions made within model system **4.**

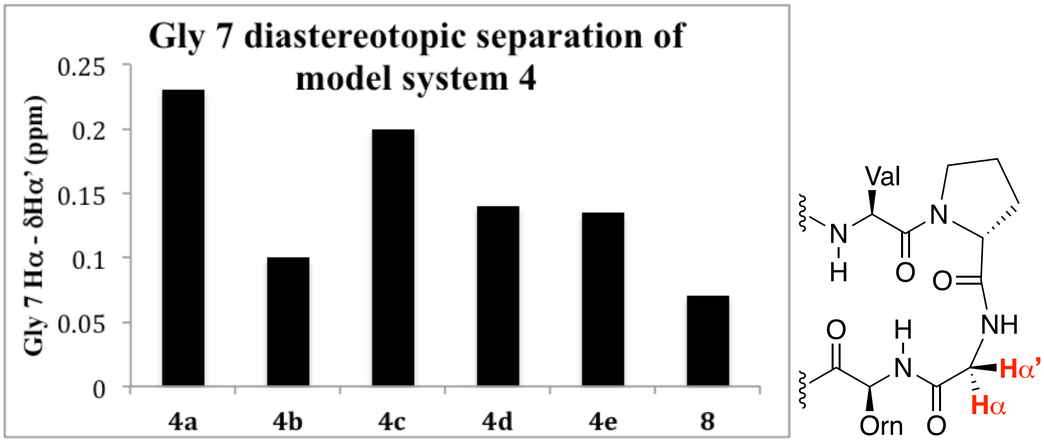


**Figure 3.3.** Glycine splitting of **4a-e** and compound **8** to see relative hairpin formation among the substitutions.

Compared to **4a**, it can be seen that all of the new peptide analogs synthesized in this series (**4b-4e**) decrease β-hairpin stability overall. The most destabilizing substitution is that of azaVal$^{3}$, followed by Gly$^{3}$ and azaGly$^{3}$. Glycine has been reported as one of least tolerant amino acids to adopt β-sheet conformation due to its inherent flexibility and lack of side chain chemistry.[7] It is important to note, however, that the aza-glycine analog (**4d**) does have conformational restrictions as inferred by the diacylhydrazine computational (Figure 1.7, p. 12), as well as additional hydrogen-bonding opportunities. However, as can be seen here, this did not lead to increased β-hairpin stability relative to the glycine$^{3}$ analog (**4e**). In accordance with what was observed with peptide **3c**, D-Val$^{3}$ substitution in peptide **4c** was less disruptive than aza-Val$^{3}$ substitution (**4b**). D-Val$^{3}$ substitution also appears to be less destabilizing than both Gly$^{3}$ (**4e**) and azaGly$^{3}$ (**4d**) substitutions.

While glycine splitting in these systems can provide qualitative information about relative β-hairpin stability in these analogs, for a more stringent analysis in sequences possessing D-Pro-Gly turn sequences, downfield shifting of α-protons in the strand segments relative to the negative control (**8**) needs to be used instead (Figure 3.3). Residue 3, denoted as X, was omitted from analysis due to the absence of CαH in aza-derivatives.

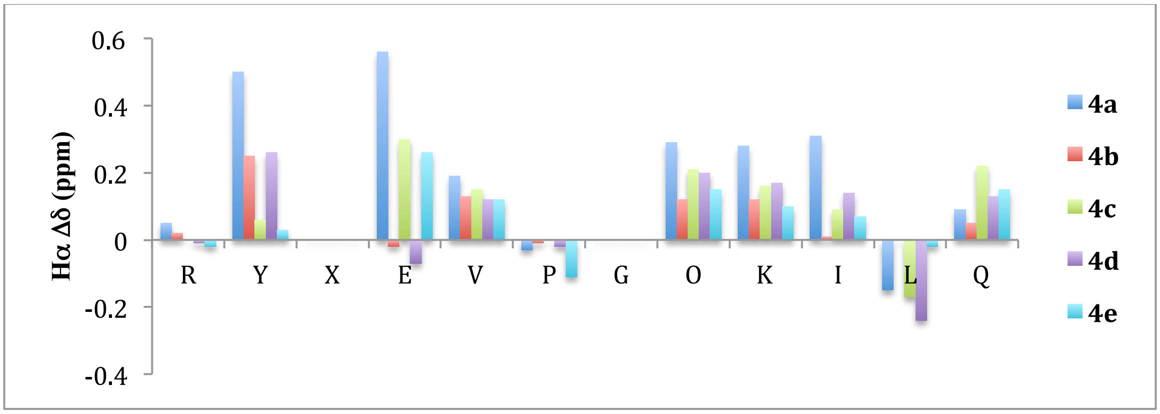


**Figure 3.4.** difference in α-proton shift from L-Pro control peptide **8**.

In the analysis of β-hairpin formation, the amino acids in the hydrogen-bonding regions of the sheet segment will be affected the most by β-hairpin formation ($Arg^1$, $X^3$, $Val^5$, $Orn^8$, $Ile^{10}$, and $Gln^{12}$). The downfield shifting of the α-protons in these residues is indicative of anti-parallel β-sheet formation from the β-hairpin folding, but the pairs of hydrogen-bonded residues are not equal. $Arg^1$ and $Gln^{12}$ positioned at the termini of the peptide suffer from peptide fraying, where the terminal residues experience a large influence of disorder, and $Val^5$ and $Orn^8$ are influenced by the immediately adjacent β-turn sequence.[8] X in position 3 and Ile in position 10 are the most reliable residues to measure β-hairpin formation as they are isolated in the center of each strand and are singularly influenced by the formation of the β-hairpin, but $X^3$ must be omitted for the variability backbone C to N in substitution. Using the α-protons shifts from literature for fully folded controls, the population of folding could be calculated in Table 3.1 (eq. 1, page 4).[1] As it can be seen in Table 3.1, the relative shifting of $Val^5$ and $Orn^8$ gives an overestimation of β-hairpin formation relative to $Ile^{10}$ and even glycine splitting calculations. Glycine splitting calculations of hairpin formation either closely matched or was lower than the values obtained from the average α-proton shifting of $Val^5$, $Orn^8$, and $Ile^{10}$. This is surprising as, historically, the use of D-Pro in the turn sequence caused Gly splitting calculations to overestimate β-hairpin formation (see Chapter 1, section 1.2). The β-hairpin stabilities of peptides **4d** and **4e** ($azaGly^3$ and $Gly^3$, respectively) calculated using glycine splitting were found to be identical; however using the proton shifting values for $Ile^{10}$, **4d** appears to have greater β-hairpin stability relative to **4e**. In agreement with values obtained from glycine splitting, $Ile^{10}$ proton shifting values demonstrate that the $azaVal^3$ analog **4b** exhibits the least amount of β-hairpin folding (14%). Interestingly, while D-$val^3$ analog **4c** shows the highest % β-hairpin folding among our synthesized analogs using glycine splitting and the average of α-proton shifts (48-49%), when considering only the CaH shift of $Ile^{10}$, azaGly analog **4d** has the highest β-hairpin stability (26%), excluding control peptide **4a** (58%).

**Table 3.1.** Calculated percent folding of the β-hairpin for each residue in the sheets hydrogen bonding region with average folding populations for each peptide and ΔΔG values.

| Peptide | $Val^5$ | $Orn^8$ | $Ile^{10}$ | Average by α-proton | % hairpin formation by Gly splitting | ΔΔG |
|---|---|---|---|---|---|---|
| **4a** | 83 | 91 | 58 | 77 | 76 | - |
| **4b** | 57 | 38 | 2 | 32 | 14 | +1.16 |
| **4c** | 65 | 66 | 17 | 49 | 48 | +.76 |
| **4d** | 52 | 63 | 26 | 47 | 33 | +.79 |
| **4e** | 52 | 47 | 13 | 37 | 33 | +.25 |

As an additional tool for secondary structure assessment, circular dichroism (CD) spectroscopy analyses were performed on compounds **4a**, **4b**, and **4d**. The CD curve of the natural analog (**4a**) was similar to the previously published CD spectrum[1] and showed a minimum at ~217 nm with a maximum at ~233 nm, characteristic of β-hairpin formation (antiparallel β-sheet).[9] In contrast, the CD curve of the aza-valine[3] analog (**4b**) showed instead a *maximum* at ~215 nm and a *minimum* at ~233 nm.[10] This CD signature is more consistent with a β-turn rather than an antiparallel β-sheet. As previously observed in short sequences, it is possible that the aza-amino acid induces and occupies the $i + 1$ or $i + 2$ position of a β-turn, rather than adopting the extended conformation required for accommodating a β-hairpin structure.[11] The CD spectrum of the aza-glycine[3] analog (**4d**) shows no clear minimum or maximum. Peptides **4c** and **e** were omitted due to reproducibility issues during CD analysis.

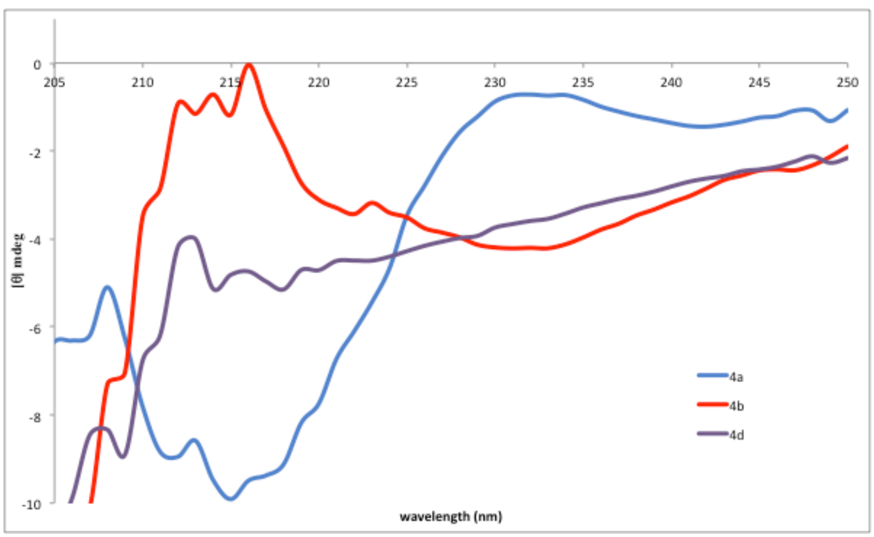


**Figure 3.5.** Circular dichroism spectra of **4a** (blue), **4b** (red **4d** (purple). Peptides were run at 100 μM concentration in 100 mM sodium acetate buffer at pH 3.8.

### 3.2 Conclusion

This research contributes valuable information to the growing wealth of knowledge of azapeptides and their applicability in peptidomimicry. With the combined 1D NMR analysis of glycine peak separation and α-proton shifting as well as CD spectroscopy, this research proves that aza-substitutions at the third position in the upper β-strand portion in β-hairpin model peptides impart a destabilizing effect that weakens, if not completely disrupts, the β-hairpin secondary structure. As can be seen through spectroscopic analysis, aza-glycine[3] substitution retained some population of β-hairpin, and destabilization from aza-substitution appears to be minimal compared to the natural glycine counterpart. This can be in part due to the stabilization of hydrogen bonding, both with neighboring residues as well with cross-strand residues. Such hydrogen-bonding interactions may counteract the lone pair repulsion aza-glycine experiences in the extended conformation. In contrast, it is possible that aza-valine imparts such a detrimental impact on the sheet formation due to the loss of one of the additional hydrogen bond present in azaGly residues. It has been seen before that methylation of a singular nitrogen on a in a diacylhydrazine model compound raised the rotational barrier to achieve the extended conformation by 5 kcal/mol.[12] Thus, our experimental findings validate the earlier computational hypothesis that aza-amino acid are not tolerated within β-sheet secondary structures, even in the presence of a templating bottom β-strand.

## 3.3 REFERENCES


[1] Sarnowski, M. P.; Kang, C. W.; Elbatrawi, Y. M.; Wojtas, L.; Del Valle, J. R. Peptide N-Amination Supports β-sheet conformations. *Angew. Chem. Int. Ed.* **2017**, *56*, 2083-2086.

[2] Tatko, C. D.; Waters, M. L. Comparison of C-H•••π and Hydrophobic Interactions in a β-Hairpin Peptide: Impact on Stability and Specificity. *J. Am. Chem. Soc*. **2004**, *126*, 2028-2034.

[3] Mahalakshmi, R.; Balaram, P. The Use of D-Amino Acids in Peptide Design. *D-Amino Acids: A New Frontier in Amino Acid and Protein Research− Practical Methods and Protocols.* **2007**, 415-430.

[4] Lee, D. L.; Powers, J.P. S.; Pflegerl, K.; Vasil, M. L.; Hancock, R. E. W.; Hodges, R. S. Effects of Single D-Amino Acid Substitutions on Disruption of β-Sheet Structure and Hydrophobicity in Cyclic 14-Residue Antimicrobial Peptide Analogs Related to Gramicidin S. *J. Peptide Res.* **2004**, *63*, 69-84.

[5] Wouters, M. A.; Curmi, P. M. An Analysis of Side Chain Interactions and Pair Correlations Within Antiparallel β-Sheets: The Differences Between Backbone Hydrogen-Bonded and Non-Hydrogen-Bonded Residue Pairs. *Proteins: Struct, Funct. Gen.* **1995**, *22*, 119-131.

[6] Butterfield, S. M.; Waters, M. L. A Designed β-Hairpin Peptide for Molecular Recognition of ATP in Water. *J. Am. Chem. Soc.* **2003**, *125*, 9580-9581.

[7] Kim, C.; Berg, J. Thermodynamic β-sheet propensities measured using a zinc-finger host peptide. *Nature* **1993**, *362*, 267-270.

[8] Kiehna, S. E.; Waters, M. L. Sequence Dependence of β-Hairpin Structure: Comparison of a Salt Bridge and an Aromatic Interaction. *Protein Sci.* **2003**, *12*, 2657-2667.

[9] Greenfield, N. J. Using Circular Dichroism Spectra to Estimate Protein Secondary Structure. *Nature Protocols* **2006**, *1*, 2876-2890.

[10] Brahms, S.; Brahms, J. Determination of Protein Secondary Structure in Solution by Vacuum Ultraviolet Circular Dichroism. *J. Mol. Biol.* **1980**, *138*, 149-178.

[11] Thormann, M.; Hoffmann, H. Conformational properties of azapeptides. *Theochem.* **1999**, *469*, 63-76.

[12] Reynolds, C.; Hormann, R. Theoretical study of the structure and rotational flexibility of diacylhydrazines: Implications for the structure of nonsteroidal ecdysone agonists and azapeptides. *J. Am. Chem. Soc.* **1996**, *118*, 9395-9401.

## CHAPTER 4

# Experimental Methods

### 4.1 General Methods

**General:** Polystyrene Rink Amide resin (0.78 mmol/g) was purchased from Protein Technology Inc™, and the manufacturer's reported loading of the resin was used in the calculation of the yields of the final products. Solid phase peptide synthesis was performed using an automated Biotage Syro Wave$^{TM}$ peptide synthesizer in 10 mL parallel reactors with PTFE frits. Incorporation of aza-amino acids and further elongations were performed manually in disposable filter columns with 20 μM PE frit filters and caps purchased from Applied Separations (cat # 2413 and 2416 for 3 mL and 6 mL filter columns, respectively) with gentle agitation on a Thermo Fisher vortex mixer equipped with a microplate tray. Solution draining and washing of the resin was accomplished by connecting the filter columns to a water aspirator vacuum *via* a waste trap. Analytical LCMS analyses were performed using an Agilent Technologies 1260 Infinity II series LCMS Single Quad instrument with ESI ion-source and positive mode ionization, equipped with a 5 μM, 150 x 4.6 mm C18 Vydac column purchased from Mac-Mod Analytical, Inc (cat # 218TP5415). A flow rate of 0.5 mL/min and 5-95%, 20-60%, or 15-60% gradients of $CH_3CN$ [0.1% trifluoroacetic acid (TFA)] in water (0.1% TFA) over 12 minutes (total run time = 22 minutes) were used for all LCMS analyses. Peptides were purified on a preparative HPLC (Agilent 218 purification system) using a preparative column (10-20 μM, 250 mm x 22 mm, C18 Vydac column, cat # 218TP101522) at a flow rate of 10 mL/min with gradients of $CH_3CN$ [0.1% trifluoroacetic acid (TFA)] in water (0.1% TFA) over 30 minutes (total run time = 60 minutes).

**Reagents**: Amino acids, *N,N*-diisopropylethylamine (DIEA), *N*, *N*'-Disuccinimidyl carbonate (DSC), Fmoc chloride, and triphosgene (BTC) were purchased from Chem Impex Int'l, Inc. Reagents such as piperidine, lithium chloride, sodium cyanoborohydride ($NaBH_3CN$), and triisopropylsilane (TIPS) were purchased from Sigma Aldrich. Reagents such as hydrazine monohydrate, Acetic anhydride, and 2,4,6-collidine were purchased from Alfa Aesar. Trifluoroacetic acid, glacial acetic acid, and solvents were purchased from Fisher. HBTU was burchased from Oakwood Chemical.

## 4.2 Experimental procedures and Characterization Data

### 4.2.1 Fmoc-based SPPS: Fmoc Deprotection and HBTU couplings

Peptide syntheses were performed under standard manual conditions on an automated shaker or using a Biotage Syro Wave™ peptide synthesizer using Polystyrene Rink Amide resin (0.78 mmol/g). Couplings of amino acids (3 equiv) were performed in DMF using HBTU (3 equiv) as coupling reagent and DIEA (6 equiv). After the 9th residue, 0.4 M LiCl was added to the coupling reaction to help break up on-resin peptide aggregation.[1] Fmoc deprotections were performed initially by treating the resin with 20% piperidine in DMF (v/v) for 5 minutes, followed by treatment with a fresh solution of 20% piperidine in DMF (v/v) for 15 minutes. After witnessing incomplete Fmoc deprotections after the 7th amino acid incorporation, where on-resin peptide aggregation may begin to hinder Fmoc deprotection reactions, a solution of 2/2/96 DBU/piperidine/DMF (v/v/v) solution was used instead.[2] Resin was washed after each coupling with DMF (3 x 1 mL) and deprotection reaction with DMF, MeOH, and $CH_2Cl_2$ (2 x 1 mL). Prior to cleavage from the resin or storage, resin was washed with $CH_2Cl_2$ (3 x 1 mL).

### 4.2.2 Synthesis of 9*H*-fluoren-9-ylmethyl hydrazinecarboxylate 20

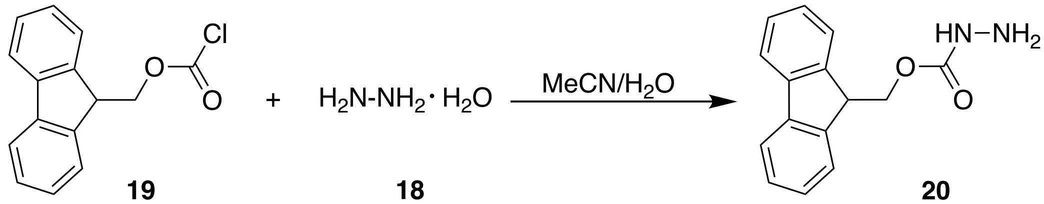


**19** **18** **20**

9*H*-fluoren-9-ylmethyl hydrazinecarboxylate **20** was synthesized according to literature procedures.[3] A solution of FmocCl (2.00 g, 7.73 mmol) in 120 mL of $CH_3CN$ was added dropwise over 2 hours at 0 ºC to a solution of excess hydrazine (3.8 mL, 78.0 mmol, 10 equiv) in 26.2 mL of $CH_3CN/H_2O$ (1:1, v/v). The solution was warmed to room temperature and left stirring for 12 h, prior to being concentrated *in vacuo* to 5 mL and filtered to give 1.92 g of white solid in 98% yield. The resulting solid was washed with water, followed by hexanes. NMR (DMSO) spectra matched literature values.[3]

### 4.2.3 Synthesis of *N*'-isopropyl-fluoren-9-ylmethyl carbazate 21

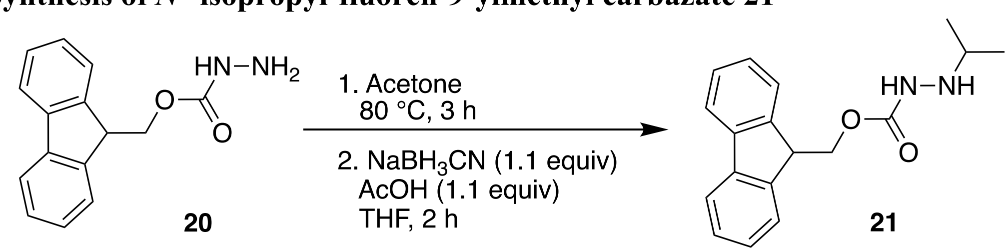


**20** **21**

N'-isopropyl-fluoren-9-ylmethyl carbazate **21** was synthesized according to literature procedures with minor modifications.[3] Specifically, 9H-fluoren-9-ylmethyl hydrazinecarboxylate **20** (1.92 g, 7.55 mmol) was suspended in acetone (50 mL) and heated at reflux for 2 h. The acetone was evaporated in vacuo, and the resulting hydrazone intermediate was dissolved in THF (50 mL), treated with acetic acid (0.48 mL, 8.39 mmol, 1.1 equiv) and $NaBH_3CN$ (521 mg, 8.31 mmol, 1.1 equiv), and stirred for 2 h. The volatiles were removed and the crude was dissolved in EtOAc (100 mL), washed with 1 M aqueous $KHSO_4$ (4 x 50 mL) and brine (2 x 50 mL), dried over $Na_2SO_4$, and concentrated to give a white solid. The obtained product was dissolved in EtOH and heated for 1 h, followed by evaporation of EtOH to yield N'-isopropyl-fluoren-9-ylmethyl carbazate **21** as a white solid (1.32 g, 59% yield) after column chromatography using a 20-100% gradient of EtOAc in hexanes. NMR ($CDCl_3$) spectra matched literature values.[3,4]

### 4.2.4 Representative procedure for the incorporation of aza-valine

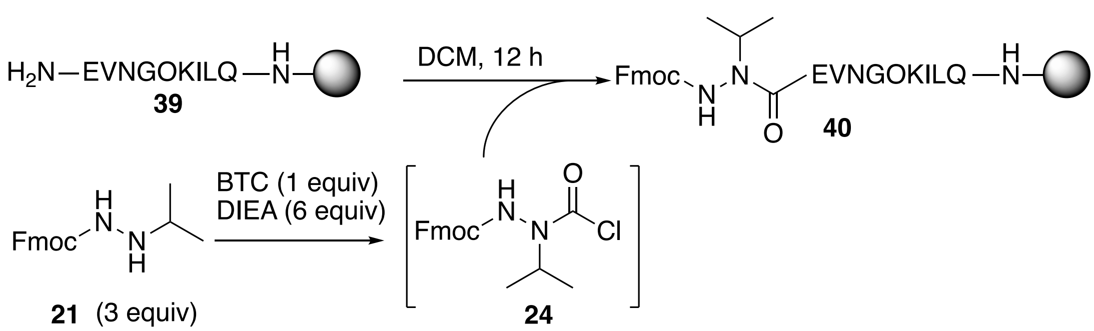


*N*'-isopropyl-fluoren-9-ylmethyl carbazate **21** (138 mg, 0.466 mmol) was dissolved in dry DCM (1 mL) and cooled to 0°C. A solution of bis(trichloromethyl)carbonate (BTC, 46.4 mg, 0.156 mmol, 1 equiv) dissolved in dry DCM (1 mL) and cooled to 0 °C was added dropwise to the carbazate suspension. The reaction mixture was left stirring at 0 °C for 5 minutes, allowed to warm to room temperature, and stirred for another 25 minutes. DIEA (0.163 mL, 0.930 mmol, 6.0 equiv) was added to the solution and the solution was stirred for 5 minutes prior to being transferred to a SPPS cartridge containing resin-bound peptide **39** (200 mg, 0.156 mmol) swollen in DCM. The SPPS cartridge was left shaking for 12 h, after which the solution was drained and the resin was washed with DCM (3 x 2 mL). The procedure was repeated to ensure full conversion.

### 4.2.5 Representative procedure for the incorporation of aza-glycine

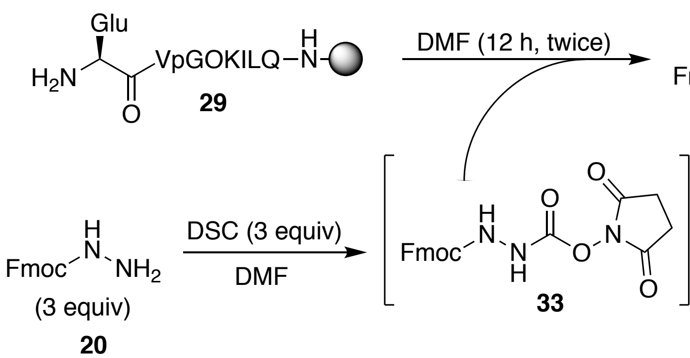


*N*, *N*'-Disuccinimidyl carbonate (DSC) (120 mg, 0.466 mmol, 3.0 equiv) was added to a solution of 9*H*-fluoren-9-ylmethyl hydrazinecarboxylate **19** (123 mg, 0.484 mmol, 3.1 equiv) in DMF and stirred for 5 minutes. The solution was then transferred to resin-bound peptide **27** (200 mg, 0.156 mmol) swollen in DMF and left shaking for 12 h. The solution was drained and the resin was washed with DMF (3 x 2 mL). The coupling was repeated to ensure complete conversion to the desired product.

### 4.2.6 Representative procedure for coupling onto the aza-amino acid residue

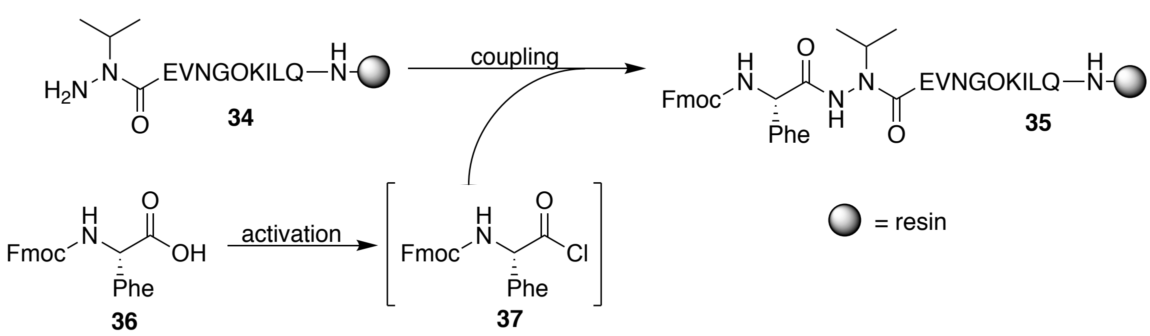


Fmoc-Phe-OH ( 188 mg, 0.484 mol, 3.1 equiv) was dissolved in dry THF (1 mL), cooled to 0 °C, and treated dropwise with a cold solution of BTC (46.4 mg, 0.156 mmol, 1.0

equiv) in dry THF (1 mL). The reaction mixture was left stirring at 0 °C for 15 minutes prior to adding 2,4,6-collidine (0.206 mL, 1.56 mmol, 10.0 equiv). The solution was stirred at 0 °C for 2 minutes, allowed to warm to room temperature, and stirred another 5 minutes. The resulting activated amino acid solution was then added to an SPPS cartridge containing resin-bound peptide **34** (200 mg, 0.156 mmol) previously swollen with 0.4 M LiCl in dry THF. LiCl (0.339 g, 0.8 mmol, 0.4 M) was added to the resin to prevent aggregation and the reaction was left shaking for 3 h. The solution was drained and the resin was treated with fresh reagents and left stirring for an additional 12 h. The resin was washed with DMF (2 x 2 mL), MeOH (2 x 2 mL), and THF (2 x 2 mL). The reaction conversion was monitored by LCMS and the procedure was repeated until a satisfactory conversion (> 50%) was reached, or starting material was completely consumed.

### 4.2.7 *N*-terminal acetylation of peptides

Resin-bound, Fmoc deprotected peptide (200. mg, 0.156 mmol) was swollen in DMF (2 mL) for 30 minutes. The DMF solution was drained and the resin was suspended in 15% $Ac_2O$ in DMF and left shaking for 10 minutes. The solution was drained and the resin was washed with DMF (3 x 2 mL) and $CH_2Cl_2$ (3 x 3 mL).

### 4.2.8 Cleavage test of resin-bound peptides

A small aliquot of resin (1-5 mg) was washed with $CH_2Cl_2$ to remove traces of DMF, drained, and treated with a freshly made solution of TFA/$H_2O$/TIPS (90:5:5, v/v/v, 0.5 mL) for 2 h at room temperature. The cleavage solution was collected by filtering the resin through a disposable, PP fritted cartridge. The filtrate was evaporated to dryness and the crude peptide was precipitated twice with cold ether (4 mL) followed by decanting. The pellet (crude peptide sample) was dissolved in 1:1 MeCN/$H_2O$ v/v (1 mg/mL) and subjected to LCMS analysis.

### 4.2.9 Full cleavage

The resin-bound peptide was washed with $CH_2Cl_2$ to remove traces of DMF, drained, transferred into a 20 mL scintillation glass vial, and treated a freshly made solution of TFA/$H_2O$/TIPS (90:5: 5, v/v/v, 5 mL). The vial was capped and agitated for 2 hours at room temperature on an orbital shaker. The cleavage mixture was filtered through a disposable, PP fritted cartridge into a 50 mL falcon tube containing cold ether (~20 mL). The ether was decanted following centrifugation at 8000 rpm for 2 minutes. The peptide pellet was suspended in 1:9 MeCN/$H_2O$ v/v (5 mL). The sample was frozen and lyophilized.

### 4.2.10 NMR spectroscopy:

Lyophilized peptide samples containing Trp or Tyr residues (peptides **2a-c**, **4a-e**) were solvated in $D_2O$ to give a stock solution of 4-8 mM, as determined by UV-Vis spectroscopy (extinction coefficient of Tyr = 1490 cm $M^{-1}$ at 280 nm and Trp = 2357 cm $M^{-1}$ at 294.4 nm). The concentration of peptide stock solutions for peptides **1a-b**, which lack Tyr or Trp residues, was determined by weighing > 8 mg of lyophilized peptide. The stock solutions were diluted to concentrations of 1-4 mM in $D_2O$ buffered with 50 mM NaOAc-$d_3$ buffer at pH 4.2 (uncorrected), pH adjusted with AcOH-$d_3$. All NMR spectra were collected at the Molecular Education, Technology, and Research Innovation Center (METRIC) at NC State University on a Bruker AvanceIII 700 MHz instrument at 25 °C. 1D spectra were collected with 32K data points and at least 32 scans and water suppression with a presaturation pulse or with a 1D-1H NOESY. 2D-experiments were collected on the same instrumentation, using the Bruker water suppression versions of ROESY. 2D scans were done with 8 scans in the first dimesion and 256 or 512 in the 2nd dimension. TOCSY spectra were collected with 80 ms spin-lock and ROESY spectra were collected with a mixing time of 250 ms. Spectral analysis was performed with Mnova software. NMR spectra of control peptide samples **1a, 2a**, **4,a**, **6**, **7a**, and **8** matched that of literature with CαH shifts and minor variance in further branching protons.[5,6]

Quantification of β-hairpin % folding was calculated from CαH for residues in the hydrogen-bonded region and Gly chemical shifts compared to random coil (7 mers) and fully folded (cyclic) control peptides using equation 1. Chemical shifts for the cyclic peptides (fully folded control) were taken from the literature.[3,5]

$$\text{Fraction folded} = (\delta_{\text{observed}} - \delta_0) / (\delta_{100} - \delta_0) \quad \text{eq. 1}$$

where δ represents the separation, in ppm, of the glycine peaks splitting and the magnitude of separation in the sample relative to the random coil control is put in reference to the fully folded control.

Alternatively, chemical shift difference between the diastereotopic $H_\alpha$ and $H_\alpha$' of glycine in the turn region (Gly $H_\alpha/H_\alpha$' splitting) has been found to provide similar β-hairpin folding values compared to $H_\alpha$ chemical shifts (equation 2).

$$\text{Fraction Folded} = \delta_{\text{Gly Obs}} / \delta_{\text{Gly 100}} \quad \text{eq. 2}$$

where $\Delta\delta_{Gly\ Obs}$ is the Glycine chemical shift splitting between $H_{\alpha}/H_{\alpha}$' observed for the peptides under stud, and $\Delta\delta_{Gly\ 100}$ is the Glycine chemical shift splitting for the cyclic, fully folded control.

### 4.2.11 Circular dichroism spectroscopy

CD spectroscopy was used to qualitatively analyze the secondary structure of the peptide variants.[6] Samples were analyzed by UV-Vis spectroscopy to find stock concentration (see NMR spectroscopy) and diluted to a peptide concentration of 100 μm in a solution of 100 mM acetate buffer at pH 3.8. Peptides were analyzed on a Jasco J-815 CD Spectrometer at 25 °C with a time constant of 1 s, in 1 nm steps, and a 1 mm quartz cell. Measurements were taken in triplicate and averaged. Smoothing software set to 5 iterations was used to yield the final spectra traces.

## 4.3 REFERENCES


[1] Thaler, A.; Seebach, D. Lithium-Salt Effects in Peptide Synthesis. Part I. Conditions for the Use of Lithium-Salts in Coupling Reactions. *Helv. Chim. Acta.* **1991**, *74*, 617-627.

[2] Tickler, A. K.; Barrow, C. J.; Wade, J. D. Improved Preparation of amyloid-β Peptides using DBU as $N^{\alpha}$-Fmoc Deprotection reagent. *J. Pept. Sci.* **2001**, *7*, 488-494.

[3] Boeglin, D.; Lubell, W. D. Aza-Amino Acid Scanning of Secondary Structure Suited for Solid-Phase Peptide Synthesis with Fmoc Chemistry and Aza-Amino Acids with Heteroatomic Side Chains. *J. Comb. Chem.* **2005**, *7*, 864-878.

[4] Spiegel, J.; Mas-Moruno, C.; Kessler, H.; Lubell, W. D. Cyclic aza-Peptide Integrin Ligand Synthesis and Biological Activity. *J. Org. Chem.* **2012**, *77*, 5271–5278.

[5] Tatko, C. D.; Waters, M. L. Comparison of C-H•••π and Hydrophobic Interactions in a β-Hairpin Peptide: Impact on Stability and Specificity. *J. Am. Chem. Soc*. **2004**, *126*, 2028-2034.

[6] Sarnowski, M. P.; Kang, C. W.; Elbatrawi, Y. M.; Wojtas, L.; Del Valle, J. R. Peptide N-Amination Supports β-sheet conformations. *Angew. Chem. Int. Ed.* **2017**, *56*, 2083-2086.

## APPENDIX

## Appendix A

### LC-MS and NMR Characterization

**1a** Ac-RFVEVNGOKILQ-$NH_2$

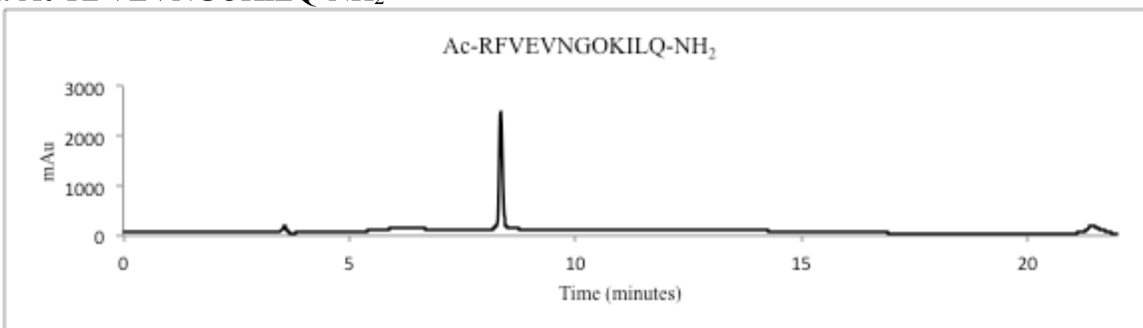


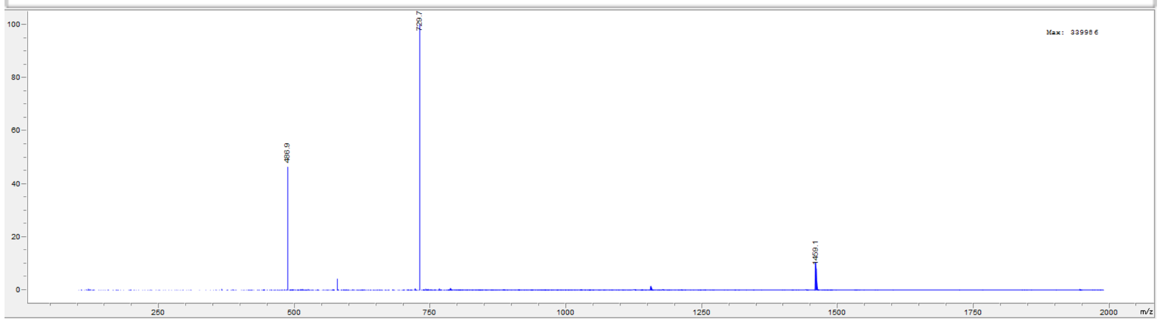


| | α | β | γ | δ | ε |
|---|---|---|---|---|---|
| R | 4.38 | 1.71 | 1.50 | 3.17 | |
| F | 5.01 | 2.96, 3.03 | | 7.17 | 7.35 |
| V | 4.2 | 1.94 | 0.95 | | |
| E | 4.75 | 2.03 | 2.34 | | |
| V | 4.28 | 2.05 | 0.9 | | |
| N | 4.54 | 2.77, 3.03 | | | |
| G | 4.05, 3.83 | | | | |
| O | 4.52 | 1.83 | 1.71 | 3.03 | |
| K | 4.53 | 1.65 | 1.23 | 1.40, 1.49 | 2.77 |
| I | 4.34 | 1.9 | .9, 1.23, 1.4 | 0.85 | |
| L | 4.31 | 1.55 | 1.6 | 0.78 | |
| Q | 4.31 | 1.94, 2.10 | 2.27 | | |

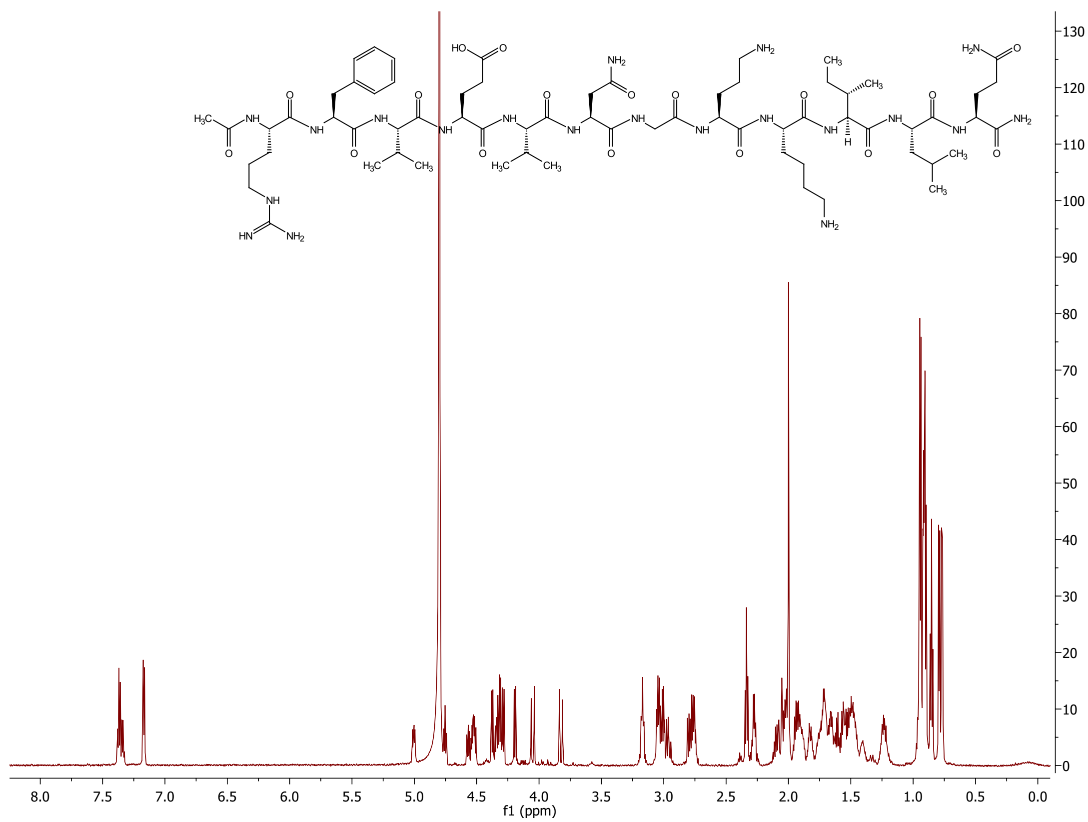
f1 (ppm)

**2a** Ac-RF**azaV**EVNGOKILQ-$NH_2$

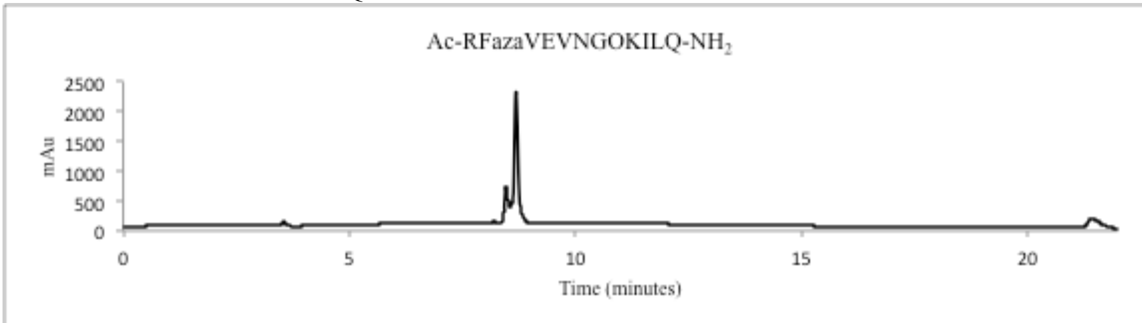


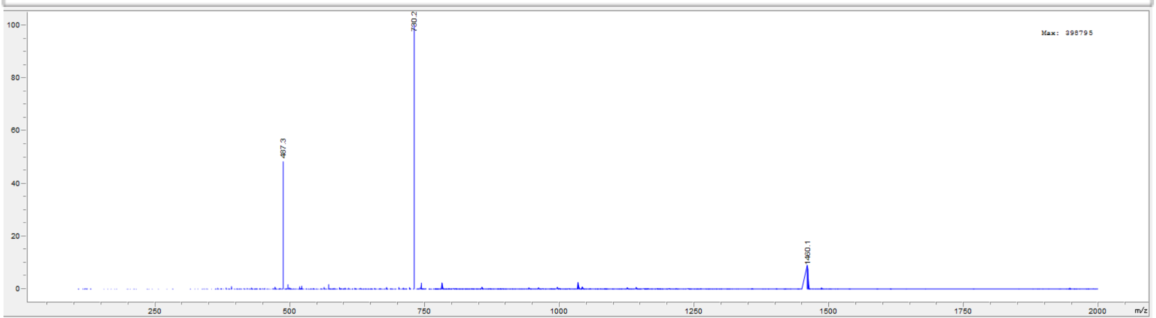


| | α | β | γ | δ | ε |
|---|---|---|---|---|---|
| R | 4.25 | 1.99 | 1.63 | 3.21 | |
| F | 4.58 | 3.02 | | 7.43 | 7.37 |
| azaV | | 1.8 | 0.56 | | |
| E | 4.33 | 2.03 | 2.27 | | |
| V | 4.13 | 2.07 | 0.94 | | |
| N | 4.7 | 2.79, 2.9 | | | |
| G | 3.95 | | | | |
| O | 4.39 | 1.88 | 1.7 | 3.01 | |
| K | 4.32 | 1.8 | 1.48 | 3.1 | |
| I | 4.15 | 1.78 | 1.4, 1.21, .87 | 0.87 | |
| L | 4.4 | 1.62 | 1.62 | 0.94 | |
| Q | 4.29 | 2.13 | 2.38 | | |

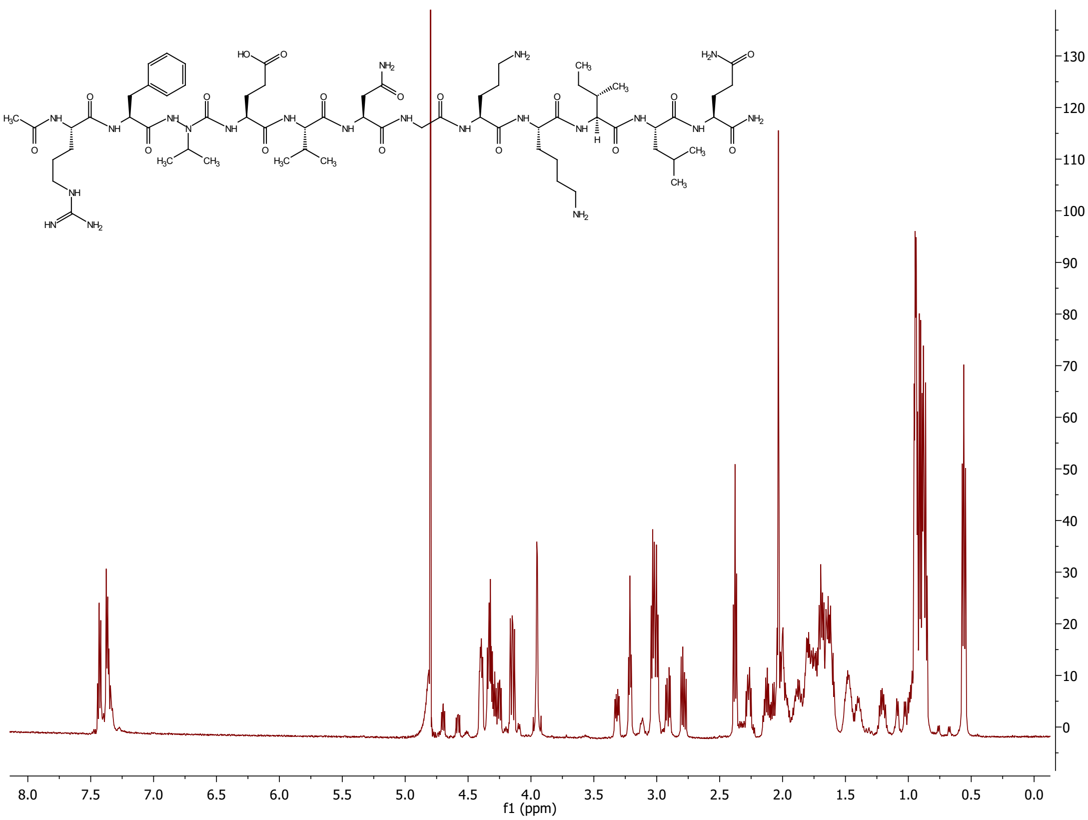

**2a** Ac-RWVEVNGOKILQ-$NH_2$

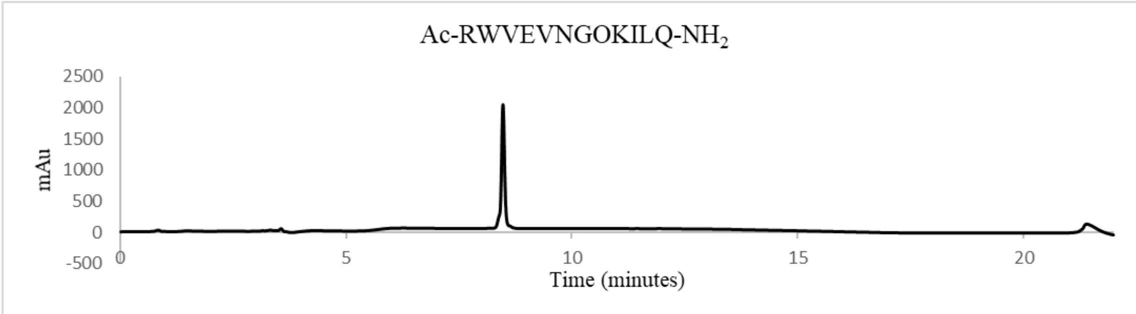


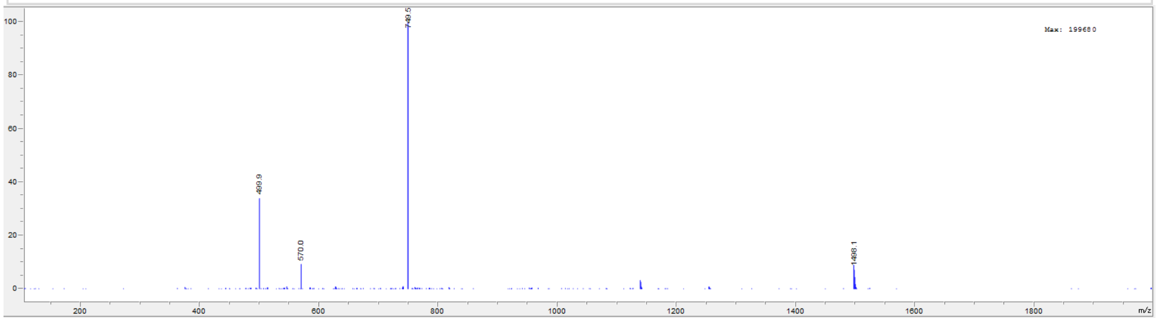

| | α | β | γ | δ | ε |
|---|---|---|---|---|---|
| R | 4.31 | 1.68 | 1.5 | 3.14 | |
| W | 5.06 | 3.13, 3.06 | 7.23(s), 7.32 7.47 (d), 7.05 7.21(t) | | |
| V | 4.2 | 1.97 | 0.93 | | |
| E | 4.89 | 2.03, 1.95 | 2.26 | | |
| V | 4.43 | 1.88 | 0.85 | | |
| N | 4.46 | 2.75, 3.09 | | | |
| G | 4.07, 3.73 | | | | |
| O | 4.6 | 1.87 | 1.72 | 3.03 | |
| K | 4.73 | 1.7 | 1.34 | 1.37 | 2.58 |
| I | 4.54 | 1.9 | .89, 1.19 | 0.9 | |
| L | 4.07 | 1.37 | 1.06 | .51, .29 | |
| Q | 4.37 | 2.04 | 2.36 | | |

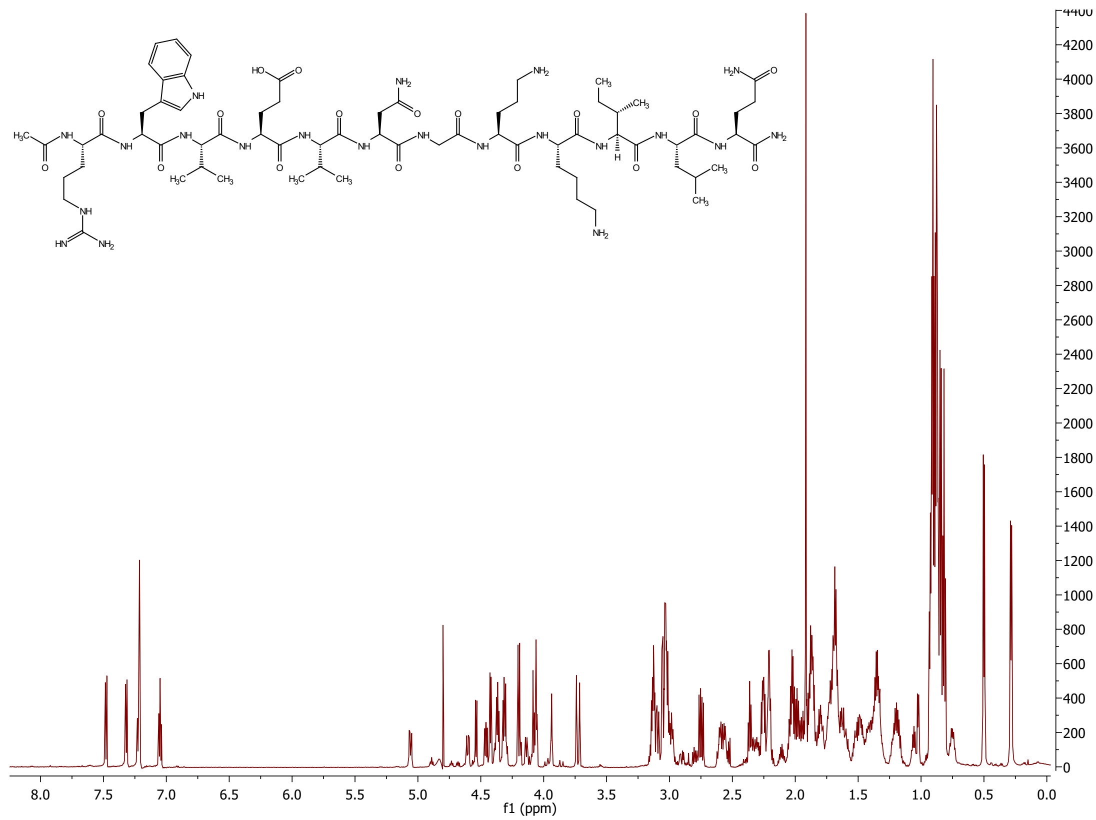
f1 (ppm)

**2b** Ac-RW**azaV**EVNGOKILQ-$NH_2$

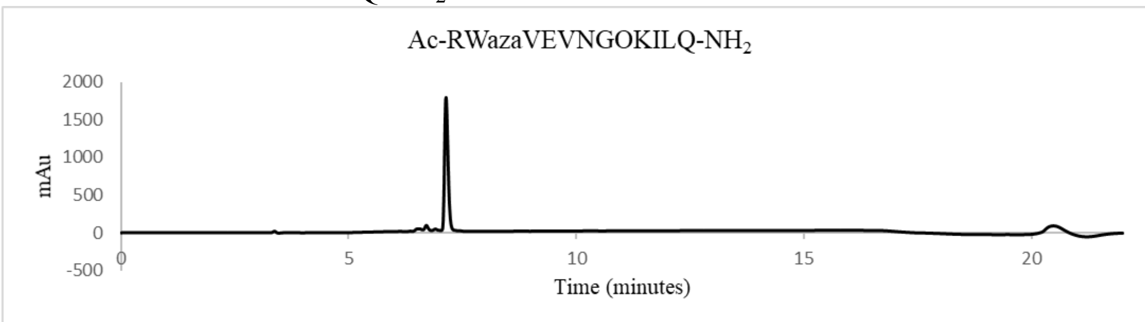


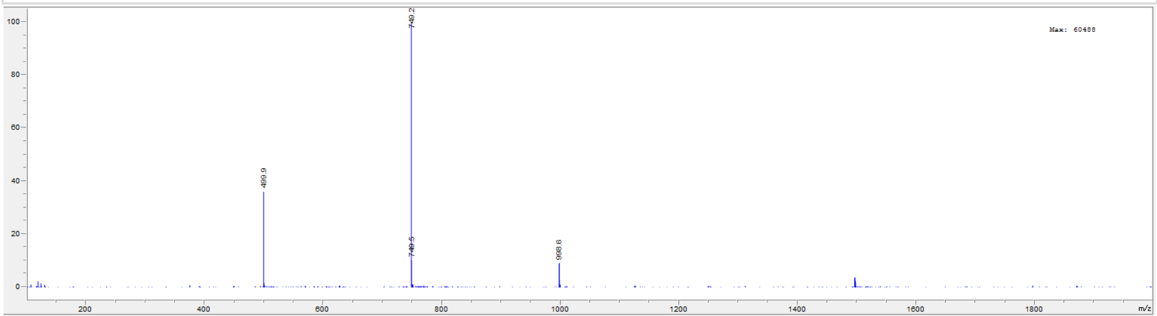


| | α | β | γ | δ | ε |
|---|---|---|---|---|---|
| R | 4.17 | 1.63 | 1.46 | 3.02 | |
| W | 4.68 | 3.21, 3.26 | 7.3(s), 7.72 7.52(d), 7.26 7.19(t) | | |
| azaVal | | 2.13 | 0.92 | | |
| E | 4.22 | 1.99, 2.09 | 2.37 | | |
| V | 4.1 | 2.1 | 0.85 | | |
| N | 4.69 | 2.76 | | | |
| G | 3.94 | | | | |
| O | 4.35 | 1.87 | 1.69 | 2.99 | |
| K | 4.33 | 1.79 | 1.48 | 1.67 | 2.98 |
| I | 4.14 | 1.79 | .89, 1.19, 1.37 | 0.85 | |
| L | 4.39 | 1.63 | 1.47 | .37, .26 | |
| Q | 4.31 | 2.01 | 2.26 | | |

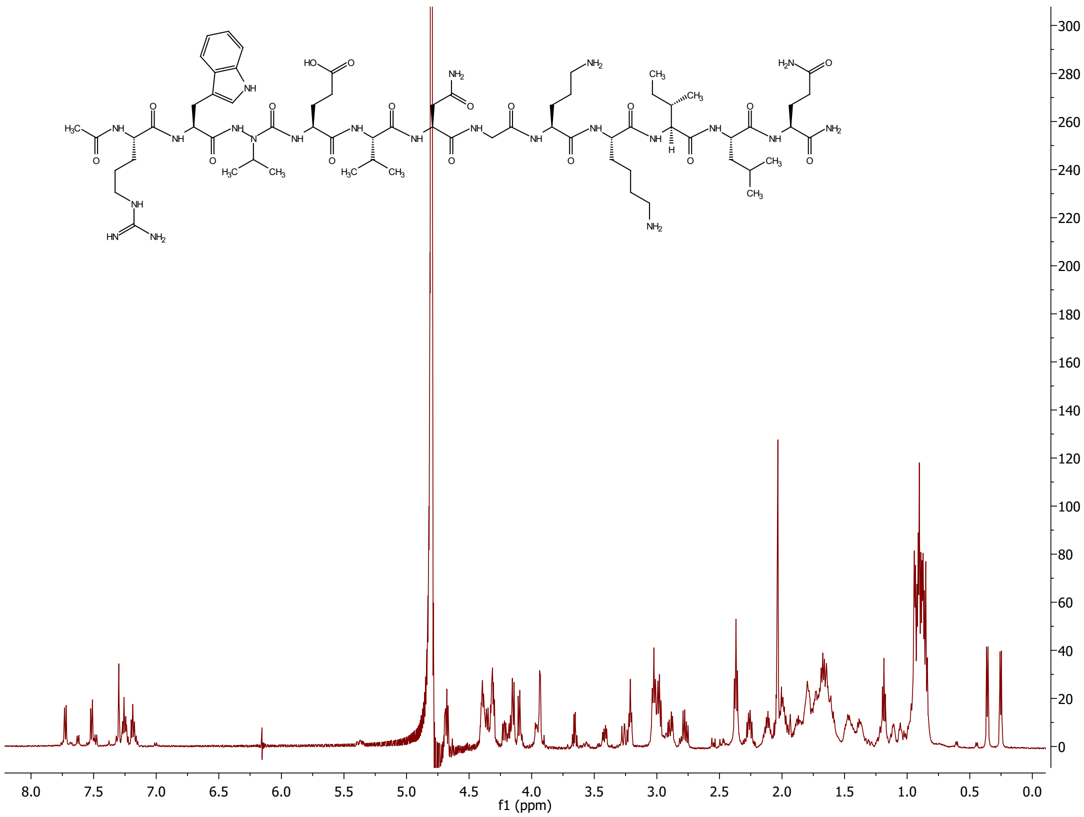

**4a** H-RYVEVpGOKILQ-NH$_2$

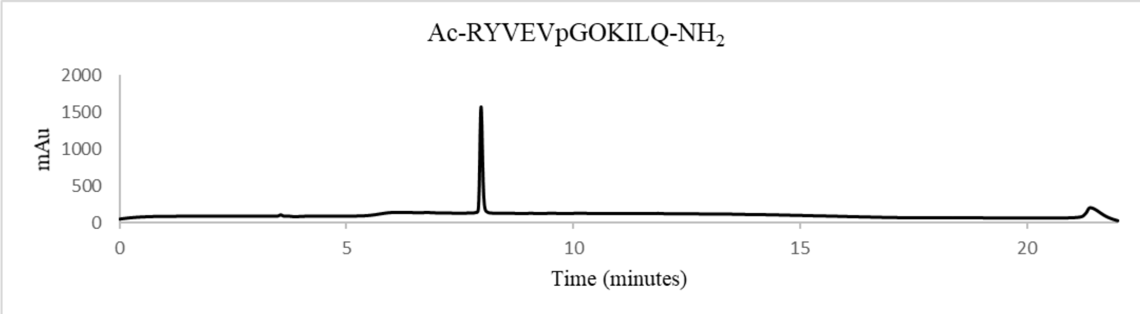


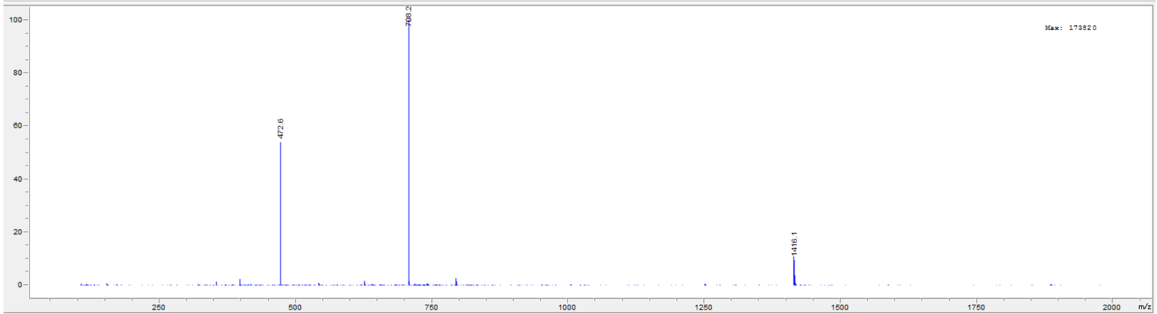


| | α | β | γ | δ | ε |
|---|---|---|---|---|---|
| R | 4.08 | 1.93 | 1.57 | 3.24 | |
| Y | 5.15 | 2.83, 2.89 | | 7.01 | 6.82 |
| V | 4.36 | 2.01 | 0.89 | | |
| E | 4.93 | 1.89, 1.98 | 2.27 | | |
| V | 4.6 | 1.99 | 0.94 | | |
| p | 4.39 | 2.38 | 2.13 | 3.87 | |
| G | 4.03, 3.80 | | | | |
| O | 4.62 | 1.84 | 1.7 | 3.03 | |
| K | 4.59 | 1.56, 1.63 | 1.16 | 2.67 | 3.02 |
| I | 4.45 | 1.9 | .87, 1.22, 1.38 | 0.82 | |
| L | 4.23 | 1.62 | 1.47 | .69, .76 | |
| Q | 4.34 | 1.85, 2.05 | 2.3 | | |

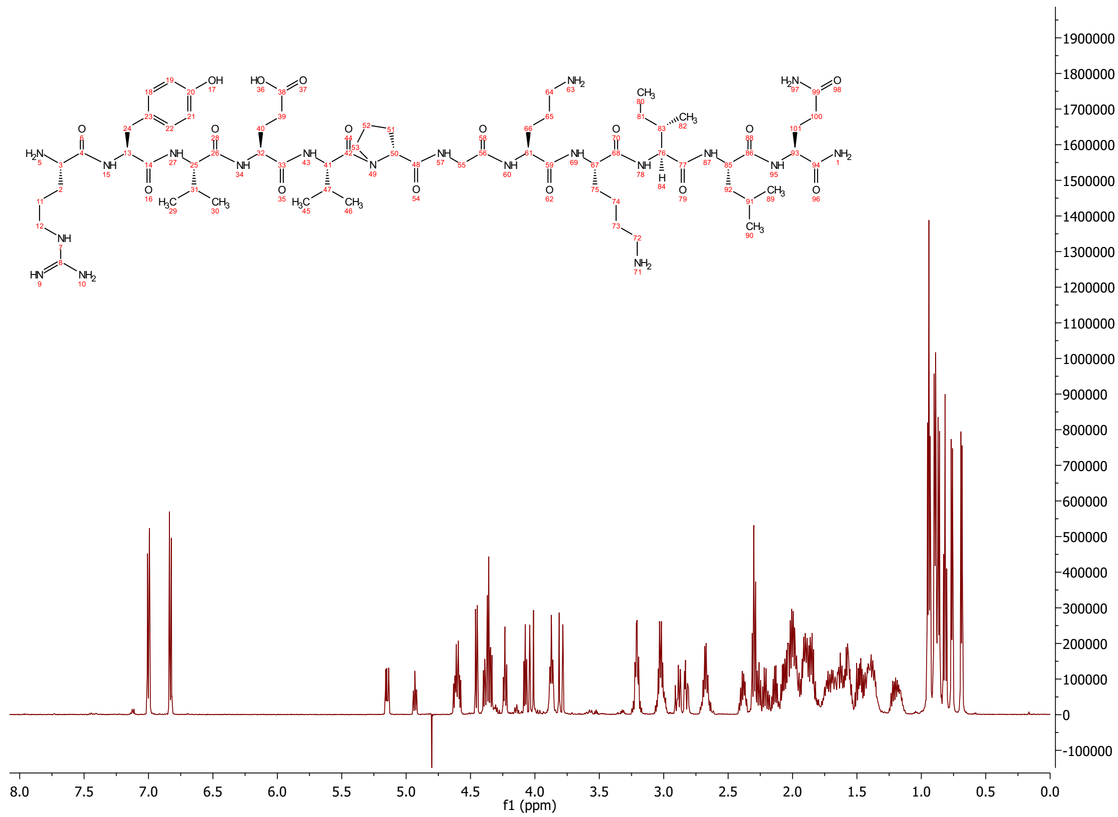

**4b** H-RY**azaV**EVpGOKILQ-$NH_2$

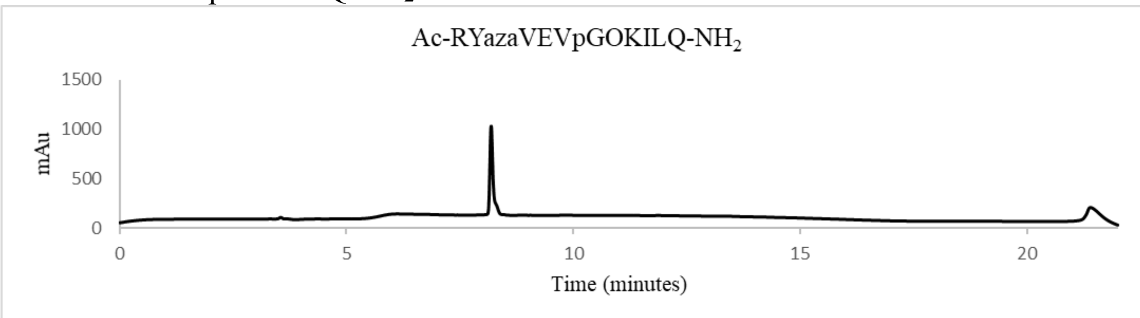


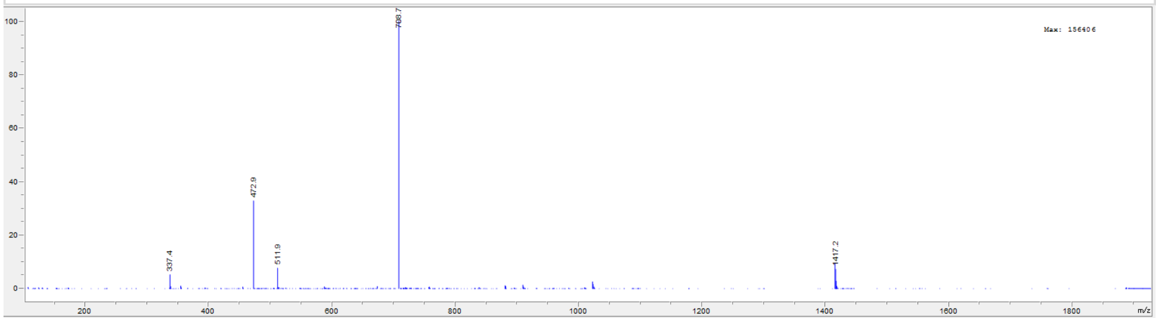


| | α | β | γ | δ | ε |
|---|---|---|---|---|---|
| R | 4.05 | 1.89 | 1.64 | 3.22 | |
| Y | 4.9 | 2.89, 2.99 | | 7.23 | 6.89 |
| azaV | | 1.79 | 0.52 | | |
| E | 4.35 | 1.89 | 2.35 | | |
| V | 4.54 | 2.05 | 0.93 | | |
| p | 4.41 | 2.35 | 2.1, 1.98 | 3.80, 3.86 | |
| G | 3.84, 3.94 | | | | |
| O | 4.45 | 1.88 | 1.8 | 3.01 | |
| K | 4.43 | 1.68 | 1.44, 1.38 | 1.63 | 2.97 |
| I | 4.15 | 1.98 | 1.44, 1.18, .88 | 0.82 | |
| L | 4.38 | 1.67 | 1.59 | 0.86 | |
| Q | 4.3 | 1.99 | 2.36 | | |

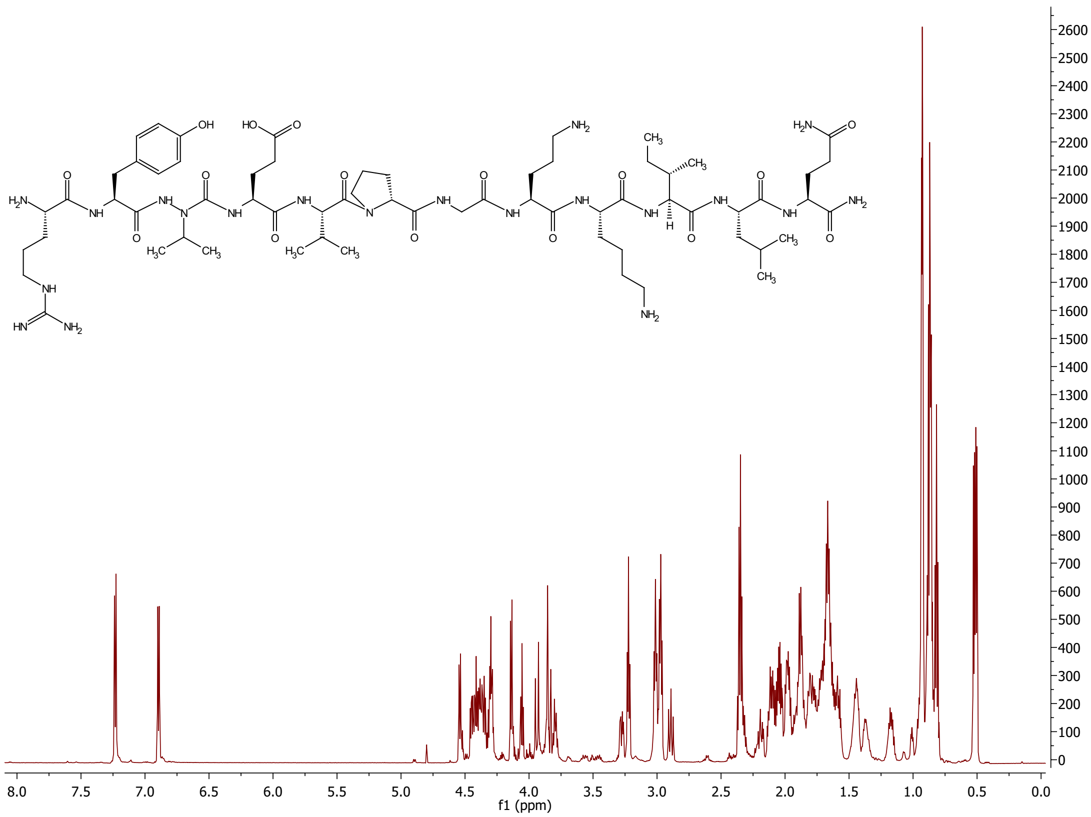
f1 (ppm)

**4c** H-RYvEVpGOKILQ-$NH_2$

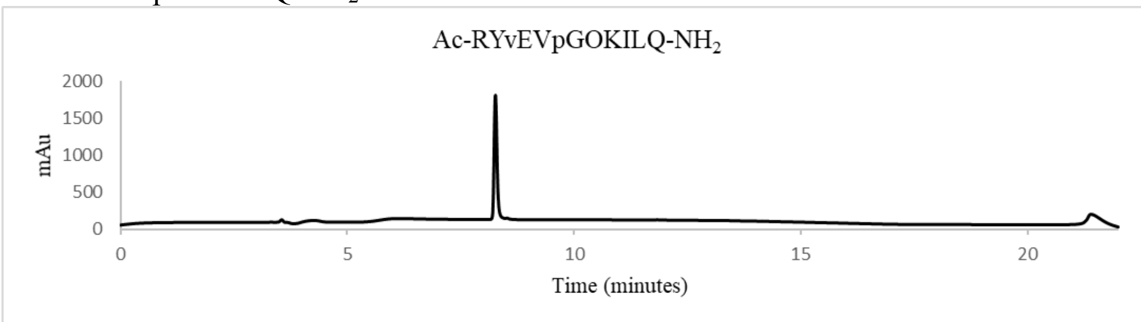



| | α | β | γ | δ | ε |
|---|---|---|---|---|---|
| R | 4.03 | 1.92 | 1.63 | 3.24 | |
| Y | 4.71 | 3.01, 3.09 | | 7.15 | 6.86 |
| v | 4.06 | 2.03 | 0.9 | | |
| E | 4.67 | 2.01, 1.89 | 2.26 | | |
| V | 4.56 | 2.05 | 0.95 | | |
| p | 4.42 | 2.39 | 2.14, 2.05 | 3.83, 3.89 | |
| G | 3.85, 4.02 | | | | |
| O | 4.54 | 1.78 | 1.71 | 3.05 | |
| K | 4.47 | 1.65 | 1.66 | 1.47 | 3.01 |
| I | 4.23 | 1.93 | 1.38, 1.22, .93 | 0.84 | |
| L | 4.21 | 1.63 | 1.46 | .71, .61 | |
| Q | 4.47 | 2.03, 1.88 | 2.3 | | |

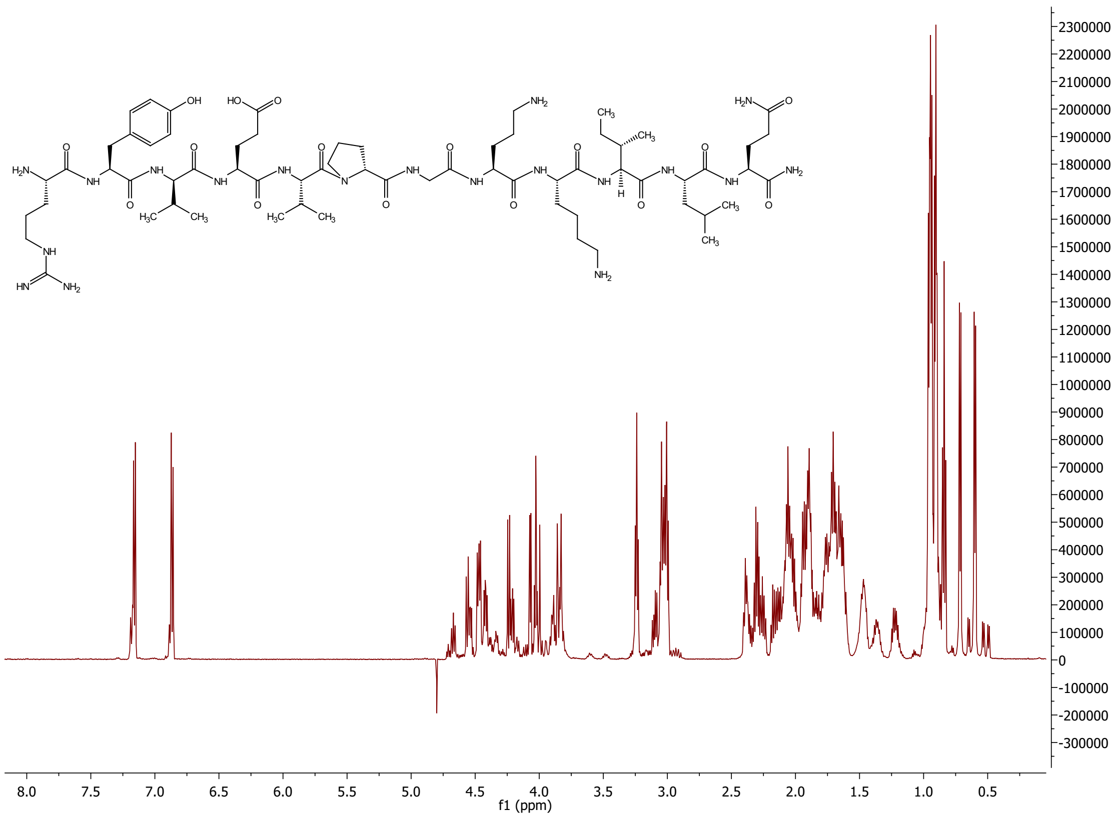
f1 (ppm)

**4d** H-RY**azaG**EVpGOKILQ-$NH_2$

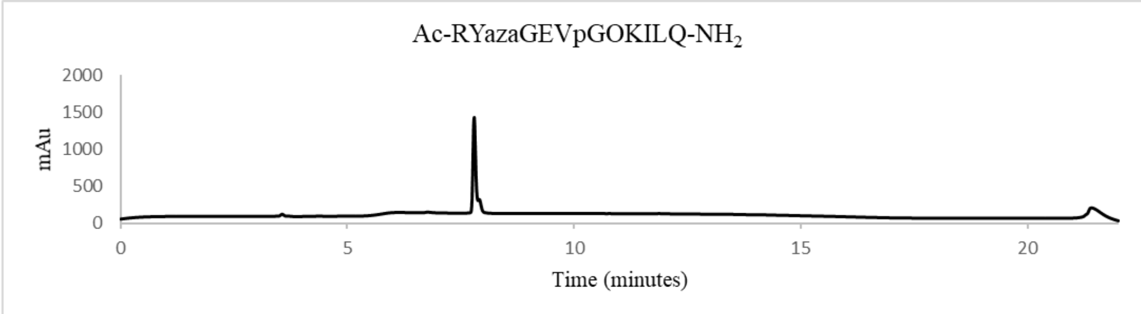


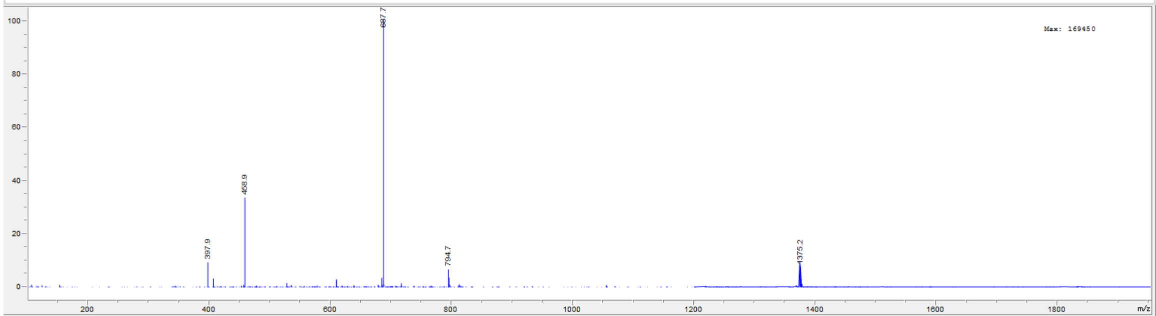


| | α | β | γ | δ | ε |
|---|---|---|---|---|---|
| R | 4.02 | 1.95 | 1.59 | 3.19 | |
| Y | 4.91 | 2.96, 2.99 | | 7.15 | 6.87 |
| azaG | | | | | |
| E | 4.3 | 1.88, 1.96 | 2.35 | | |
| V | 4.53 | 2.02 | 0.93 | | |
| p | 4.4 | 2.36 | 2.08. 1.98 | 3.82, 3.88 | |
| G | 3.82, 3.96 | | | | |
| O | 4.53 | 1.86 | 1.71, 1.73 | 3.02 | |
| K | 4.48 | 1.66 | 1.37, 1.41 | 1.17 | 2.98 |
| I | 4.28 | 1.97 | 1.45, 1.19, .91 | 0.81 | |
| L | 4.14 | 1.66, 1.61 | 1.58 | .85, .87 | |
| Q | 4.38 | 2.00, 1.99 | 2.36 | | |

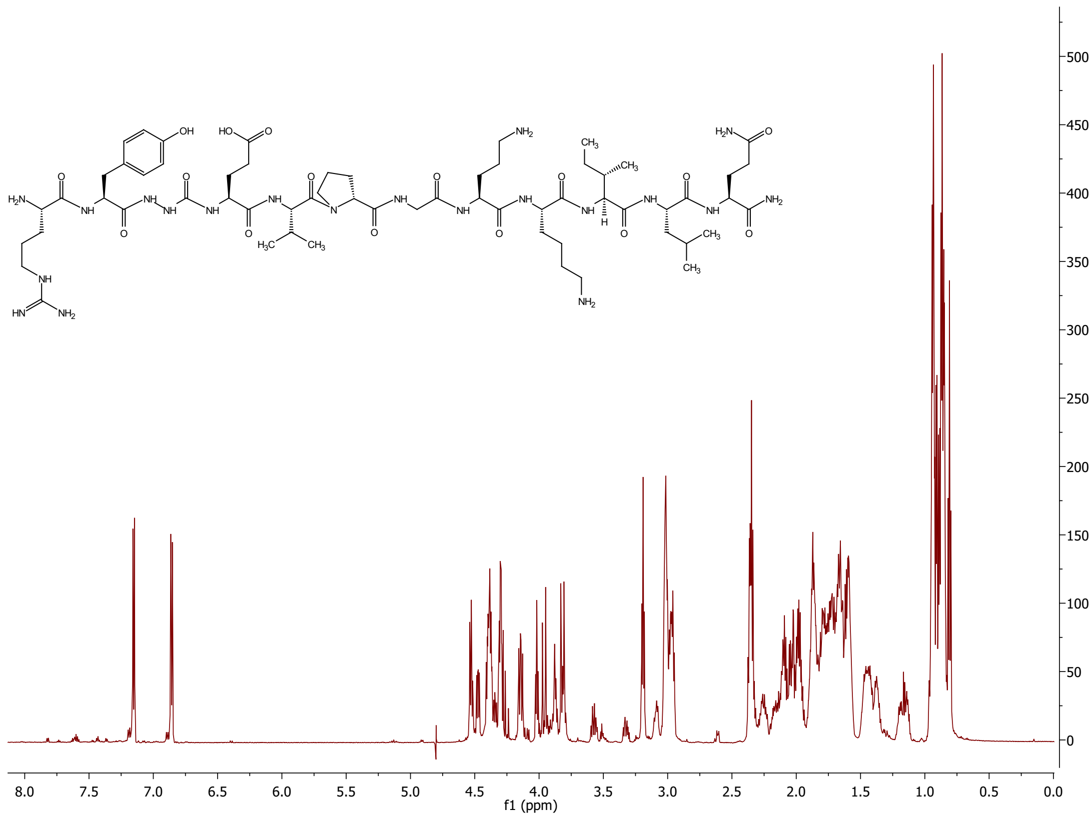

f1 (ppm)

**4e** H-RYGEVpGOKILQ-$NH_2$

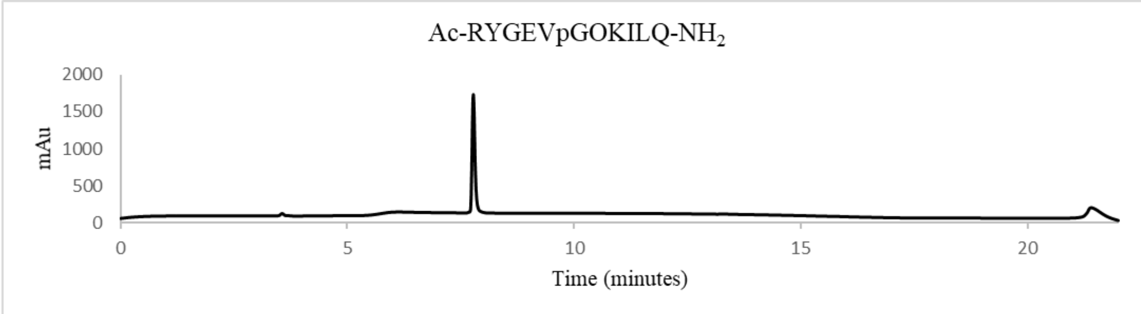


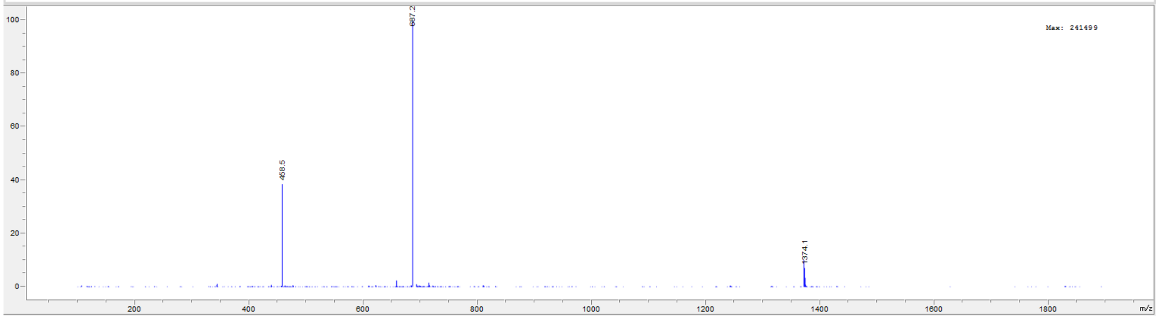


| | α | β | γ | δ | ε |
|---|---|---|---|---|---|
| R | 4.01 | 1.87 | 1.59 | 3.18 | |
| Y | 4.68 | 3.02 | | 7.13 | 6.85 |
| G | 3.90, 3.83 | | | | |
| E | 4.63 | 1.97, 1.82 | 2.26, 2.20 | | |
| V | 4.53 | 2.03 | 0.93 | | |
| p | 4.31 | 2.34 | 2.08, 1.95 | 3.89, 3.81 | |
| G | 3.97, 3.84 | | | | |
| O | 4.48 | 1.86 | 1.73 | 3.02 | |
| K | 4.41 | 1.71 | 1.62 | 1.44 | 2.92 |
| I | 4.21 | 1.8 | 1.43, 1.16, .88 | 0.82 | |
| L | 4.36 | 1.61 | 1.43 | 0.85 | |
| Q | 4.4 | 2.04 | 2.34 | | |

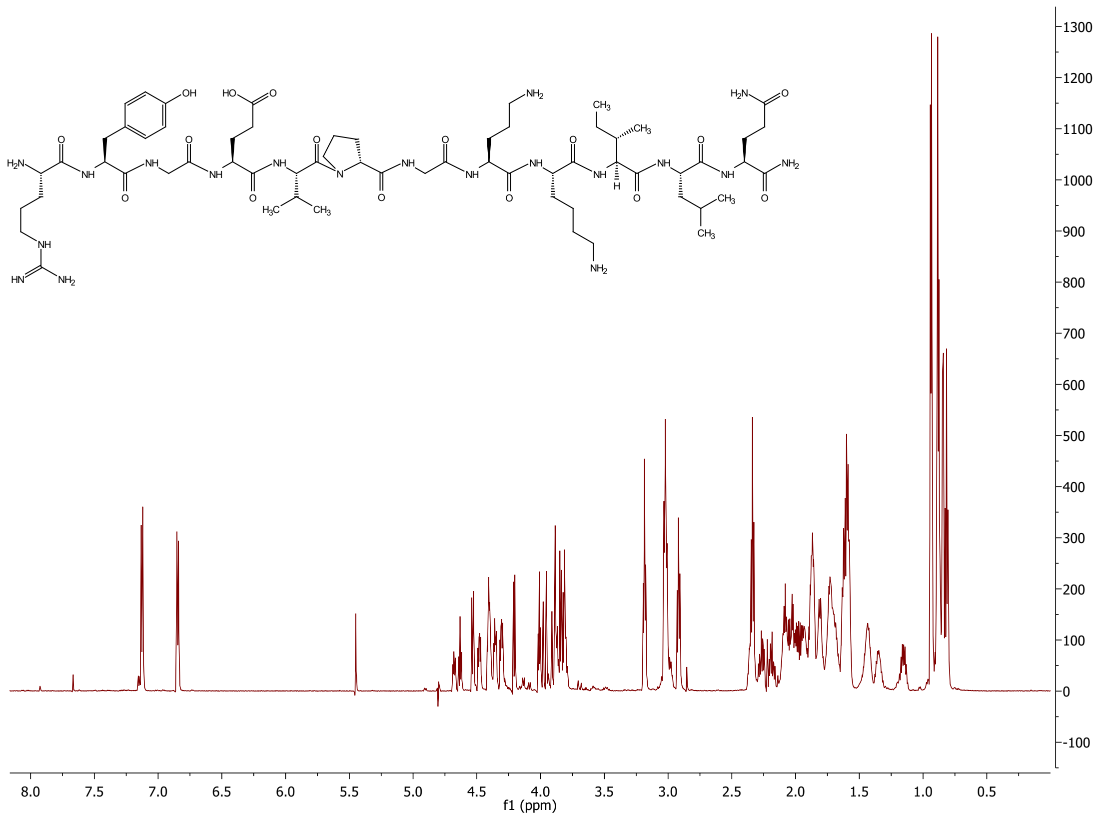
f1 (ppm)

**5b** Ac-RF**azaV**EVNG-$NH_2$

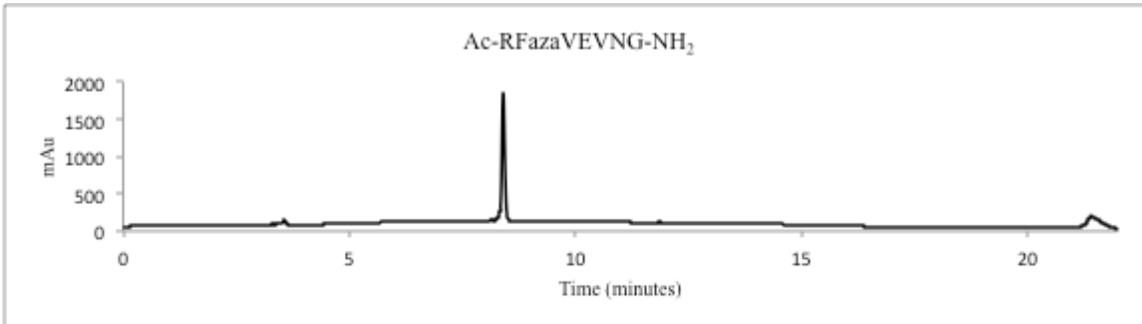


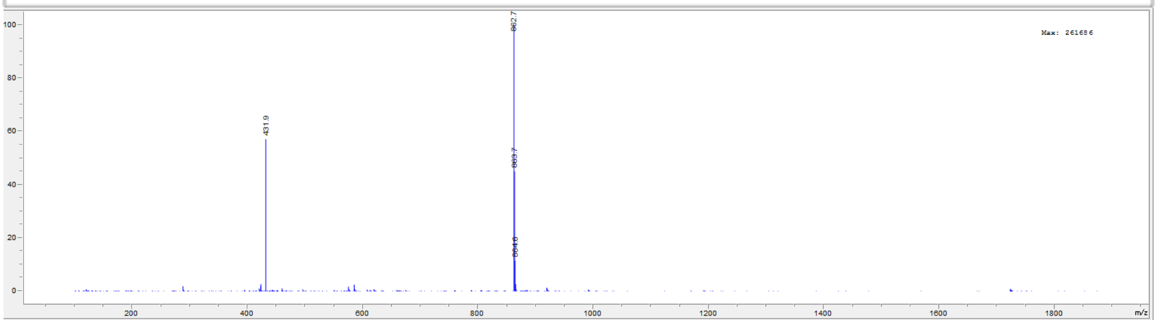

| | α | β | γ | δ | ε |
|---|---|---|---|---|---|
| R | 4.26 | 1.95, 1.91 | 1.62 | 3.21 | |
| F | 4.57 | 3.02 | | 7.43 | 7.36 |
| azaVal | | 1.8 | 0.55 | | |
| E | 4.33 | 2.04 | 2.32 | | |
| V | 4.11 | 2.08 | 0.94 | | |
| N | 4.7 | 2.9, 2.79 | | | |
| G | 3.91 | | | | |

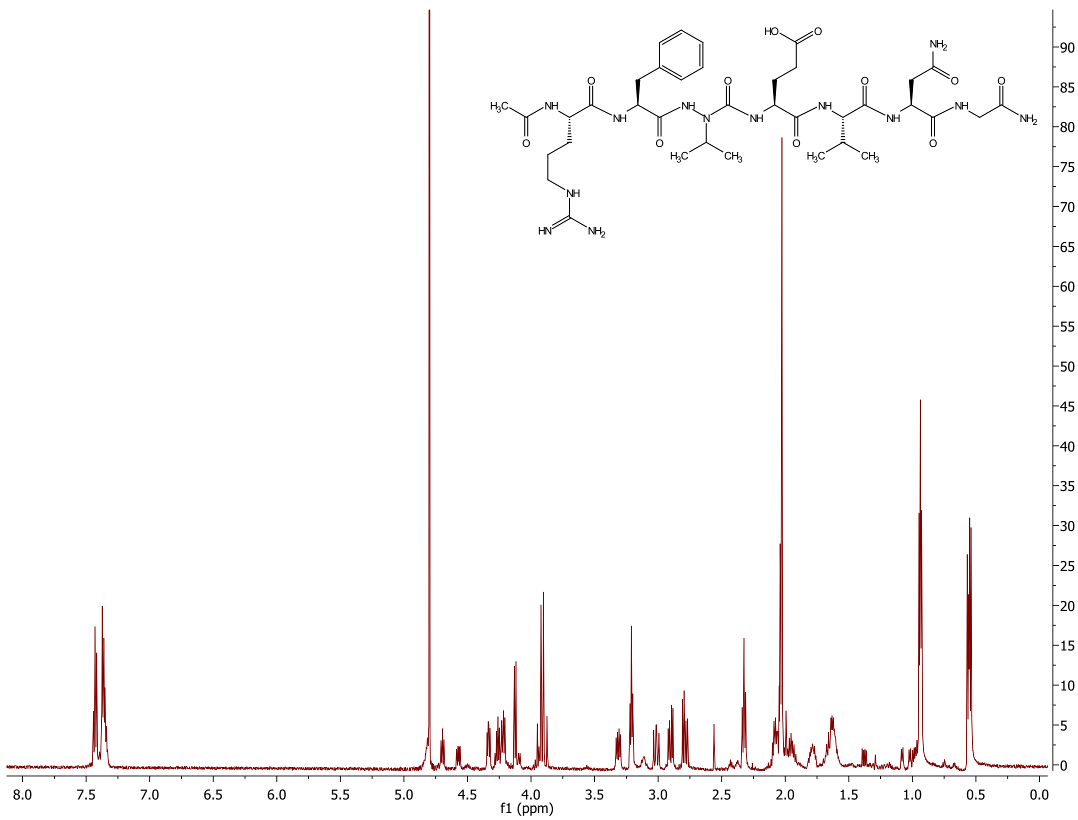
f1 (ppm)

**6** Ac-NGOKILQ-$NH_2$

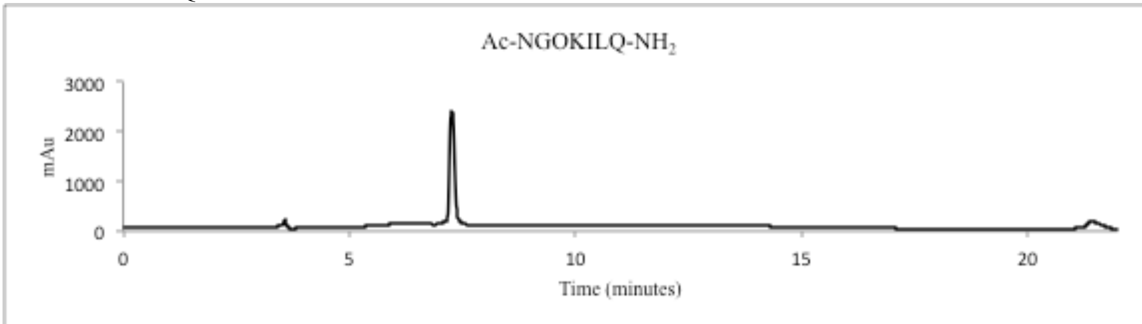


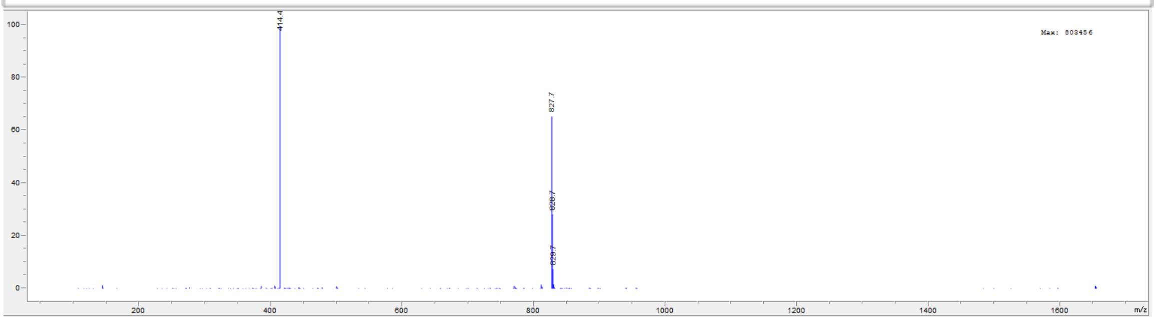


| | α | β | γ | δ | ε |
|---|---|---|---|---|---|
| N | 4.69 | 2.83 | | | |
| G | 3.96 | | | | |
| O | 4.37 | 1.87 | 1.7 | 3.04 | |
| K | 4.33 | 1.8 | 1.49 | 1.7 | 3 |
| I | 4.15 | 1.76 | .88, 1.21, 1.4 | 0.88 | |
| L | 4.4 | 1.65 | 1.6 | 0.95 | |
| Q | 4.31 | 2, 2.13 | 2.38 | | |

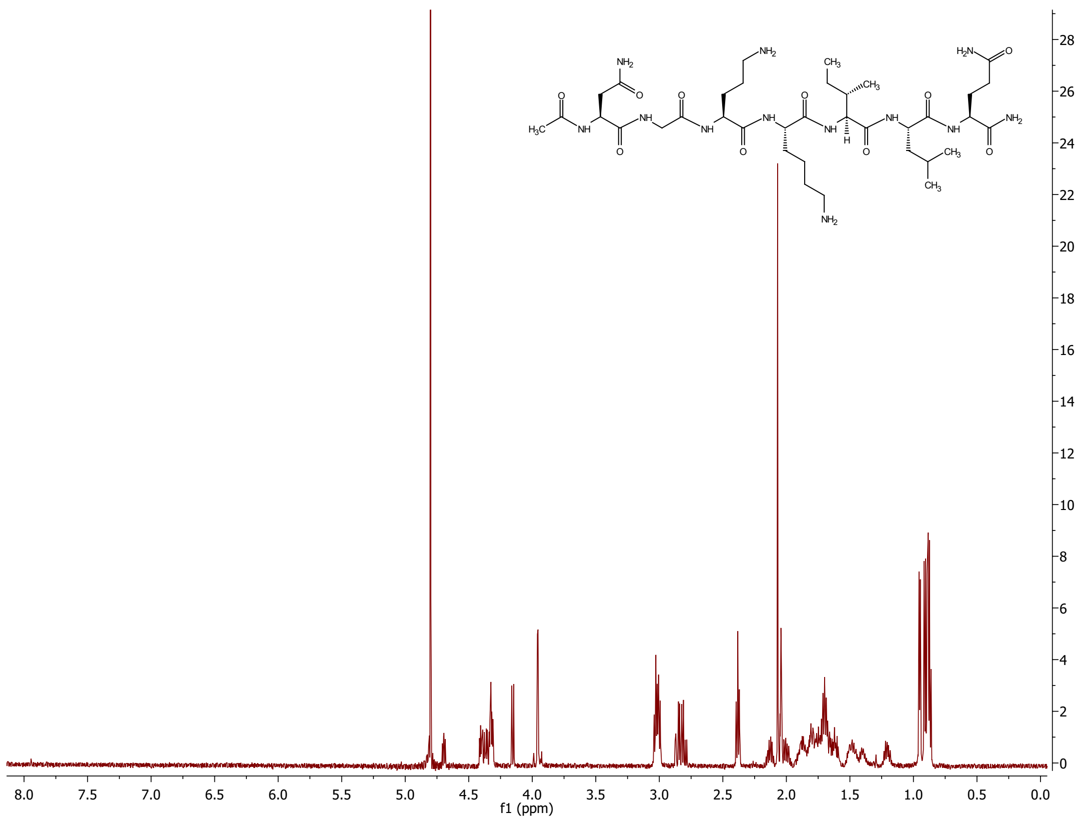
f1 (ppm)

**7a** Ac-RWVEVNG-$NH_2$

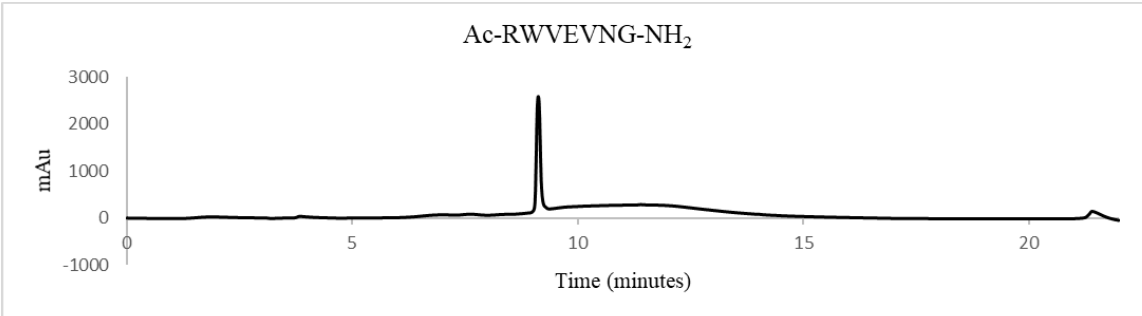


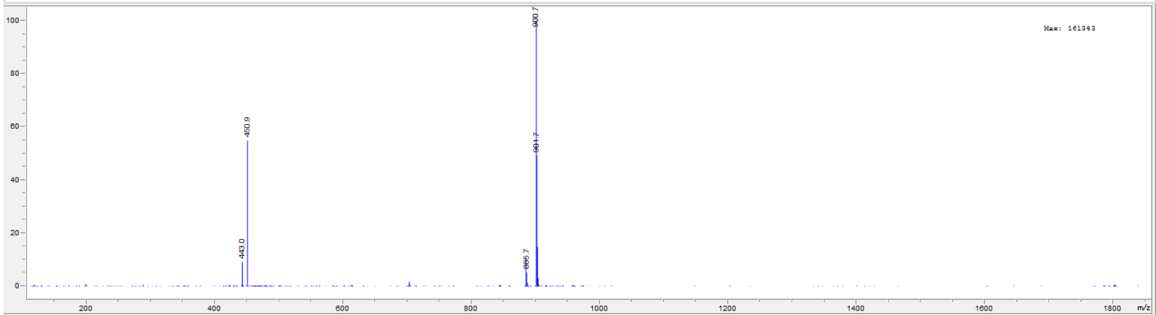


| | α | β | γ | δ | ε |
|---|---|---|---|---|---|
| R | 4.16 | 1.59 | 1.42 | 3.07 | |
| W | 4.67 | 3.22, 3.30 | | 7.21(s), 7.60 7.48(d), 7.23 7.14(t) | |
| V | 3.98 | 2.02 | 0.92 | | |
| E | 4.24 | 2.05, 1.92 | 2.35 | | |
| V | 4.07 | 2.01 | 0.82 | | |
| N | 4.69 | 2.75, 2.85 | | | |
| G | 3.89 | | | | |

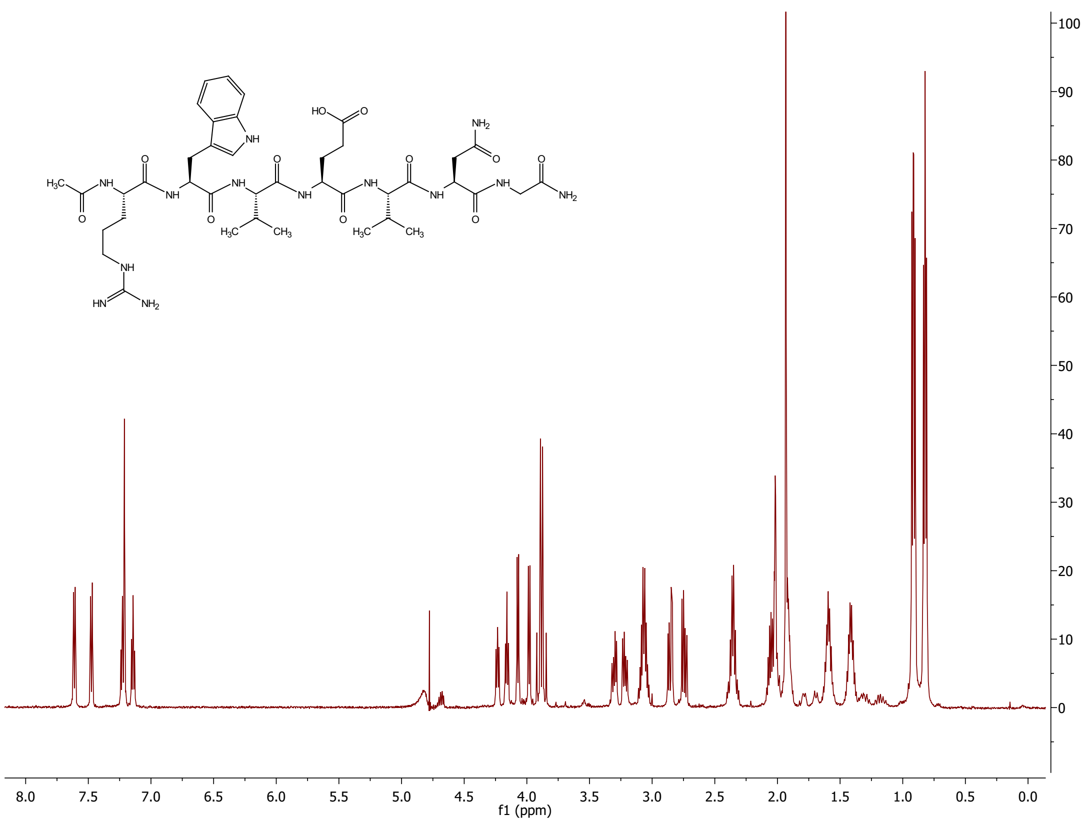

H3C
NH
O
NH
HN
NH2
NH
NH
O
NH
H3C
CH3
HO
O
NH
O
NH
H3C
CH3
NH2
O
NH
O
NH
O
NH2
f1 (ppm)
8.0
7.5
7.0
6.5
6.0
5.5
5.0
4.5
4.0
3.5
3.0
2.5
2.0
1.5
1.0
0.5
0.0
100
90
80
70
60
50
40
30
20
10
0

**8** H-RYVEVPGOKILQ-$NH_2$

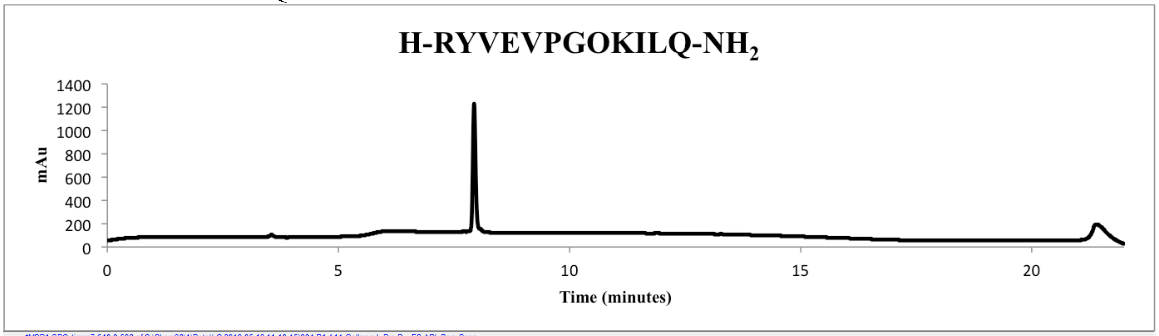


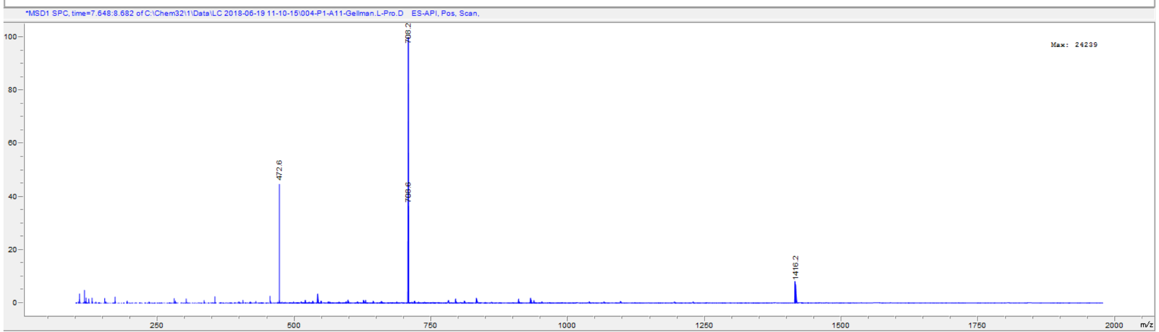


| | α | β | γ | δ | ε |
|---|---|---|---|---|---|
| R | 4.03 | 1.9 | 1.59 | 3.2 | |
| Y | 4.65 | 2.96, 3.03 | | 7.11 | 3.83 |
| V | 3.96 | 1.87 | 0.85 | | |
| E | 4.37 | 1.99 | 2.37 | | |
| V | 4.41 | 2.07 | 0.97 | | |
| P | 4.42 | 2.32 | 1.98 | 3.88, 3.71 | |
| G | 4.01,, 3.94 | | | | |
| O | 4.33 | 1.87 | 1.78 | 3.01 | |
| K | 4.31 | 1.75 | 1.45, 1.39 | 1.69 | 2.98 |
| I | 4.14 | 1.86 | 1.47, 1.21, .9 | 0.94 | |
| L | 4.38 | 1.66 | 1.59 | 0.86 | |
| Q | 4.25 | 2.11, 1.96 | 2.37 | | |

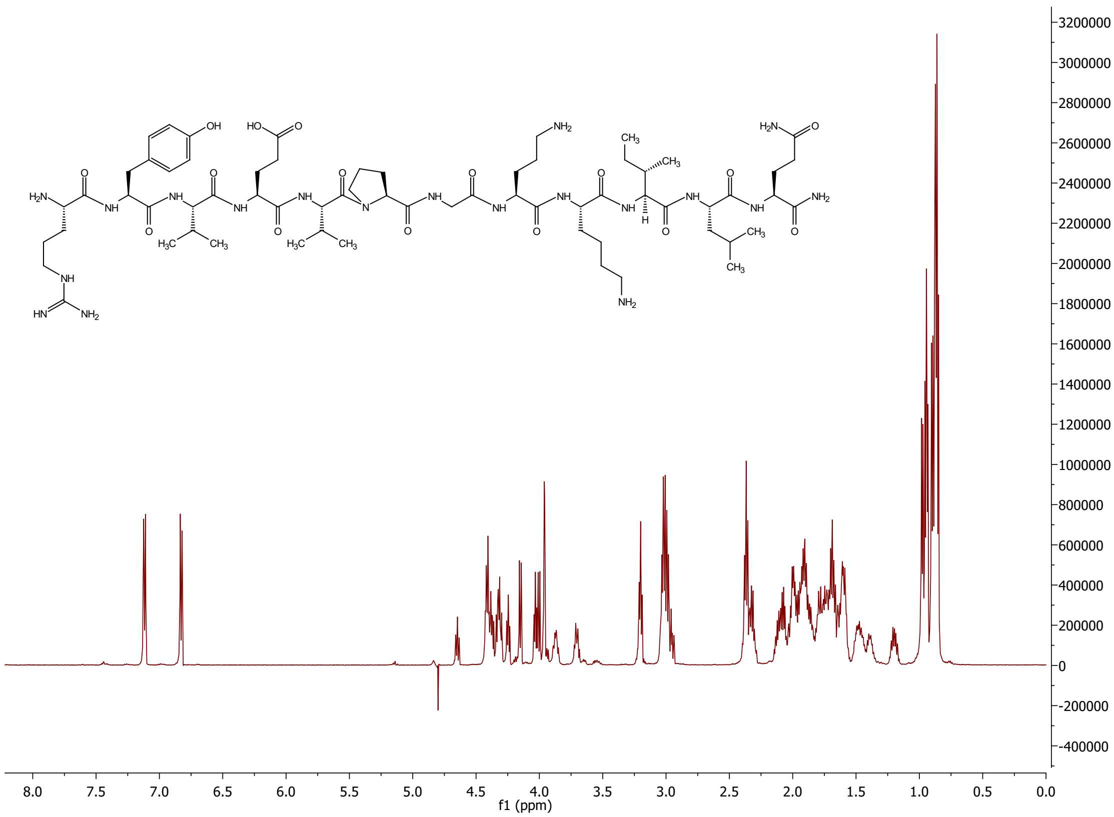
f1 (ppm)